UNIVERSITA' DEGLI STUDI DI VERONA

DEPARTMENT OF

Neuroscience, Biomedicine and Movement Science

GRADUATE SCHOOL OF

Life and Health Sciences

DOCTORAL PROGRAM IN

Neuroscience, Psychological and Psychiatric Sciences

WITH THE FINANCIAL CONTRIBUTION OF

CARI Verona foundation

Cycle: XXXII°

TITLE OF THE DOCTORAL THESIS

Mechanics and energetics of running at steady and non-steady speed (sprint and shuttles): the effects of muscle-tendon behaviour

S.S.D. M/EDF-01

Coordinator: Prof. Gianluigi Zanusso

Tutor: Prof. Paola Zamparo

Doctoral Student: Andrea Monte

Author's address

Andrea Monte
Department of Neuroscience, Biomedicine and Movement sciences
University of Verona, Italy
andrea.monte@univr.it

Supervisor

Prof. Paola Zamparo, Ph.D.
Department of Neuroscience, Biomedicine and Movement sciences
University of Verona, Italy
paola.zamparo@univr.it

Reviewers

Prof. Adamantios Arampatzis, Ph.D.
Department of Training and Movement Sciences
Humboldt-Universität zu Berlin, Germany
a.arampatzis@hu-berlin.de

Prof. Leonardo Alexandre Peyré-Tartaruga, Ph.D.
School of Physical Education, Physical Therapy and Dance
University of Rio Grande do Soul, Brasil
leonardo.tartaruga@ufrgs.br

Acknowledgements

This PhD program has been a great and challenging experience. In undertaking a doctoral thesis, one also embarks on a journey to both create and absorb as much knowledge from both themselves and their peers. During this travel, I have found a passion for science; new life skills, new communication skills, patience, but above all I have found great friendships. Over the course of my study I have met some amazing people, who have helped me no end, and whom I hope I can always call friends. I would like to specifically thank some of those here, whose help is greatly appreciated.

First and foremost, I would like to thank my Ph.D. supervisor, prof. Paola Zamparo for always supporting me and teaching me so much during this period. You have motivated, challenged and intrigued me. I cannot thank you enough for your outstanding guidance, help, patience, for always having an open door, enduring my stubbornness, all the discussions, and last but not least you taught me valuable lessons in science, critical and analytical thinking. Your teachings will never be forgotten.

Sofia and family. Without the close support and endless encouragement of my girlfriend and family, this wouldn't have been possible. Studying in another country for 6 months can be difficult at times, but the support I received from all of you, all over the world made all of the difference.

I would like to show my immense gratitude to some other individuals who have helped along the way. Prof Baltzopoulos and prof. Maganaris, thank you all so much for the help, the patience, the guidance and the continuous support you showed me through this journey. You are an amazing role model: extraordinary scientists from who I learnt a lot, and two really good persons. Costis, thank you very much for the time spent with me to write the papers. Your teachings will never be forgotten.

All my colleagues. Particularly, I would like to thank Gaspare Pavei for his help in several research projects (Study 2 and 3), for his support and discussions about several research projects, as well as for the fun at the congresses.

Finally, the acknowledgments are a very important part of a work, because you thank all people that made this possible. I'm partially writing them in my native language, so everyone can understand.

Siamo alla fine dei tre anni di dottorato e di acqua sotto i ponti ne è passata parecchia. Non mi dilungherò troppo, anche se la mia natura mi rende prolisso nei discorsi.
Ho sempre affermato che il dottorato è uno stile vita, molto spesso fatto di sacrifici che ti portano a togliere del tempo a te stesso e alle persone che ti stanno accanto. Quello che porta il piatto della bilancia a tuo favore è il viaggio che intraprendi, fatto di persone e luoghi che possono cambiarti dentro.

Proprio per questo non posso che ringraziare Paola Zamparo, la mia tutto di dottorato, che per tre anni mi ha sopportato e supportato. Non ho parole per esprimere la gratitudine che ho per lei.

Restando tra i professori, voglio ringraziare anche Vasilios Baltzopoulos e Costantinos Maganaris per il loro aiuto durante il periodo di studio a Liverpool. Ho trovato due persone eccezionali che mi hanno aiutato a crescere sotto diversi aspetti.

Vorrei anche ringraziare Gaspare Pavei per tutto il lavoro fatto insieme, e per tutto quello che avremo da fare. Grazie per i momenti di sfogo e per quelli di svago passati ai congressi. Sei stato un esempio per me.

Grazie a tutti i colleghi, a tutte le "cavie da laboratorio" e a tutte le persone che hanno fatto parte di questi tre anni e che hanno reso il tutto più spensierato, interessante e piacevole.

Grazie a Sofia per avermi supportato in questi anni e non essersi mai lamentata delle mie idee e scelte, anche quando sarei andato via di casa per sei mesi. In fine, grazie alla mia famiglia per esserci sempre.

E' stato un bel viaggio…(TO BE CONTINUED)
Grazie, thank you

December 2019-12-09

Andrea Monte

Table of contents

Figure Captions

Table Captions

Background

When humans move, they could do it in steady or non-steady conditions. In the former case the speed of locomotion is constant (or with minimal oscillations) and occurs in a definite direction (e.g. walking or running along a linear path), whereas in the latter case the body accelerates, decelerates or moves in different directions. In both cases, the minimum work required to sustain locomotion is given by the product of the resistance offered by the environment and the distance covered. Finally, the efficiency of the locomotor apparatus may be expressed as the ratio between the work necessary to maintain motion and the chemical energy transformed by the muscles. However, whereas the energetics and mechanics of running at constant speed are well known, only few studies have investigated so far non-steady running conditions (e.g. accelerated or decelerated running as well as running with changes of direction).

The role of muscles and tendons in determining the mechanical and physiological responses during human locomotion is another topic that needs to be further investigated, both in steady and unsteady conditions. As an example, when humans run at constant speed muscles and tendons stretch and recoil; into this succession of stretch-shortening cycles, tendons could play an important role as energy savers allowing this form of locomotion to be particularly efficient. Locomotion (apparent) efficiency during constant speed running can be, indeed, as high as 0.70 at high running speeds whereas in un-steady conditions (e.g. shuttle runs) the efficiency is much lower, approaching the values of muscle efficiency (0.25) when fast accelerations and decelerations are required; locomotion (apparent) efficiency is thus enhanced when tendon elastic recoil is maximized.

Investigating the role of muscle and tendon behaviour during steady and non-steady state running could, therefore, provide important information about the underpinning mechanisms that determine the mechanical and energetic demands of human locomotion. For these reasons, this thesis focuses on two main topics (running at non-steady speeds and running at constant speed), each with its own specific aims.

Aims

Non-steady speed running

To investigate the mechanical and energetic demands during non-steady locomotion using two different models: sprints (an acceleration phase) and shuttles (where an acceleration is followed by a deceleration and a change of direction). Given the difficulties in measuring muscle and tendon behaviour *in vivo* in these conditions, a further study was conducted to investigate the role of muscle architecture and Achilles tendon geometry (measured at rest) in determining the mechanical output during a sprint running acceleration phase.

The specific aims were:

1. To investigate the role of muscle and tendon geometry of the lower limb muscles in determining the force and the (horizontal) power during a sprint running acceleration phase.
2. To provide a detailed description of the mechanical power (internal and external) generated in the sprint running acceleration phase and to create an equation to predict internal mechanical power in these conditions.
3. To investigate the interplay between mechanics and energetics (e.g. locomotion efficiency) during non-steady locomotion, using as a model shuttle runs over different distances covered at different speeds.

Constant speed running

To provide a detailed description of muscle and tendon behaviour during running at constant (and increasing) speed, as well as to investigate the influence of the muscle-tendon unit components in determining the mechanical and energetic demands of running.

The specific aims were:

4. To describe the mechanical behaviour of different muscle-tendon units (and their components: muscle fascicles and tendons) at increasing running speeds.
5. To investigate the relative contribution of muscle fascicles and tendons in determining the physiological demands of running (energy cost and efficiency) at increasing speeds.

Structure of the thesis

In the first chapter a general overview of muscle and tendon characteristics, from a structural and a functional point of view, is reported. The mechanics and energetics of running at steady and non-steady speed are then reviewed. Finally, the role of muscles and tendons in determining the mechanical output and the energy demands of this form of locomotion is discussed. The aims of the thesis are then re-formulated and the research strategy defined.

The five studies are described and discussed in chapters 2-7.

The last chapter is devoted to the conclusions.

CHAPTER 1
GENERAL INTRODUCTION

Summary

In this chapter, a general overview of muscle and tendon characteristics, from a structural and a functional point of view, is firstly reported. The mechanics and energetics of running at steady and non-steady speed are then reviewed. Finally, the role of muscles and tendons in determining the mechanical output and the energy demands of this form of locomotion is discussed.

MUSCLE AND TENDON CHARACTERISTICS

SKELETAL MUSCLE STRUCTURE

Skeletal muscle is the most abundant tissue of the human body (40-45% of its total composition); it has the capability to generate force and to promote movement and therefore plays a key role in human locomotion. This particular type of tissue has the ability to adapt to a large variety of exogenous or endogenous stimuli, such as training, disuse and pathological conditions. Skeletal muscle fibres are highly specialised multinucleated cells that have the capacity to contract. Besides the functional unit (the sarcomere, that allows the muscle to contract) skeletal muscle presents different levels of collagenous connective tissue that, at the same time, divide and link muscle fibres together.

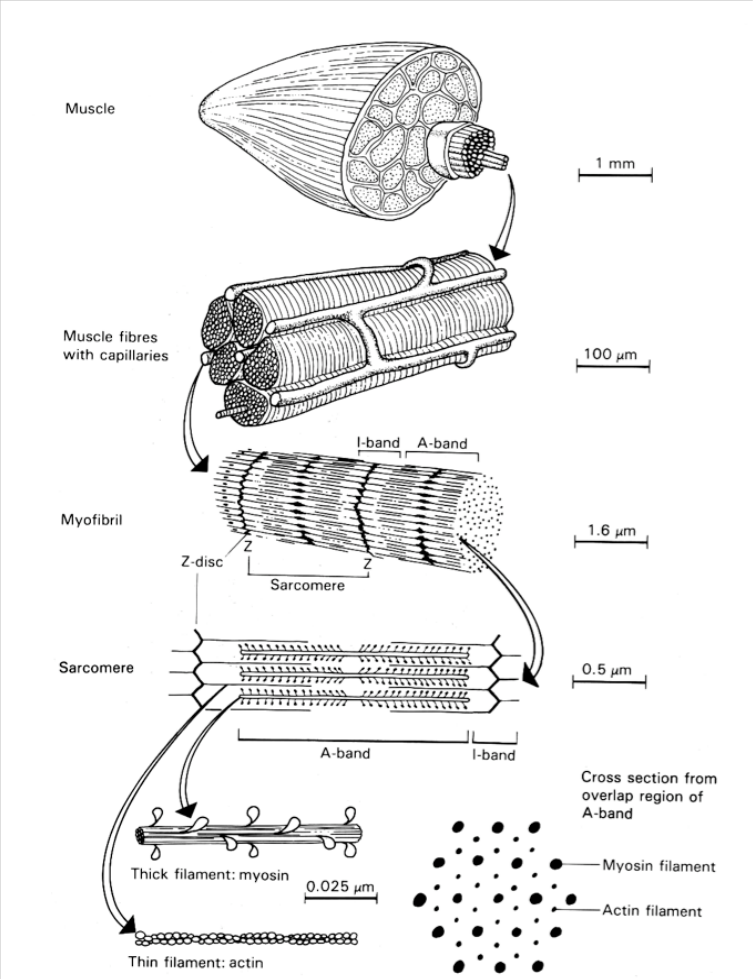

Figure 1.1: skeletal muscle structure. (Billeter & Hoppeler, 2003)

The muscle fascia wraps the muscle itself and, just beneath the fascia, a layer of connective tissue, the epimisyum, covers the whole muscle (Figure 1.1). Beneath the epimisyum, there are bundles of 10 to 100 of muscle fibres, the muscle fascicles, each surrounded by the perimisyum. Another, thinner, matrix of connective tissue (the endomysium) divides each single fibre from another one. The cell membrane surrounding each muscle fibre is known as sarcolemma and a fluid called

sarcoplasm is enclosed within them.

A muscle fibre is constituted of myofibrils arranged in parallel, which are simply 1μm diameter strings of sarcomeres (i.e. subunits of the myofibrils arranged in series). The muscle's contractile unit is the sarcomere (from 2 to 2.5 μm long) which is composed by a specific arrangement of two major protein filaments: actin and myosin. Bundles of 100 to 400 myofilaments form myofibrils and about 2000 myofibrils form an adult muscle fibre (Figure 1.1).

Contractile proteins (actin and myosin)

Sarcomeres are the functional units of muscle contraction and are composed by contractile and structural proteins. A relatively thick myofilament called myosin and a thinner one called actin are the proteins that allow the muscle to contract. Myosin presents an anti-parallel tail-to-tail arrangement and is characterized by two heavy chains (MHCs) and two light chains (MLCs) which form the thick myofilament structure. The myosin molecule can be "divided" into two major fragments: head and tail. The head has a globular portion that contains the ATPase activity (i.e. is the portion that can combine with actin) and one portion that includes the flexible region of the molecule (Figure 1.2). Actin is a globular protein composed by two strands of polymerized actin monomers forming a double helical arrangement. In order to promote muscle contraction, two different proteins interact with actin: troponin and tropomyosin, which regulate the relationship between actin and myosin. Whereas tropomyosin lies on seven actin subunits and blocks the sites where the myosin head can bind, troponin is positioned every seven monomers of actin and consists of three different components: troponin T that binds tropomyosin, troponin C that acts as a receptor for calcium ions (Ca^{++}) and Troponin I that represents the inhibitory subunit.

Actin and myosin are spatially organized in a hexagonal arrangement, that allows the muscle to shorten and generate muscle force. During the shortening process, each of the six actin filaments that surround a myosin filament has the possibility to serve as an attach site for the thick filament. Conversely each actin filament can interact with three different myosin filaments (Figure 1.2).

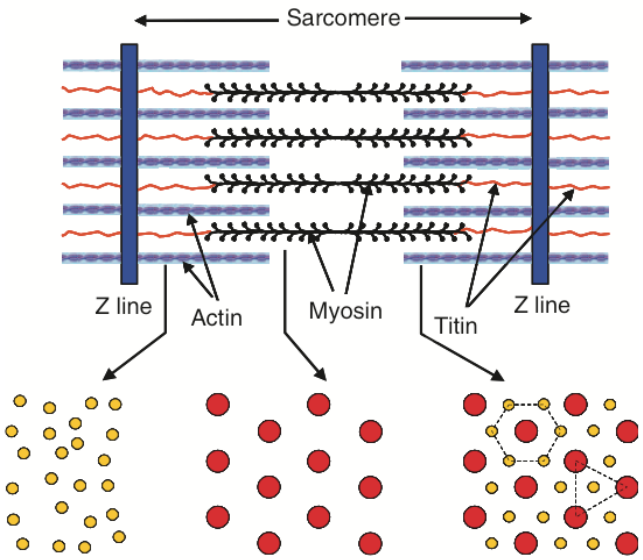

Figure 1.2: representation of a sarcomere with the spatial arrangement of the contractile (actin and myosin) and structural (e.g. titin) proteins. (Jones et al., 2004).

Inside the sarcomere, various regions can be described (Figure 1.3) the myosin filaments are situated mostly in the middle of the sarcomere; the area known as A-band is the zone where there is overlap between the different protein filaments whereas the H-band is the zone where there is no overlap between actin and myosin (Figure 1); the region containing the actin filaments, called I- band is situated next to the Z line (that represents the end of the single sarcomere unit). Therefore, one sarcomere dimension can be calculated from one Z- band to the other.

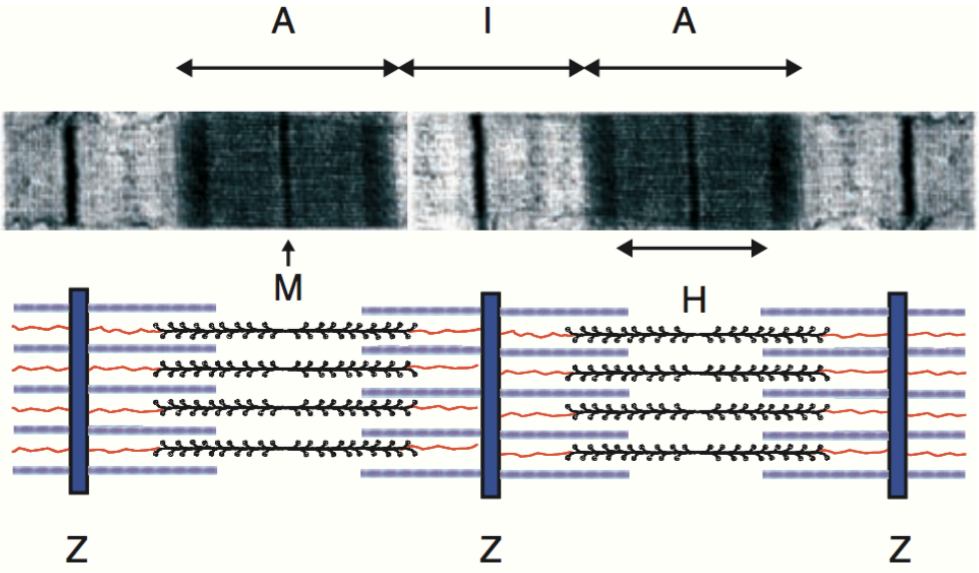

Figure 1.3: sarcomere structure during resting (a) and shortening (b). (Jones et al., 2004).

Structural proteins (the cytoskeletal complex)

Besides actin and myosin, there are several other proteins inside the muscle many of which are structural proteins that constitute the cytoskeleton. The primary role of the entire cytoskeletal complex is to maintain the arrangement of actin and myosin within the sarcomere and the alignment of myofibrils between each other. The two main structural proteins of the sarcomere are titin and nebulin, which are responsible to connect myosin to the Z band, keeping myofilaments aligned and regulating the length of actin filaments, respectively (Figure 1.3). Another sarcomere structural protein, α-actinin, binds the actin filaments together at the Z line.

Other proteins (such as desmin) and focal adhesions work "outside the sarcomere" to link adjacent myofibrils and to maintain the alignment of Z lines, as well as to connect intracellular proteins to extracellular space, connecting myofibrils to sarcolemma and muscle fibres to the myotendinous junction.

Cross-bridge generation: the sliding filament theory

As previously mentioned, myosin interacts with actin to generate force: the process through which the globular heads of myosin interact with the actin filament takes the name of cross-bridge cycle. This cycle consists of three main phases: detachment, activation and attachment of the myosin globular head (Huxley and Simmons, 1971) and begins with ATP (adenosine triphosphate) binding to the myosin head and causing the detachment of the latter from actin; myosin head is weakly attached to actin at this state and ATP has been hydrolysed to adenosine diphosphate (ADP) and inorganic phosphate. Successively, Ca^{++} binds to troponin, freeing the myosin-binding sites of the actin filament, so that the globular head can attach to actin: the inorganic phosphate is released whilst the power stroke of the cross-bridge cycle occurs, resulting in exertion of force at the contractile site. Myosin filaments are arranged so that actin filaments can slide between them and thus myosin can bind to actin at the same time; this is possible because while thick filaments remain fixed, thin filaments can slide in and out (Huxley,1974). This mechanism constitutes the sliding filament theory of muscle contraction (Huxley, 1974).

MECHANICAL CHARACTERISTICS OF SKELETAL MUSCLE

Our knowledge of how muscle proteins generate force and movement has come about by investigating the structure of the actin and myosin filaments and their organization in the sarcomere but in order to better understand the mechanisms of muscle force generation, we need to acknowledge two important features of muscle contraction. The first takes into account how force varies with the length of the muscle, and the second is the relationship between the force that can be developed and the velocity of movement, during either shortening or lengthening. These properties can be described by two different relationships: the Force-Length and the Force-Velocity relationships.

Force-Length or Length-Tension relationship

Muscle force generation depends on the interaction between the contractile protein filaments; as a consequence, the production of force is proportional to the extent of myosin and actin overlap. For this reason, the force developed by a muscle (during an isometric contraction) depends on the length of the sarcomeres (and thus of the muscle itself).

The relationship between sarcomere tension development and sarcomere length was firstly investigated on frog muscle (Gordon et al. 1966; Huxley & Simmons, 1971; Huxley, 1974). The sarcomere Length-Tension curve (Figure 4) presents three distinct parts: 1) an ascending part, where force and sarcomere length increase; 2) a small plateau, where force is constant for a specific sarcomere length; and 3) a descending profile, where force decreases whereas sarcomere length continue to shorten. Gordon and co-workers observed that no active muscle fascicles force is developed at a length of 3.65 μm (micrometres) in frog muscle (Gordon et al., 1966) because no sliding between myosin and actin filaments is possible at this length, as thick filaments are 1.65 μm long and thin filaments are 2 μm long; therefore, there could be no overlap between contractile proteins unless sarcomere length decreases and contractile filaments are able to interact and produce force. As described in Figure 1.4, in frog skeletal muscle the tension generated starts to increase as sarcomere length goes from 3.65 μm to 2.2 μm: the force (tension) generated by the sarcomeres reache a plateau (e.g. maximum tetanic tension) between 2.2 and 2 μm of sarcomere length. In this phase, the force results to be maximum due to the greater filament overlap. Following this phase, no more cross-bridge interactions are able to occur. Indeed, if the sarcomeres are further shortened, the actin filaments from one side of the sarcomere overlap with the ones of the opposite side, causing a "double-overlap" situation, which affects cross-bridges formation and, as a consequence, the force generated by the contractile material. As a result, the tension registered between 2 and 1.7 μm declines as the sarcomere shortens: after further shortening (sarcomere length < 1.7 μm) the myosin filaments come into contact with the Z line and fibres and tension production dramatically drop.

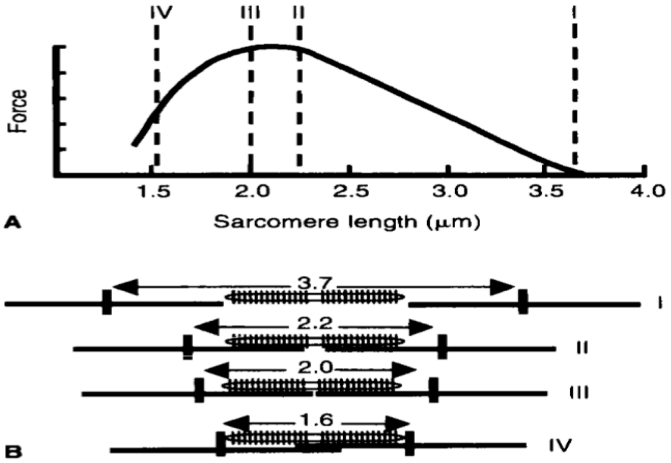

Figure 1.4: Isometric force at different sarcomere lengths. Force generated (A); arrangement of filaments at different lengths (B). Values are for frog muscle. (Gordon et al., 1966).

The F-L relationship of human skeletal muscle is very similar to that of frog skeletal muscle but the optimal sarcomere length (where maximum tetanic tension can be developed) is higher (between 2.6 and 2.8 μm) because of the longer actin filaments of human sarcomeres compared to frog (whereas myosin length is essentially the same) (Walker & Schrodt, 1974).

In Figure 1.5, the dotted line represents the tension generated when a muscle is stretched to various lengths without stimulation. Passive tension below or near the optimal length is almost zero but when the muscle is lengthened, passive tension increases dramatically. These relatively long lengths can be attained physiologically and, therefore, passive tension can play a role in providing resistive force even if the muscle is not stimulated (Lieber, 2003). Magid & Law (1985) demonstrated that the origin of the passive muscle tension is within the myofibrils themselves, and that titin is strongly related with the capability of the muscle to generated passive force.

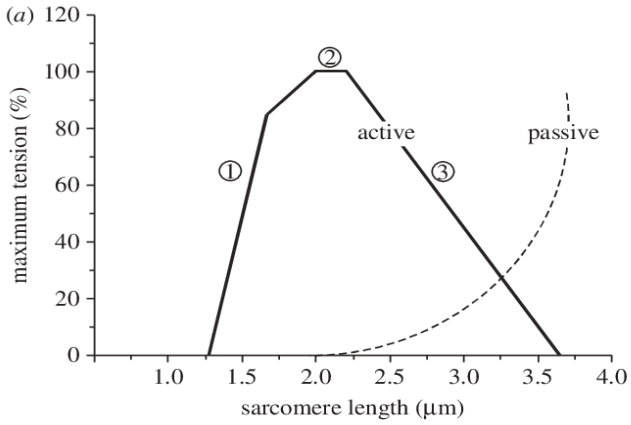

Figure 1. 5: Length-Tension relationship for frog sarcomere obtained using sequential isometric contractions in single muscle fibre. Bold solid line: active force generated by the sarcomere; dotted line: passive muscle tension. (Lieber, 2003).

To determine the active force generated at long muscle lengths it is thus necessary to subtract the passive force from the total. This process results to be difficult because the passive force itself varies. Whatever gives rise to the passive force, it is not perfectly elastic and shows the property of hysteresis, that is, there is a greater passive force at the same overall muscle length when the muscle is being stretched than when it is shortening (Jones, 2004).

Force-Velocity relationship

The force developed by a muscle, besides on its length, depends on contraction velocity. Hill in 1938 and Katz in 1939, showed how force values change with the increase or decrease of shortening and lengthening velocity of human skeletal muscle (see Figure 1.6).

The first study conducted by Katz (1939) used isotonic contraction to investigate the capability of an isolated muscle to generate force at different contraction speeds. The F-V relationship is a curve that represents the results of many experiments plotted on the same graph. Experimentally, a muscle is stimulated maximally and allowed to shorten against a constant load, while the velocity is measured and plotted against the force.

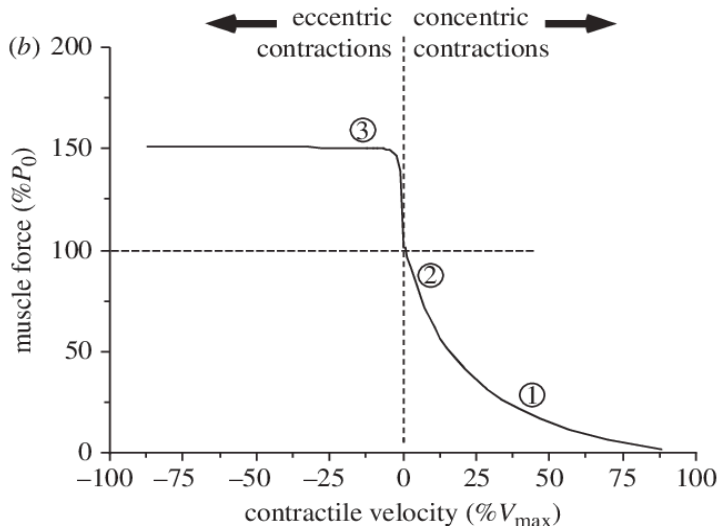

Figure 1.6: Force-Velocity relationships of a skeletal muscle fibre obtained using isotonic contractions. Force increases rapidly upon forced sarcomere lengthening and drops upon muscle shortening. The circled numbers represent the force and velocity data from two concentric contractions (1,2) and one eccentric contraction (3). Note that force increases dramatically upon forced muscle lengthening and drops precipitously upon muscle shortening (Lieber, & Ward, 2011).

During voluntary muscle activation (e.g. when lifting a load), the contractions that permit the muscle to shorten are known as concentric contractions. During a concentric contraction, the force that a muscle could generate is always lower than the maximum isometric force (point 2 in Figure 1.6). When the force necessary to move the load decreases, the contraction velocity increases (e.g.

"point" 1 in Figure 1.6). This physiological behaviour occurs until the muscle finally reaches its maximum shortening velocity. Thus, the heavier is the load to lift, the slower will be the velocity of shortening, until the latter will get close to 0 value. In this last case, when the velocity of movement is 0, the force generated by the muscle is defined as maximum isometric force, in which muscle exerts tension but with no real joint movement. This kind of contraction represents the maximum value of force that can be generated while the muscle shortens.

It is then possible that, as the load on the muscle increases, it reaches a point where "the external force on the muscle is greater than the force the muscle can generate" (Lieber, 1992). As a consequence, the muscle will be lengthening even if it may be fully activated (point 3 in Figure 1.6). This kind of contraction, when a muscle exerts tension while lengthening, is called eccentric contraction. As suggested by Katz (1939) in the eccentric part of the F-V curve, it can be easily observed that: 1) the maximum tension that can be generated while the muscle actively lengthens is greater than the one developed in isometric and shortening contractions and, 2) the absolute tension does not depend of lengthening velocity. In fact, with the increase of lengthening velocity, muscle force rises until it reaches a plateau at a value close to 1.8 times the maximum isometric one (Katz, 1939, Lombardi & Piazzesi, 1990). Even though *in vivo* the force values differ from the *in vitro* situation (for reasons that will be explained in the next sections), eccentric muscle force still reaches greater values than the ones generated by either isometric or concentric actions (about 1.2 times) (Aagaard et al., 2000; Westing et al., 1988).

Length-Tension-Velocity relationship

During real life, both relationships (F-L and F-V) describe "unrealistic" conditions since force generation at constant length or velocity of contraction at constant force are not common during daily activities. However, since muscle force changes with length and velocity in a specific manner, it is possible to define the muscle force produced in a variety of conditions. Indeed, the F-L relationship can be considered as a series of length-force-velocity experiments performed at constant velocity, whereas the F-V relationship could be viewed as a length-force-velocity relationship performed at constant length. In that case, the common point between the F-L and F-V relationships is the point of maximum isometric tension, whereas if both length and velocity change, the result is the superposition of the two curves (Fridén & Lieber, 1992)

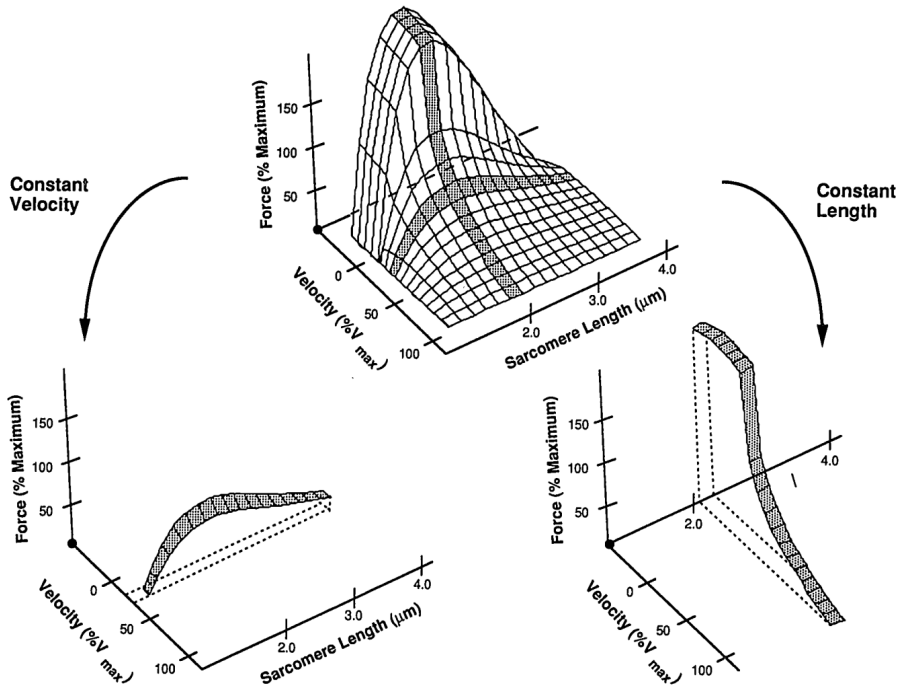

Figure 1.7: The hypothetical muscle length-force-velocity surface for skeletal muscle. Shaded regions represent a "slice" of the surface at either constant length or velocity. A "slice" of the surface at constant length is simply a force-velocity curve measured at that length while a "slice" of the surface at constant velocity is simply a length-tension curve measured at that velocity (Fridén & Lieber, 1992).

As indicated in Figure 1.7, when contraction velocity is high, the force will be low no matter the length; as a consequence, at high contraction speeds muscle length is not determinant; whereas at low velocity (and high force), muscle length becomes an important parameter. Of course, neural control is important in determining the length-force-velocity relationship, and it should be kept in mind that the F-L and F-V relationships are determined on a maximally activated muscle, whereas during daily activities the muscles are generally submaximal activated (Fridén & Lieber, 1992).

MUSCLE ARCHITECTURE

The F-V and F-L relationship well explain how muscles work in order to produce force and how the latter is dependent on contraction velocity and muscle length. The internal macroscopic design of how muscle fascicles are arranged within the muscle is described as muscle architecture and can influence the functional properties of muscles (Narici & Maganaris, 2006). Indeed, muscle fibres exert forces along their longitudinal axes, whereas the muscle as a whole exert forces via its tendons. In various muscles, fascicles are connected to tendons at different angles, and hence the direction of an individual muscle fibre force and the muscle force direction can be different.

Fascicle architectural arrangements

Human skeletal muscle presents two main typologies of architectural models: parallel or fusiform muscles and pennate muscles (Figure 1.8).

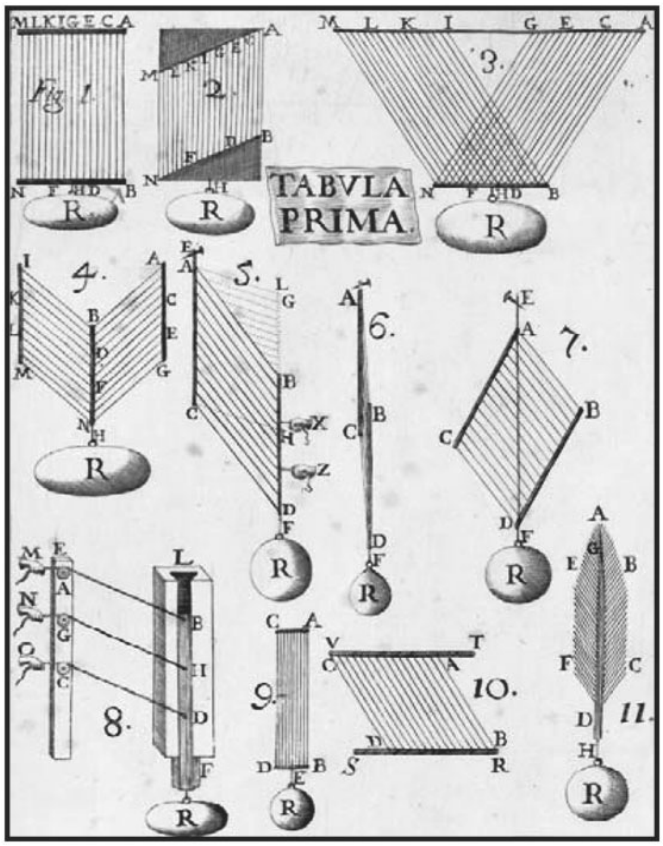

Figure 1. 8: different possible arrangements of parallel (1,2 and 9) and pennate (3-7 and 10) muscles (Borelli, 1680).

In parallel fibred muscles, fascicles run longitudinally and in the same direction of the muscle-tendon unit line of action whereas pennate muscles fascicles are placed to form an angle (pennation angle, PA) with the muscle-tendon line. In the case of a muscle with the fibres that insert onto the tendon aponeurosis with the same pennation angle, the muscle is classified as unipennate, whereas, when different PA are present within the same muscle, the muscle is classified as a multipennate. Most of the muscles of the human body appear to show a pennate architecture (Friederich & Brand, 1990).

Pennation angle influences fibre length as it constrains the muscle fibres to extend to only part of the whole muscle length (Narici & Maganaris 2006). Fibre length is also dependent on the number of sarcomeres in series that form that fibre: shorter fibres have less contractile units in series and present a slower velocity of shortening, and this phenomenon affects the speed of contraction of the whole muscle. On the other hand, pennation angle plays an important role in the spatial arrangement of muscle fascicles, allowing more fibres to be placed within the muscle (Gans & Bock, 1965; Gans, 1982). Therefore, the larger the pennation angle the larger the amount of muscle mass for the same

amount of area (i. e. the larger the physiological cross sectional area for a given anatomical cross sectional area) (Kawakami et al.,1993; Reeves et al., 2009).

Pennate muscles are thus able to develop higher contractile force due to the higher muscle mass in the same area. However, this gain of contractile units in-parallel could also represent a problem for muscle force exertion, as the fascicle are placed in a non-longitudinal arrangement, if related to the muscle-tendon line of action. Thus, because muscle force must act through the tendon and then onto the bone to ultimately create joint movement, the force developed in the direction of the fibres will have to be transferred longitudinally to the tendon aponeurosis. The amount of "effective force transmitted" could be calculated with planar geometrical models, by using trigonometric formulas. The first theoretical model was suggested by Steno in 1667 and was followed by several studies where the "muscle geometry model" was better defined (e.g. Gans & Bock 1965, Alexander & Vernon 1975, Gans 1982, Wickiewicz et al., 1983, Fukunaga et al., 1997); an example of a two-dimensional model of pennate muscle is reported in Figure 1.9.

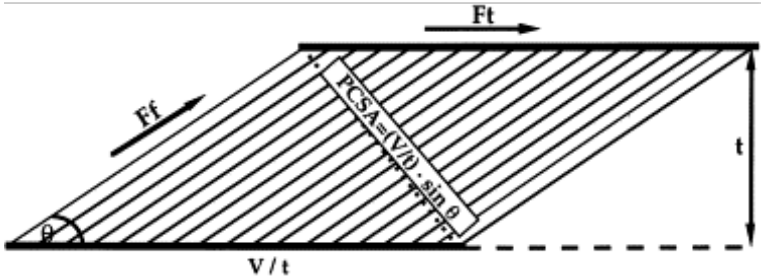

Figure 1. 9: two-dimensional model of a pennate muscle. Ff: fibre force; Ft: force transmitted; t: muscle thickness, V: muscle volume; PCSA: physiological cross sectional area. (Narici et al., 1996).

For fusiform muscles (i.e. with parallel muscle fibres), the cross-section can be determined at any distance between muscle origin and insertion whereas for pennate muscles the only valid cross-section is the one through all muscle fibres: this is called the *physiological cross-section* and the corresponding area is known as the *physiological cross-sectional area* (PCSA). If all the fibres in a muscle were arranged in parallel, the PCSA would equal their total cross-sectional area. In addition to the PCSA, the area of the muscle slices cut perpendicularly to the longitudinal muscle direction or to the muscle centroid can be determined. This area is called the *anatomical cross-sectional area* (ACSA) or *simply cross-sectional area* (CSA). For fusiform muscles, the PCSA and ACSA are similar, whereas for pennate muscles, the PCSA is larger than the ACSA (e.g. Lieber, 2002).

The variable that better describes the capacity of a muscle to generate maximum voluntary force and to transmit it through its tendon is the physiological cross-sectional area (PCSA) which represents a good measure of the amount of sarcomeres arranged in parallel within the muscle and which is directly proportional to the maximum tetanic tension that can be generated by the muscle (Haxton, 1944; Alexander & Vernon 1975; Narici, 1999; Narici & Maganaris, 2006). By using

trigonometry, PCSA can be calculated as:

$$PCSA = (V/t) \cdot \sin\theta$$

where V is muscle volume, t is muscle thickness and θ is the angle of pennation.
Whereas the effective force acting on the muscle-tendon line (Ft) can be calculated as:

$$Ft = Ff \cdot \cos\theta$$

where Ff represents the force acting along the fascicles.

As indicated in Table 1, the muscles with the higher pennation angle are those with the lower fascicle length and the length of the muscle fibres never extends the entire muscle length (e.g. the larger the pennation angle the shorter the muscle fibres compared the muscle length). As a consequence, also PCSA is higher in the muscles with the higher pennation angle.

Muscle and the number of studied specimen	Muscle length, cm	Fiber length, cm	Lf coefficient of variation, %	Sarcomere length, μm	Pennation angle, °	Physiological cross-sectional area, cm^2
Psoas, $n = 19$	24.25 ± 4.75	11.69 ± 1.66	12.4 ± 5.9	3.11 ± 0.0.28	10.6 ± 3.2	7.7 ± 2.3
Gluteus medius, $n = 16$	19.99 ± 6.42	7.33 ± 1.57	20.3 ± 11.8	2.40 ± 0.18	20.5 ± 17.3	33.8 ± 14.4
Sartorius, $n = 20$	44.81 ± 4.19	40.30 ± 4.63	6.4 ± 4.2	3.11 ± 0.19	1.3 ± 1.8	1.9 ± 0.7
Rectus femoris, $n = 21$	36.28 ± 4.73	7.59 ± 1.28	9.7 ± 4.6	2.42 ± 0.30	13.9 ± 3.5	13.5 ± 5.0
Vastus lateralis, $n = 19$	27.34 ± 4.62	9.94 ± 1.76	9.1 ± 6.1	2.14 ± 0.29	18.4 ± 6.8	35.1 ± 16.1
Vastus medialis, $n = 19$	43.90 ± 9.85	9.68 ± 2.30	10.7 ± 5.7	2.24 ± 0.46	29.6 ± 6.9	20.6 ± 7.2
Tibialis anterior, $n = 21$	25.98 ± 3.25	6.83 ± 0.79	6.6 ± 4.0	3.14 ± 0.16	9.6 ± 3.1	10.9 ± 3.0
Gastrocnemius medial head, $n = 20$	26.94 ± 4.65	5.10 ± 0.98	13.4 ± 7.0	2.59 ± 0.26	9.9 ± 4.4	21.1 ± 5.7
Gastrocnemius lateral head, $n = 20$	22.35 ± 3.70	5.88 ± 0.95	15.8 ± 11.2	2.71 ± 0.24	12.0 ± 3.1	9.7 ± 3.3
Soleus, $n = 19$	40.54 ± 8.32	4.40 ± 0.99	16.7 ± 6.9	2.12 ± 0.24	28.3 ± 10.1	51.8 ± 14.9

Table 1. 1: Architecture of Lower Extremity Muscles. Lf is the fibre length normalized to a sarcomere length of 2.7um. (Liber, 2009).

Influence of muscle architecture on the F-L and F-V relationships

Pennate muscles have shorter fibres but more contractile material in-parallel, compared to parallel-fibred muscles and these differences in the geometrical characteristics have important functional consequences: 1) the larger the pennation angle, the larger the voluntary force that could be exerted; 2) the larger the number of sarcomeres in series (i.e. the larger the fascicle length) the larger the velocity of shortening. Even small changes in fascicle length or PCSA are thus expected to affect the F-L and F-V relationships of a muscle (Jones, 2004; Lieber, 2002).

As an example, if we consider two muscles with an identical PCSA (same total number of sarcomeres in parallel) but with different fibre lengths (different number of sarcomeres in series), the two muscles will have distinctly different force-length and force-velocity relationships (Figure 1.10). Both muscles will generate the same absolute force (since their PCSA will be the same) but the longer muscle will be able to generate force over a greater range of lengths and will display a greater optimum length than the shorter-fibred muscle. As a consequence, the length-force relationship of a pennate muscle presents a smaller operating range than that of a parallel muscle (Woittiez et al. 1984; Gasier et al. 1992). If we consider the force-velocity relationship, a muscle with longer fibres will not only display a higher maximum shortening velocity but will also shorten at a faster velocity at any given submaximal force.

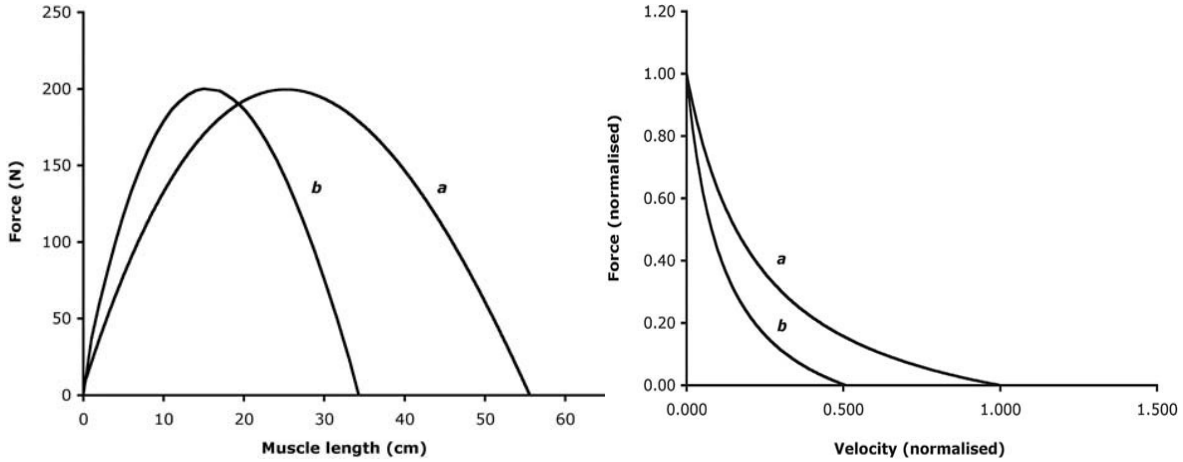

Figure 1. 10: The F-L (on the left) and F-V (on the right) relationships of two muscles (a and b) with the same PCSA but with different fibre lengths. In the F-L relationship, the muscle with longer fibres (a) is able to generate force over a much larger range of lengths than muscle b (with smaller fibre length) and has a greater optimum length for maximum force generation. Because their PCSA is the same, both muscles generate the same maximum isometric force. In the F-V relationship, the muscle with longer fibres (a) has a much higher maximum shortening velocity than the muscle with shorter fibres (b). Again, since the PCSA of a and b is the same, their maximum isometric force does not differ but the force generated at any given submaximal shortening velocity is lower for muscle b. (Lieber, 2002).

On the contrary, if we consider two muscles with the same fibre length (the same amount of sarcomere in series) but a different PCSA (different amounts of sarcomeres in parallel), the muscles will have the same optimum length and excursion, but different absolute force (Figure 1.11). Furthermore, no differences will be observed in maximum shortening velocity but the muscle with

the larger PCSA will be able to develop greater isometric force and also greater dynamic force at any given submaximal velocity (Figure 1.11). Hence its force-velocity relation will also be different from that of the muscle with a smaller PCSA (Lieber, 2002).

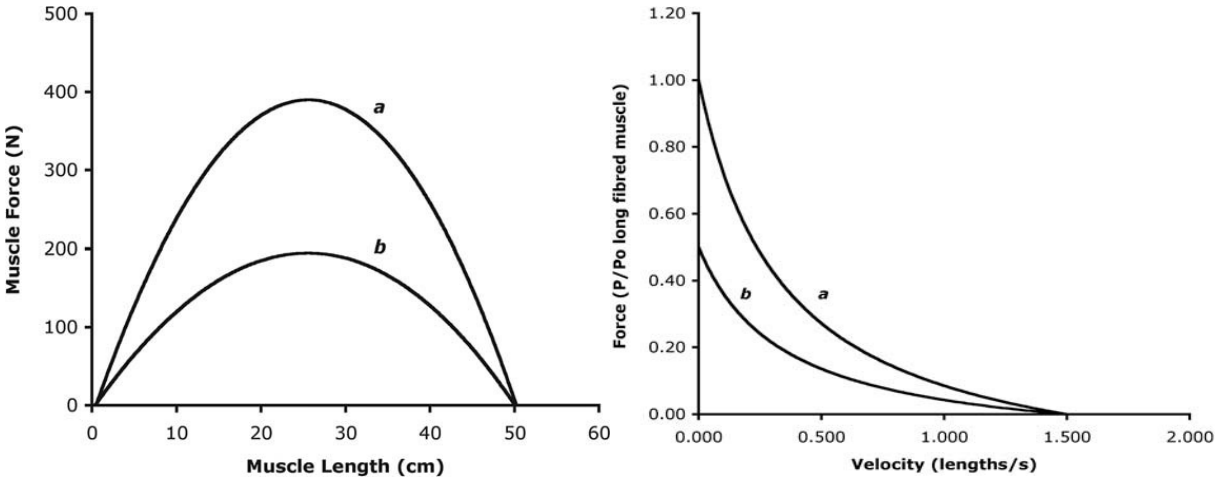

Figure 1. 11: The F-L (on the left) and F-V (on the right) relationships of two muscles with the same fascicle length but with different PCSA. On the left, the muscle a with a larger PCSA (a) generates a much larger force than muscle b with a smaller PCSA. The optimum length as well as the range of contraction are, however, the same for both muscles. On the right, the muscle with a larger PCSA generates a much higher isometric force and a larger dynamic force at any given submaximal shortening velocity than muscle b; however, their maximum shortening velocity are the same. (Lieber, 2002).

When combining all these properties, the muscles with relatively long fibres are muscles with high contraction velocities and large excursions; conversely, the muscles with larger PCSA are those able to develop the greater tensions (Lieber, 2002). The F-V relationship for two muscles, one pennate (with larger PCSA and shorter muscle fibres) and one fusiform (with lower PCSA but larger fascicle length) is represented, as an example, in Figure 1.12.

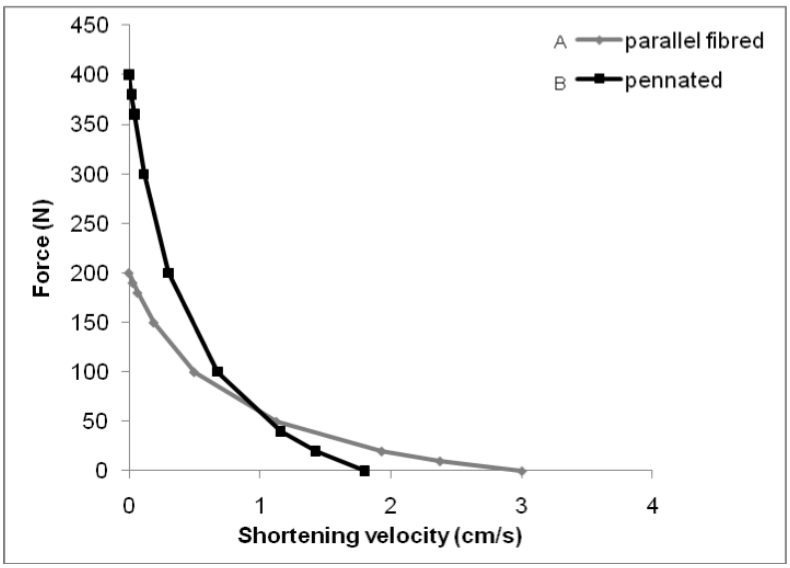

Figure 1. 12: F-V relationship for parallel and pennate muscles with same volume but different PCSA and fibre length. (Jones, 2004).

The maximum shortening velocity of a muscle does not only depend on its fibre length but also on the changes in pennation angle that occur during contraction. Indeed, during shortening, the fibres pivot about their origin, pulling the opposite aponeurosis towards the proximal end of the muscle and this results in a linear shortening of the muscle (Figure 1.13).

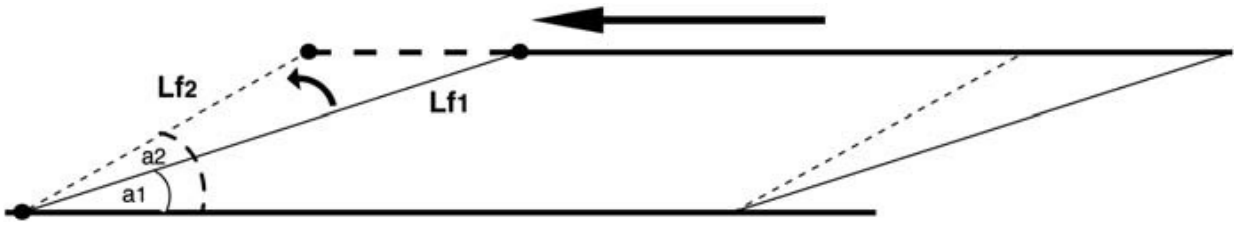

Figure 1. 13: pennate muscle at rest (solid line) and during contraction (dashed line). As the muscle contracts, fibres pivot about their origin increasing pennation angle from a1 to a2 and shortening their lengths from Lf1 to Lf2. (Bottinelli, 2000).

Hence, the shortening of a muscle will depend on three factors: a) the resting length of the fibre, b) the resting pennation angle and, c) the pennation angle during contraction. It is thus possible to estimate shortening velocity by simultaneously taking into account the changes in fibre length and pennation angle:

$$v = \frac{(Lf1 \cdot \cos \alpha 1 - Lf2 \cdot \cos \alpha 2)}{t}$$

(where Lf_1 is fibre length at rest, Lf_2 is fibre length in the contracted state, α_1 is pennation angle at rest, α_2 is pennation angle in the contracted state and t is the time/duration of the shortening phase).

TENDON STRUCTURE AND COMPOSITION

Tendon structure

Tendon structures are interposed between muscles and bones. Tendons could have different shapes and sizes, depending on the characteristics of the respective muscle and bone (Józsa and Kannus, 1997). In most case, the tendon connect directly distal to the joint on which the respective muscle principally acts thus, allowing for joint movements (Benjamin and Ralphs, 1997). The part of the tendon that links the muscle to the bone is called free or external tendon, whereas the aponeurosis, or internal tendon, is the part that provides the attachment area for the muscle fibres (Magnusson et al., 2008; Nigg and Herzog, 1999).

As reported in in Figure 1.14, tendons are characterized by a multi-unit hierarchical structure (Benjamin and Ralphs, 1997; Elliott, 1965; Kastelic et al., 1978), where the smallest structural unit is the fibril, consisting of a quarter-staggered arrangement of aligned collagen molecules.

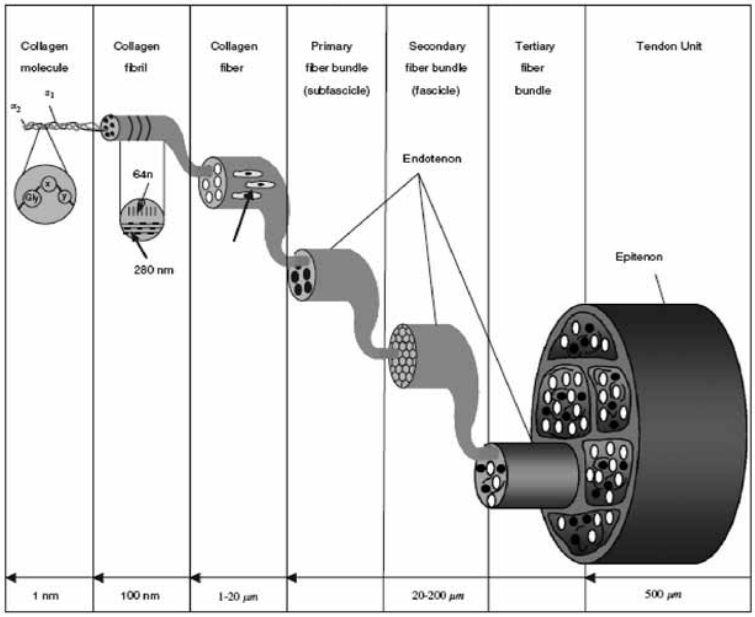

Figure 1. 14: Schematic illustration of the multi-unit hierarchical structure of the tendon (Wang, 2006).

Collagen molecules are long and are arranged in stiff rods, containing three helical polypeptide alpha-chains that wind around each other to form a triple helix, extending throughout the length of the molecule (Józsa and Kannus, 1997). Collagen fibres, that are composed by bundles of collagen fibrils form the next level of tendon structure (Figure 1.14). The endotenon, a thin layer of connective tissue that includes blood vessels, lymphatics and nerves, binds several collagen fibres to a primary fibre bundle (sub fascicle) (Figure 1.14). Primary fibre bundles form to secondary fibre bundles (fascicles) and then to tertiary fibre bundles. Each fascicle level is enclosed by endotenon tissue. The final structural level is the tendon unit, as the conjunction of the tertiary fibre bundles (Figure 1.14). The tendon unit is surrounded by the epitenon, a connective tissue that also provides vascular, lymphatic and nerve supply to the tendon. A third surrounding connective tissue layer, the paratenon, is connected with the epitenton to the so-called peritenon (Figure 1.14). It has been suggested that this layer reduces the friction with adjacent tissues (Benjamin and Ralphs, 1997; Kastelic et al., 1978; Wang, 2006).

All levels in this hierarchical structure are aligned parallel to the axis of the tendon (Elliott, 1965), allowing for an optimal mechanical load transmission (Wang et al., 2012). In an unloaded condition, the collagen fibres are characterized by a crimping or wavy formation (crimp pattern), most likely due to proteoglycan fibre cross-linking. However, when the tendon is stretched the wavy configuration disappears in correspondence to the straightening of the collagen fibres (Elliott, 1965; Józsa and Kannus, 1997).

At the end of the tendons is the tendon-bone junction, that consist of a fibrous or a fibro-

cartilaginous connection type. In the first case, the tendon directly attaches to the bone, whereas in second case, the fibro-cartilaginous end shows a transitional zone of hyaline fibrocartilage to distribute mechanical loads (Benjamin et al., 2002). The myotendinous junction connects the muscles to the tendon with a special arrangement of the terminal myofibrils (Benjamin and Ralphs, 1997). As an example, membrane folding of the terminal muscle cells increases the junction surface area, myofilament bundling at the terminal processes of muscle cells and also out branches of smaller myofibrils allow for the insertion of the tendon collagen fibrils on the muscle and, thus, for the transmission of the muscular forces (Michna, 1983; Tidball, 1991; Wang, 2006).

Tendon composition

Tendons are essentially composed by cells, collagen, proteoglycans, glycoproteins and water (Silver et al., 2003), where the collagen, particularly the type I, is the most abundant protein in the tendon extracellular matrix. Type I collagen constitutes about 60% of the tendon dry mass and about 95% of the total collagen content in tendons. Collagen type III and V constitute about 5% of the remaining part. Moreover, type III collagen is mainly located in the endotenon and epitenon, whereas type V is located in the core of type I collagen fibrils (Wang, 2006). All other types of collagen (type II, VI, IX, X and XI) are less abundant and primarily located at the tendon-bone insertion point (Fukuta et al., 1998).

Type I collagen mainly forms parallel fibres (longitudinal) but can also be organized horizontally and transversely. Furthermore, from a geometrical point of view, collagen fibres crossing each other form spirals and plaits along their course (Józsa and Kannus, 1997) and this allows the tendon to be resistant. It has been suggested that the collagen type I plays a key role for the tensile strength of tendons (Wang et al., 2012). Indeed, the collagen in the extracellular matrix is cross-linked (intra and inter-molecularly) via enzymes (e.g. lysyl oxidase) or by means of non enzymatic glycation (Avery and Bailey, 2005; Bailey et al., 1998; Eyre et al., 1984; Reiser et al., 1992) and this influences the tendon mechanical properties (i.e. Young's modulus, Thompson and Czernuszka, 1995). Moreover, also the proteoglycans (e.g. aggrecan and decorin) and glycoproteins (e.g. tenascin-C, fibronectin and elastin) account for important functions in the tendinous tissue (Halper and Kjaer, 2014; Silver et al., 2003; Wang et al., 2012). While aggrecan binds water (50 times their weight) and therewith resists compression and shear, decorin allows for collagen fibrillar slippage during mechanical deformation. Glycoproteins not only contribute to the mechanical stability of tendinous tissue through its interaction with collagen fibrils (tenascin-C) but also facilitate wound healing (fibronectin). Elastin, in particular, accounts for the length recovery following mechanical stretching (i.e. elastic tendon properties) (Halper and Kjaer, 2014; Józsa and Kannus, 1997; Pins et al., 1997)

TENDON MECHANICS

Tendon function

The main function of tendons is to transmit the force exerted by the muscle to the bone and, therefore, allow the muscle to generate movements (Józsa and Kannus, 1997; Magnusson et al., 2003). Tendons have great tensile strength, due to the molecular and sub-molecular structure of collagen, that allows to transmit the muscle forces with minimal energy exchange and deformation (Józsa and Kannus, 1997; Nigg and Herzog, 1999). On the other hand, tendons are flexible due to their elastic fibre content and, therefore, rest length is recovered following loading-induced deformation (Elliott, 1965; Józsa and Kannus, 1997). It is this spring-like characteristic that allows for a dynamic mechanical interaction between the muscle and tendon (Magnusson et al., 2003). Furthermore, the flexibility of the tendon at their insertion and origin, enables an alignment of the tendon to the different directions of the acting muscles forces (e.g. at different joint angles) (O'Brien, 1992).

Mechanical properties

Normally, in everyday live, tendons are exposed to large tensile forces. When an external stretching force is applied to a tendon, the tendon length increases; when the force is removed, the tendon returns to its initial length (i.e. resting length). If the force exceeds a certain critical magnitude, the tendon elongation will increase up to a point at which the tendon will break.

The mechanical properties of tendons can be assessed by means of loading tests. *In vitro*, single tendinous fibres are constantly elongated, and the corresponding tensile force is recorded (Butler et al., 1978), whereas, *in vivo* measurements include a maximum voluntary muscle contraction on a dynamometer while the corresponding tendon elongation is visualized using an ultrasound apparatus (Fukashiro et al., 1995; Kubo et al., 1999).

The loading test paradigm allows to determine the relationship between tendon force and tendon strain (see Figure 1.15) and therefore to determine the tendon mechanical properties. Tendon structure and composition directly affect the force-strain relationship (Silver et al., 2003): at rest, a crimp pattern of the collagen fibres and fascicles is present, but this disappears following the application of tensile forces in correspondence to the straightening of the fibres (Elliott, 1965; Józsa and Kannus, 1997). Since the initial forces are accompanied by a pronounced tendon elongation, the primary part of the force-strain relationship is concave-shaped: it is termed toe region (Butler et al., 1978; Elliott, 1965). In the subsequent increase in tendon force, the tendon elongation shows a relatively linear response (Butler et al., 1978; Elliott, 1965). The slope of this linear region of the force-strain relationship is called "tendon stiffness" (Butler et al., 1978; Heinemeier and Kjaer, 2011). Until the end of this region, the tendon has the capability to fully recover to rest length when the load

is removed (i.e. reversible strain) (Józsa and Kannus, 1997). On the contrary, if the load is further increased, at the terminal part of the linear region, micro failure of single collagen fibres may occur; this is the so-called "yield region" on the force-elongation relationship where low force increments are accompanied by a massive elongation (Nigg and Herzog, 1999): fibre cross-links are detached until macroscopic failure takes place and the load-supporting ability of the tendon is lost leading to tendon rupture (Butler et al., 1978; O'Brien, 1992).

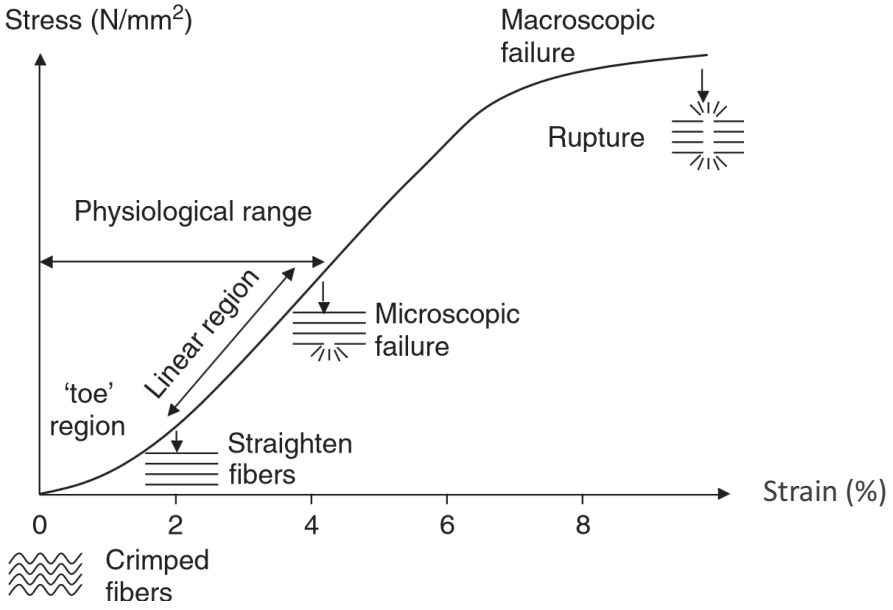

Figure 1. 15: Schematic stress-strain relationship of a tendon. (Wang, 2006).

The force-strain relationship is directly affected by the morphological properties of the tendon, such as cross-sectional area and rest length (Butler et al., 1978). Indeed, a thicker and/or shorter tendon accounts for a steeper slope of the force-elongation relationship, indicating less tendon elongation at a given tendon force and, thus, a higher tendon stiffness (Butler et al., 1978; Thompson and Czernuszka, 1995). To exclude confounding factors, the tendon force can be normalized to the tendon cross-sectional area (i.e. tendon stress) and the tendon elongation to the tendon resting length (i.e. tendon strain) (Butler et al., 1978; Heinemeier and Kjaer, 2011).

The resulting tendon stress-tendon strain relationship is quite similar in shape to the force-elongation curve, but independent of the individual tendon morphology (Butler et al., 1978). Therefore, the stress-strain relationship displays the actual material characteristics of the tendon. The linear slope of the stress-strain relationship is referred to as Young's modulus (or elastic modulus) and is the parameter most commonly utilized to describe the material properties of a tendon (Arampatzis et al., 2009; Butler et al., 1978; Heinemeier and Kjaer, 2011), where a high Young's

modulus indicates a relatively stiff tendon tissue (Heinemeier and Kjaer, 2011). For the stress - strain relationship the toe-region lies typically below 3% of tendon strain and the linear region extends to about 4-5% of tendon strain (Nigg and Herzog, 1999; Wang, 2006). When tested *in vitro*, macroscopic tendon failure was reported at strain-levels of 8-10% (O'Brien, 1992; Wang, 2006) whereas tests on whole tendons indicated that higher levels of strain might be tolerable (Józsa and Kannus, 1997).

Viscoelastic behaviour of tendons

Due to the content of collagen, elastin, water and the interactions between collagenous and non-collagenous proteins (e.g. proteoglycans), tendons feature viscous and elastic properties (Wang, 2006). The elastic component allows for a recovery of the rest length following loading-induced elongation and is a time-independent phenomenon, whereas the viscous component strongly depends on time and impedes the complete recovery of the rest length (Józsa and Kannus, 1997). Viscoelasticity accounts for several specific characteristics of tendons, like force-relaxation, creep and hysteresis (Butler et al., 1978; Józsa and Kannus, 1997; Nigg and Herzog, 1999).

As shown by Figure 1.16, stress (force) - relaxation indicates that the load, required to maintain a certain strain-level decreases over time. Creep, on the other hand, means that tendon length increases over time during a constant load application (Butler et al., 1978; Józsa and Kannus, 1997). Hysteresis, or elastic hysteresis, is the difference between the loading and unloading curves in the stress-strain cycle. Viscosity is also responsible for the sensitivity of tendons to different strain rates.

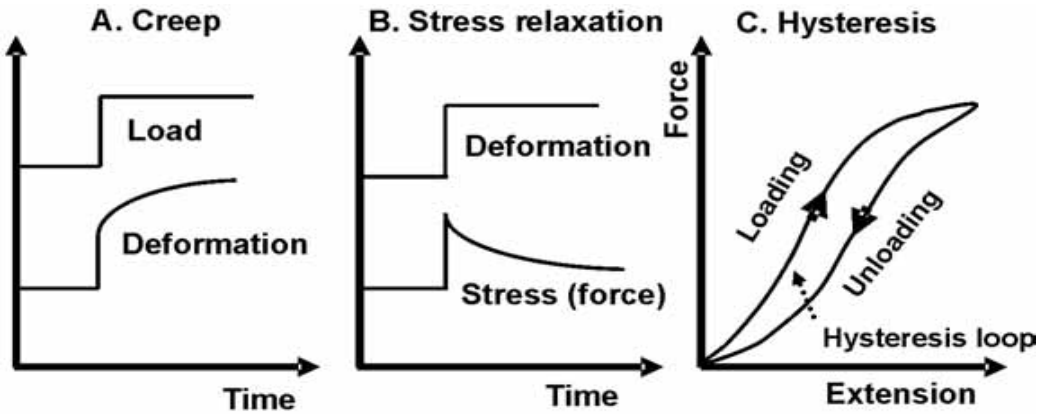

Figure 1. 16: main viscoelastic characteristic of tendos. Creep: under constant load the deformation increases; stress relaxation: under constant deformation the stress decreases; hysteresis: the force-deformation curves are different between loading and unloading periods. The "hysteresis loop" is representative of the energy loss, whereas the area under the loading phase represent the energy recoil. (Maganaris & Paul, 2000).

At lower strain rates the deformation of the tendon is higher: the tendon thus absorbs more strain energy but is less effective in transferring loads. With higher rates, the tendon elongates less

(higher stiffness) and the load transfer becomes more efficient (Józsa and Kannus, 1997; Alexander, 2000; Noyes et al., 1974; Wren et al., 2001). During a loading cycle, characterized by a stretch and recoil of the tendon, the resulting force-elongation curve forms a loop, indicating that a proportion of strain energy expended during elongation is not completely recovered when the load is removed (Butler et al., 1978; Nigg and Herzog, 1999). This phenomenon (tendon hysteresis) can be quantified by the area between the two curves that indeed indicates the energy that is dissipated (e.g. as heat). *In vitro*, the loss energy is reported to be low (i.e. 6-11%) indicating that most energy is recovered when the applied force is removed (Bennett et al., 1986; Ker, 1998) whereas *in vivo* measurements on human tendons reported higher hysteresis values; these discrepancies might be explained by the different methodological approaches used for tendon elongation measurement *in vitro* and *in vivo* (Lichtwark et al., 2013).

Effects of tendon elasticity on the F-L and F-V relationships

Muscle and tendon work as a unit within the musculoskeletal system, since the force generated by the muscle is transferred to the bone by the tendon. The non-rigidity of tendons considerably affects the performance capability of the corresponding muscle influencing its force-length and force-velocity relationships, as well as the storage and return of elastic strain energy during contraction and locomotion (Ettema et al., 1990; Fukunaga et al., 2002; Hof et al., 1983; Alexander, 2002).

The force generated by a muscle fibre, at a given level of muscle activation, is a function of fibre length and velocity, and is influenced by its "history", such as preceding shortening or stretch. If muscle fibres are considered together with their tendons, another important factor that affects force generation is the elasticity of the muscle-tendon unit; indeed, the force recorded at the ends of an isolated MTU is different from that generated by a single muscle fibre, due to the presence of series elastic elements (SEE) within the MTU (Figure 1.17). When muscles are contracted in a fixed joint position (isometric action), muscle fascicles shorten and the in-series elastic elements are stretched. The effect of the series elastic elements on the F-L relationship is described in Figure 1.17 (Gordon et al., 1966). The typical F-L relationship for an isolated sarcomere is reported on the left (panel A), whereas on the right (panel B), the sarcomere is considered as in series with elastic elements.

As shown in panel B of Figure 1.17, when a sarcomere is activated, the sarcomere ends will stretch the in-series elastic elements. In some conditions (e.g. the ascending limb of the F-L relationship), the elastic elements are not stretched and, thus, are not able to produce passive force; therefore, the amount of force (dashed line) will be lower than that of the same sarcomere activated (continuous line). On the contrary, if the initial length of passive sarcomere in-series with elastic elements is on the descending limb of the force-length relation, the elastic elements allow the

sarcomere to generate more force, due to the passive force generated by the elastic components. As a result of in-series elasticity, maximal isometric force will be attained at longer sarcomere lengths (e.g. Gordon et al., 1966).

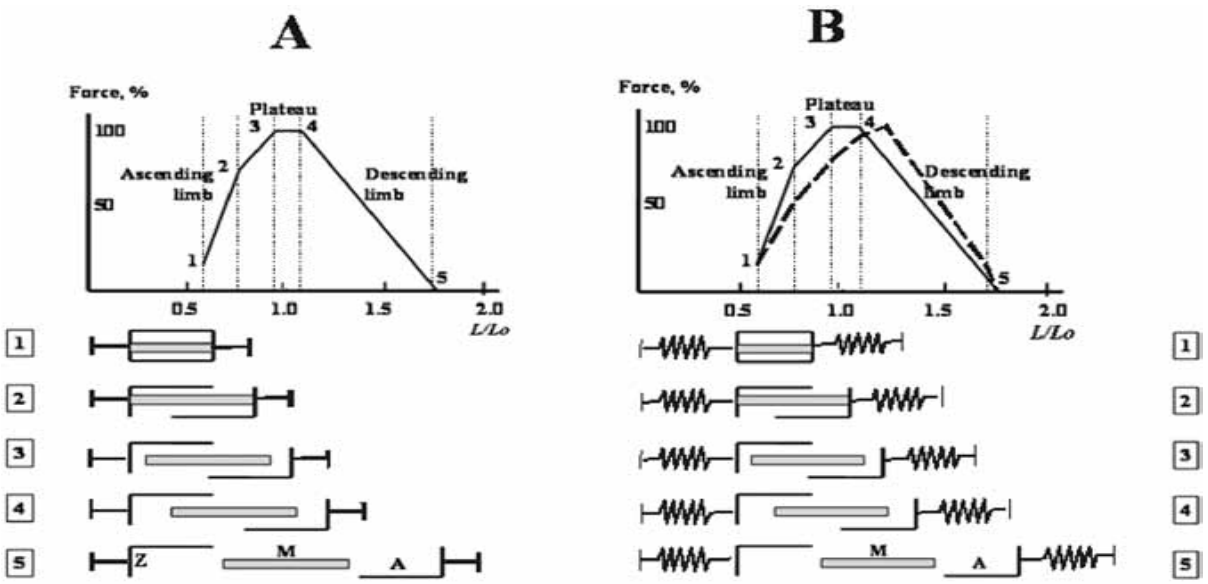

Figure 1. 17: F-L relationships for a sarcomere and relative positions of myosin (M) and Actin (A) in a sarcomere at specific sarcomere lengths: from 1 to 5. A: Classic F-L relationship for a sarcomere; B: F-L relationship taking into account the influences of the series elastic elements. (Gordon et al., 1966).

The effect of the SEE on force production essentially depends on the ratio between the tendon slack length and the optimal fibre length (Lt_{Slack}/L0). As a general rule, the longer the tendon compared with the muscle fibre length, the more the muscle fibre shortening and tendon stretch would occur during isometric muscle action. The Lt_{Slack}/L0 ratio of proximally located MTUs is lower than that of distal MTUs and this allows for a larger portion of muscle mass to be located closer to proximal joints, thus reducing the moments of inertia of the extremities. Relatively long tendons of the distal leg muscles are, moreover, advantageous for preventing excessive length changes of the relatively short muscle fibres, so they can operate close to their optimal length ranges and with low shortening velocities, thus maintain improved force production capabilities (Zajac, 1989; Wang, 2006, Muraoka et al., 2004).

Regarding the F-V relationship, the majority of the movements start slowly, with a relatively high force to begin the movement and then, as the limb accelerates, the velocity increases and the force that the muscle fibres can generate decreases. The decrement in force is, however, offset by the presence of the tendons. During the initial high-force phase of the contraction, the tendons become stretched and thus, as the movement begins, part of the overall shortening of the MTU is taken up by the tendons. Thus, the "external velocity" of a limb is not mediated by the muscle alone, but by the

combination of muscle and tendon displacement. As a consequence, the fibres are moving at a slower speed and have the possibility to generate higher force, than that they would generate without tendon (Bohm et al., 2018; Roberts et al., 1997).

The overall effect that tendons have on the force-velocity profile of muscle is to avoid the higher velocity of the muscle fibres. In the case of shortening, this increases the force and power that can be generated for any given velocity of shortening; indeed, the velocity of contraction would be the same and the muscle fibre could operate in a more isometric way and with a higher force potential (Roberts et al., 1997).

Summary

The F-V and F-L relationships have an important role in determining the muscle's mechanical output. In addition, the geometrical characteristics of muscles, such as fibre length, pennation angle and PCSA influence the force and/or the velocity of contraction while the morphological characteristics of tendons play an important role in the transmission of force from muscle to bone. Muscle and tendon work as a unit within the musculoskeletal system, and the non-rigidity of tendons considerably affects the performance capability of the corresponding muscle influencing its force-length and force-velocity relationships, as well as the storage and return of elastic strain energy during contraction and locomotion.

MECHANICS AND ENERGETICS OF RUNNING AT STEADY AND NON-STEADY SPEED

MECHANICS AND ENERGETICS OF LEGGED LOCOMOTION: GENERAL CONCEPTS

The human body can be considered as a biological machine that utilizes chemical energy to generate mechanical work. As pointed out by Rodolfo Margaria: "the study of locomotion first requires the determination of the energy cost of this exercise and secondly a detailed analysis of the mechanical work performed" (Margaria, 1976). To evaluate human locomotion, besides energy cost and mechanical work, a third parameter is generally determined: mechanical efficiency, that represents the relationship between these two.

Energy cost (cost of transport)

When human muscles contract to perform a given amount of work (e.g. to sustain locomotion) they consume a given amount of metabolic energy. Measuring the oxygen consumed in this process ($\dot{V}O_2$, $mL \cdot min^{-1}$) provides a good indication of the metabolic energy consumed, in the unit of time, at the muscle level. In human (and animal) locomotion it is, however, customary to express the metabolic energy consumed not as a function of time but as a function of distance covered. Measuring the energy expended to transport the body over a given distance is a way to investigate the economy of a locomotion mode in analogy to the liters of fuel consumed by a car to cover one kilometre, which is indeed a way to define a car's economy. Thus, the lower the cost of transport (and the higher the economy) the better.

The net cost of transport (C_{net}: the metabolic energy expended per unit distance) is defined as the net energy needed for moving a kilogram of body mass for a distance of one metre and is generally expressed in $J \cdot kg^{-1} \cdot m^{-1}$. When the exercise is based on aerobic energy sources (e.g. submaximal exercise at steady state), C_{net} can be calculated as the ratio of net oxygen uptake to the speed of progression:

$$C_{net} = \frac{(\dot{V}O_{2ex} - \dot{V}O_{2bas})}{v}$$

where $\dot{V}O_{2ex}$ is oxygen uptake during exercise (at steady state: $ml \cdot kg^{-1} \cdot min^{-1}$), $\dot{V}O_{2bas}$ is oxygen uptake at rest ($ml \cdot kg^{-1} \cdot min^{-1}$) and v is the speed ($m \cdot min^{-1}$); C_{net} thus results expressed in $ml \cdot kg^{-1} \cdot m^{-1}$. In order to express C_{net} in $J \cdot kg^{-1} \cdot m^{-1}$ the energetic equivalent of oxygen should be taken into account (e.g. in

the human body about 21 kJ of energy become available for every liter of oxygen consumed; this value depends on the respiratory exchange ratio, that should thus also be measured, along with $\dot{V}O_2$).

The energy cost is thus a parameter useful to compare individuals with different sizes, moving at different speeds and using different gaits/locomotion modes.

Mechanical work

Human locomotion is a complex action, involving the activation and coordination of many muscles exerting force via tendons and producing the movement of bones and body segments. Despite this, each gait can be described by a simple "paradigm" (e.g. a basic physical model) that helps in understanding the overall mechanics of locomotion, describing the trajectory of the body centre of mass (BCoM) and its energies time course; more specifically, each paradigm describes, for each gait, the interplay among the three fundamental energies associated with the BCoM: potential, kinetic and elastic energy. Walking has been classically described by the inverted pendulum paradigm (Margaria 1976) where potential and kinetic energy change in opposition of phase during the stride (and this allows for some exchange of energy between these two). Running has been classically described by the bouncing ball/pogo stick paradigm (Margaria 1976) where potential and kinetic energy change in phase during the stride (and no energy exchange occurs between these energies during ground contact).

The mechanical energy changes (i.e. the mechanical work) required to maintain overall motion are, ultimately, the effect of muscle action and, indeed, they affect metabolic energy expenditure (e.g. Fenn 1930). Total mechanical work (W_{tot}, $J \cdot kg^{-1} \cdot m^{-1}$) can be calculated, according to the König theorem, as the sum of external work (the work done to accelerate, decelerate and rise the BCoM; W_{ext}, ($J \cdot kg^{-1} \cdot m^{-1}$) and internal work (the work done to accelerate and decelerate limbs respect to BCoM; W_{int} ($J \cdot kg^{-1} \cdot m^{-1}$) (Cavagna e Kaneko 1977).

More specifically, W_{ext} can be calculated analysing the time course of the BCoM total energy (E_{tot}) during the stride, which is the sum of potential energy (EP) and 3D kinetic energies (EK) (progression, kx; medio-lateral, ky and vertical, kz):

$$E_{tot} = mgh + \frac{1}{2}\left(mv_x^2 + mv_y^2 + mv_z^2\right)$$

where m is the subject's body mass (kg), g is the acceleration of gravity (9.81 $m \cdot s^{-2}$), h and v are the vertical position (m) and the velocity of the BCoM ($m \cdot s^{-1}$). The sum of the increments in E_{tot} during a stride is taken as a measure of the external positive work (W_{ext}^{+}) whereas the sum of the decrements

in E_{tot} is taken as the external negative work (W_{ext}^{-}) (Cavagna & Margaria 1966, Cavagna et al. 1976).

The sum of the increments of kinetic and rotational energy of the limbs in respect to BCoM constitutes the internal work (W_{int}) (Cavagna & Kaneko 1977, Minetti 1998b):

$$Wint = \sum_{i=1}^{n} \left[\frac{1}{2}(m_i v_i^2) + \frac{1}{2}(m_i w_i^2 k_i^2) \right]$$

where i are the body segments (this number depends on the kinematic model adopted), v is the limb's speed relative to BCoM ($m \cdot s^{-1}$), k is the limb's radius of gyration (m) and w is the angular velocity of the segment ($rad \cdot s^{-1}$) (Cavagna & Kaneko 1977, Minetti 1998b; Minetti et al., 1993).

Finally, the recovery is a parameter that was introduced by Cavagna and colleagues (1976) to quantify the energy exchange in the forms locomotion that resemble a pendulum-like motion (such as walking). When a pendulum oscillates it exchanges potential to kinetic energy and without friction it will oscillate forever. Recovery (%) is the percentage of energy that can be saved by exploiting this pendulum-like motion and is calculated by computing the horizontal and vertical components of mechanical work (Wf and Wv):

$$Recovery = \frac{(Wf + Wv) - Wext}{(Wf + Wv)}$$

In walking, recovery could be at most 60-70% (in correspondence to the self-selected speed, where the energy cost reaches its minimum) whereas in running energy recovery is about nil (in this case indeed, no exchange between potential and kinetic energy takes place).

Mechanical Efficiency

Mechanical efficiency (at the whole body level) can be calculated from the ratio of total mechanical work (W_{tot}) to net energy cost (both expressed in $J \cdot kg^{-1} \cdot m^{-1}$): it represents the capability to convert metabolic energy into mechanical work:

$$Eff = \frac{W_{tot}}{C_{net}}$$

As calculated, mechanical efficiency approximates "pure" muscle efficiency values (about 0.25-0.30, as reported by Woledge et al. 1985) in the forms of locomotion where elastic recoil is negligible (e.g.

cycling, as reported by Minetti et al. 2001) whereas in the case of running the efficiency calculated in this manner can reach far larger values (e.g. up to 0.5-0.7 as reported by Cavagna and Kaneko (1977) in human running at steady speeds).

ENERGETICS AND MECHANICS OF RUNNING AT STEADY SPEED

Energetics of running (on the level)

$\dot{V}O_2$ increases as a function of speed both in walking and running (at steady speed), moreover, as indicated in Figure 1.18 (panel A): 1) walking above a speed of ~2.0 $m \cdot s^{-1}$ is energetically expensive, exceeding the $\dot{V}O_2$ required for running at a similar speed; 2) the slope of the walking curve (for speeds larger than ~ 2.0 $m \cdot s^{-1}$) is steeper than the slope of the running curve indicating a greater demand for oxidative metabolism in the latter case; and 3) at speeds slower than ~2.0 $m \cdot s^{-1}$, walking is less expensive than running; thus: 4) a transition from walking to running occurs at ~ 2.0 $m \cdot s^{-1}$ to minimize metabolic energy demands (Mercier et al., 1994; Saibene & Minetti, 2003; Margaria, 1976).

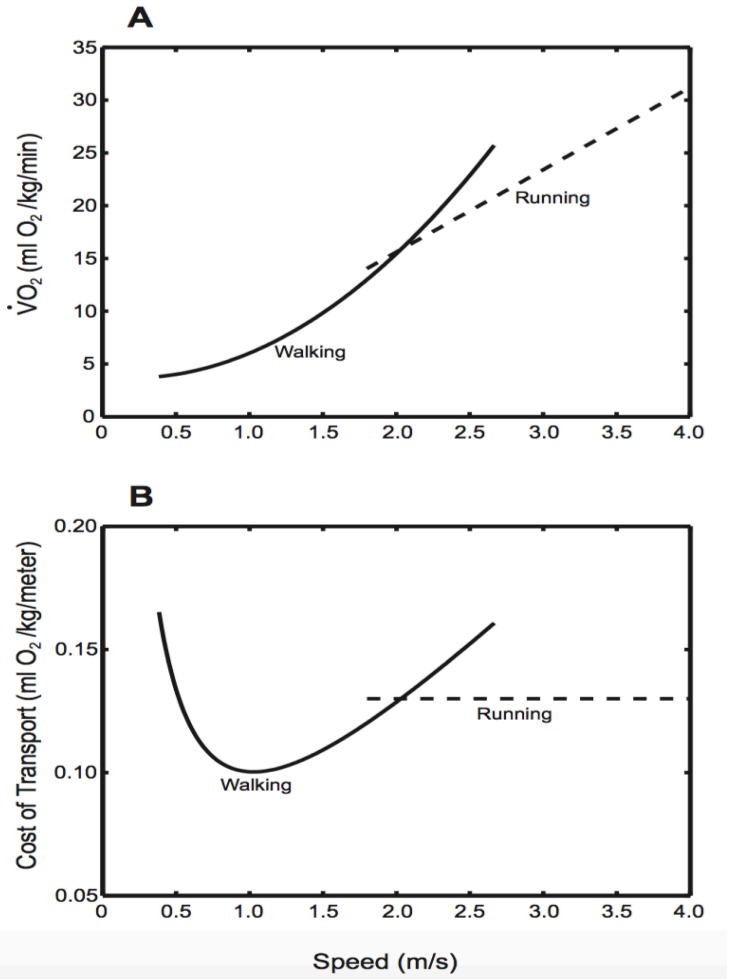

Figure 1. 18: oxygen uptake (A) and energy cost of locomotion (B) during walking and running at different speeds. The metabolic energy consumed in the unit of time (oxygen uptake) increases linearly with running speed whereas the (net) energy cost of running is almost independent of the speed and amounts to about 4 $J \cdot kg^{-1} \cdot m^{-1}$. (Margaria et al.,1963).

The relationship between the (net) cost of transport and speed depicts a U-shaped curve for walking with a minimum at ~1.1 $m \cdot s^{-1}$ (Figure 1.1, panel B); when humans are asked to walk at their freely chosen speed, they indeed walk at a speed (~1.0-1.3 $m \cdot s^{-1}$) that nearly minimizes the cost of transport (e.g. ~ 2 $J \cdot kg^{-1} \cdot m^{-1}$). The (net) cost of transport for running is, on the contrary almost independent of speed and amounts to ~ 4 $J \cdot kg^{-1} \cdot m^{-1}$ (Margaria, 1976; Margaria et al., 1963).

Mechanics of running (on the level)

From a biomechanical point of view, running is a progression of steps with an aerial phase between each ground contact, and a with a duty factor (i.e. the fraction of the stride duration at which each foot is on the ground, expressed in percentage of the stride) smaller than 0.5. This form of locomotion has been classically described by a bouncing ball model (Margaria 1976) and later refined as a spring mass model (Blickhan 1989, McGeer, 1990a; McMahon and Cheng, 1990) where the body is modelled as a point mass on the top of a spring (Figure 1.19).

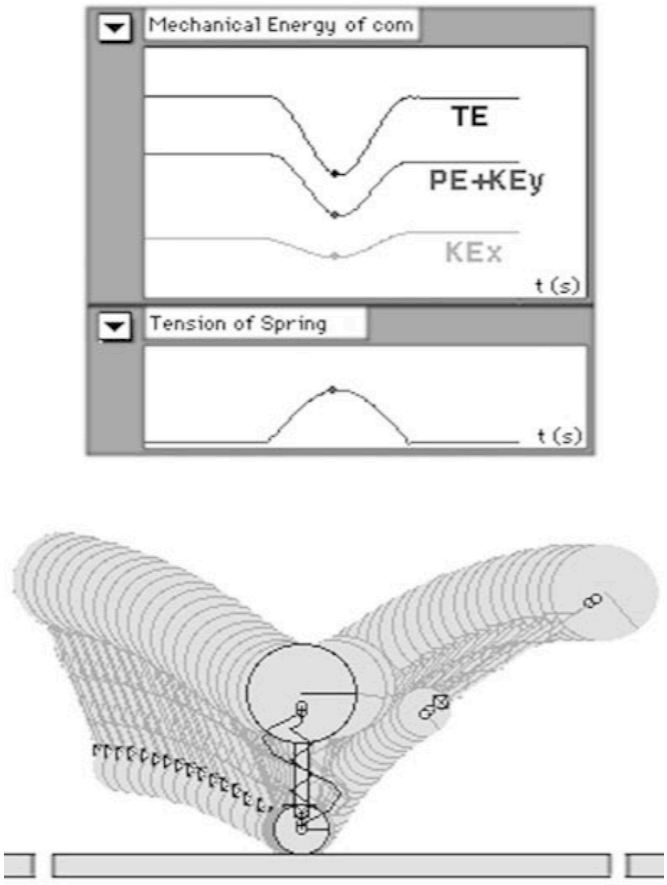

Figure 1. 19: Schematic representation of running mechanics. Upper figure: the time course of potential, kinetic and total energy during a running stride, the tension of the spring is also reported. Lower figure: the spring mass model. (Saibene & Minetti, 2003).

Both models well describe the essential "mechanical" characteristics of running: 1) potential and kinetic energies are in phase (and there is no exchange between them); 2) during ground contact part of the total energy is stored on the stretching elastic elements.

As far as the spring-mass model is regarded, the spring behaviour of the leg is attributed to the elastic stretch and recoil of muscles, tendons, and ligaments (Alexander, 1984; Ker et al., 1987). The energy released by the linear leg spring during the second part of the stance phase provides the mechanical energy for the acceleration of the body in the upward and forward direction. As shown in Figure 1.20, the vertical displacement of the BCoM (Δy) represents the amount of compression of the spring. During the first half of stance, the linear spring is compressed and elastic energy (EE) is stored within the spring. During the second half of stance, the linear leg spring recoils and releases the EE, which is converted back into kinetic and potential energy.

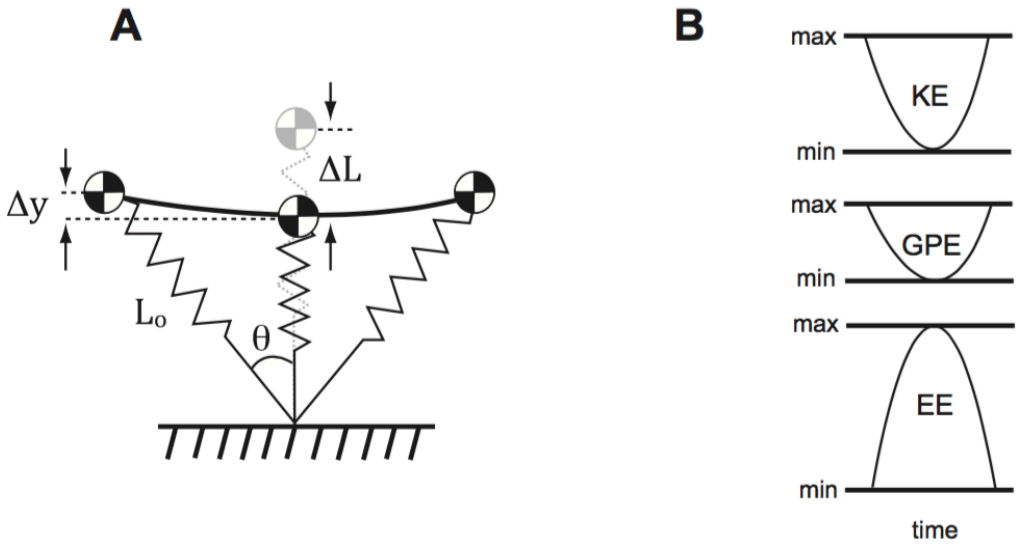

Figure 1. 20: (A) Spring-mass model of human running. The model consists of a mass and a single leg spring. This figure shows the model at the beginning of the stance phase (left most position), at the middle (leg spring is oriented vertically) and at the end of the stance phase (right most position). The vertical displacement of the BCoM represent the amount of compression of the spring. (B) This figure illustrates the fluctuations in the kinetic energy (KE), gravitational potential energy (GPE) and elastic energy (EE). During the first half of stance, the KE and GPE of the COM compress the linear leg spring and elastic energy (EE) is stored within the spring. During the second half of stance, the linear leg spring recoils and releases the EE, which is converted back into KE and GPE. (Farley & Gonzalez, 1996).

Despite the simplicity of the spring-mass model of human running, this analogy presents a paradox since this model assumes that the linear spring is perfectly elastic, meaning that the same amount of mechanical energy is stored and returned during the stance phase of running (and thus that muscle work is not necessary to sustain locomotion). Even if this is clearly not the case, these elastic mechanisms are expected to greatly reduce the energy cost of running in humans and other animals, as well as to affect mechanical work production (Alexander, 1984; Cavagna et al., 1977; Cavagna et al., 1964).

During the contact phase of running muscles perform negative and positive work (and thus consume a given amount of energy): during the first half of the stance, negative work is necessary to decelerate and lower the BCoM, whereas during the second half of the stance, positive work is required to lift and accelerate the BCoM (Cavagna et al. 1976); when negative work is performed the muscles are lengthening, whereas during the propulsion phase the muscle are shortening and produce positive work. This positive work is the external work (W_{ext}) that can be calculated as described above based on the increments in potential and kinetic energy associated to the BCoM.

As shown in Figure 1.21, W_{ext} does not change appreciably as a function of speed (eventually it slightly decreases) whereas W_{int} and W_{tot} are larger the higher the speed. Since the energy expended to cover a given distance (e.g. the energy cost) does not change as a function of speed, locomotion efficiency (calculated from the ratio of W_{tot}/C_{net}) is bound to increase as running speed increases. This suggests that positive work in running derives mainly from the passive recoil of the series elastic elements of the muscle-tendon units.

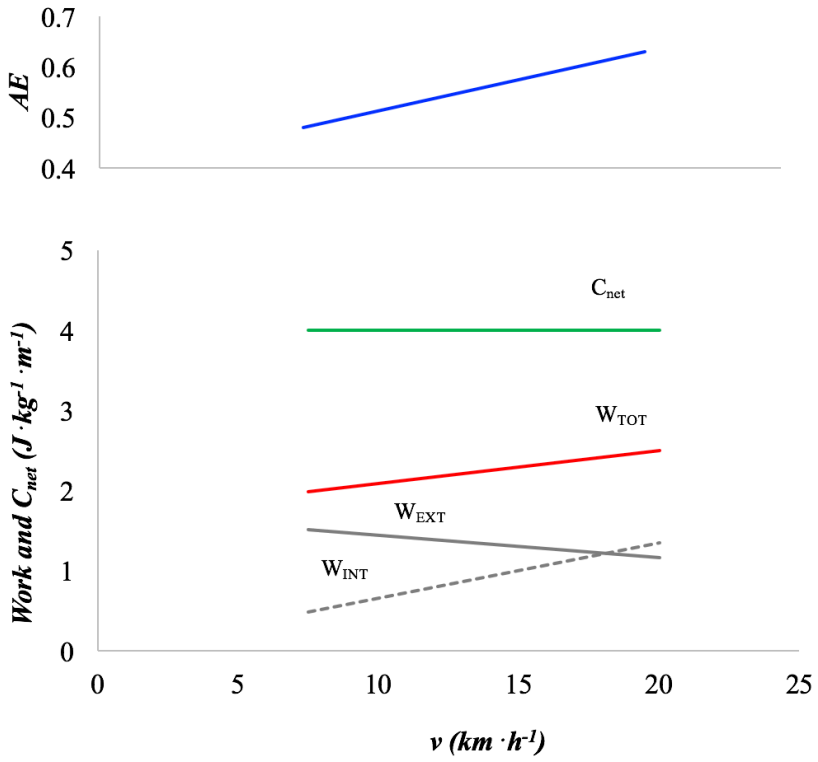

Figure 1. 21: the total mechanical work done per unit distance(Wtot) increases as a function of speed whereas the energy cost of running (Cnet) does not show appreciable changes when the velocity increases so that "apparent efficiency"(AE) increases linearly with speed. (Adapted from Cavagna and Kaneko, 1977).

"Apparent" efficiency

Running efficiency increases as a function of running speed from about 0.45 at 10 $km \cdot h^{-1}$ to about 0.65 at 20 $km \cdot h^{-1}$ (Cavagna et al., 1977; Cavagna & Kaneko, 1977). These values of efficiency exceed the values that could be measured at the muscle level, that are at most of 0.25-0.30 (Woledge et al., 1985). Traditionally, this is explained by considering that tendons and other elastic elements (in series and in parallel with the contractile elements) can store and then release elastic energy during stretch-shortening cycles and this can be considered an "energy saving" mechanism (Alexander 1991; Biewener and Roberts 2000). It has, indeed, been suggested that tendons contribute proportionally more positive work as running speed increases, thus allowing the muscle fibres to operate more efficiently than would be the case if tendon elastic strain energy were not utilized (Alexander, 1988; Alexander, 2002; Roberts, 2002; Biewener, 2003). However, the role of the re-utilisation of elastic energy, as well as the impact of muscle-tendon behaviour on the "apparent efficiency" of locomotion is still not completely understood.

ENERGETICS AND MECHANICS OF RUNNING AT NON-STEADY SPEED

Energetics of non-steady running: sprints and shuttles

Non-steady walking or running, in terms of non-linear trajectory or with speed changes, is a common occurrence in daily life, as well as in many sport activities (e.g. team sports). The mechanics and energetics of walking and running in these conditions are far less known than during steady conditions (e.g. constant speed linear running such as, as an example, when running on a treadmill).

The energetics and mechanics of walking and running at oscillating speeds were investigated by Minetti et al. (2001; 2013) but in these studies only the effects of small accelerations or decelerations about an average speed were investigated. The energy expenditure during locomotion tasks with relevant speed changes (e.g. with large accelerations or decelerations, such as sprints and shuttles) is less known because oxygen uptake does not reach a steady state and thus cannot be easily determined.

Shuttles

In 2011, Zadro and coworkers proposed a method to assess the energy cost of un-steady locomotion (shuttle runs) based on considerations about the energetics of intermittent exercise put forward by Margaria and coworkers in 1969. Shuttle runs are indeed a good model of unsteady locomotion because a rapid acceleration phase is followed by a deceleration phase and by a change of direction. In following studies Zamparo et al. (2014, 2015, 2016) applied this method to investigate the

energetics of shuttle runs covered at different speeds, over different distances and with different changes of direction. With this method bouts of exercise (e.g. shuttle runs) are separated by 30 s of recovery (that corresponds approximately to half time of the alactic oxygen deficit payment, as reported by Margaria et al. 1969) and repeated a number of times as to reach 5-6 min of total exercise duration. As shown by Figure 1.22 a sort of steady state is obtained after the first minutes of exercise so that oxygen uptake can be measured as the average of the last minutes of exercise. By taking into account the contribution of the lactic energy sources (blood lactate accumulation at the end of exercise) the total metabolic energy expended could be estimated and the energy cost can be finally calculated.

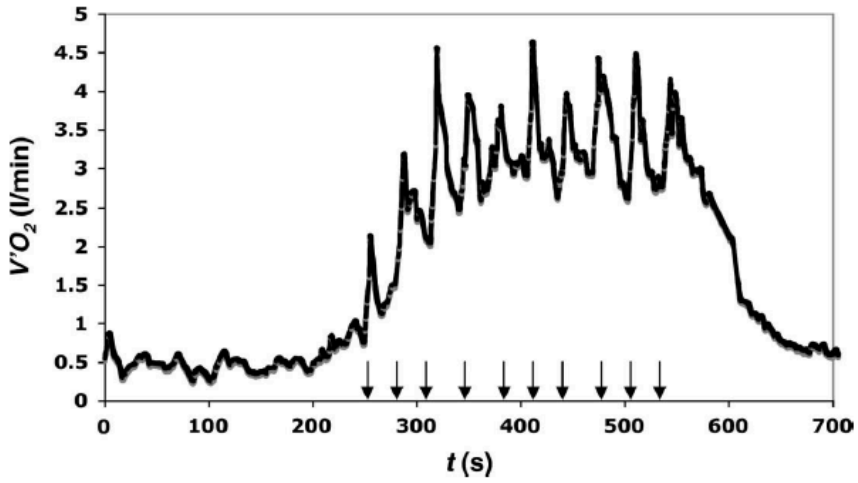

Figure 1. 22: oxygen uptake as a function of time during 10 shuttle runs (arrows) with 30 seconds of recovery in between. Oxygen consumption increases sharply after each bout of exercise to further decrease in the following 30 s of recover; after the first minutes of exercise, however, oxygen uptake reaches a sort of steady state. (Zadro et al., 2011).

Other authors investigated the energy demands of shuttle running by using different methods (Buglione and di Prampero 2013, Stevens et al. 2015, Zago et al. 2018) and obtained similar results than those reported by Zadro (2011) and Zamparo (2015, 2016) at comparable shuttle distances and shuttle speeds. Buglione and di Prampero (2013) used a mixed approach to obtain the energy expenditure of (intermittent) shuttle running, combining aerobic measurements with anaerobic alactic and lactic energy measurements whereas Stevens et al. (2015) and Zago et al. (2018) measured energy expenditure during continuous exercise (shuttle runs performed one after the other without recovery in between).

These studies have shown that the energy cost of shuttle running is far larger than that of constant speed, linear running; shuttle running indeed implies a significant increase in energy expenditure because of the accelerations and decelerations phases, as well as because of the changes of direction (Zamparo et al., 2014; 2015, 2016; Buglione and di Prampero, 2013, Stevens et al., 2015).

The difference between the energy demands of shuttle running and constant speed linear running increases as a function of shuttle speed but decreases as a function of shuttle distance: over the longer shuttle distances, the net energy cost approximates that of linear, constant speed, running especially when the shuttle speed is low (Figure 1.23). In these conditions indeed a relatively larger fraction of the shuttle distance is covered by running at relatively constant speed whereas the distance covered while accelerating, decelerating and changing direction represents only a small fraction of the total distance.

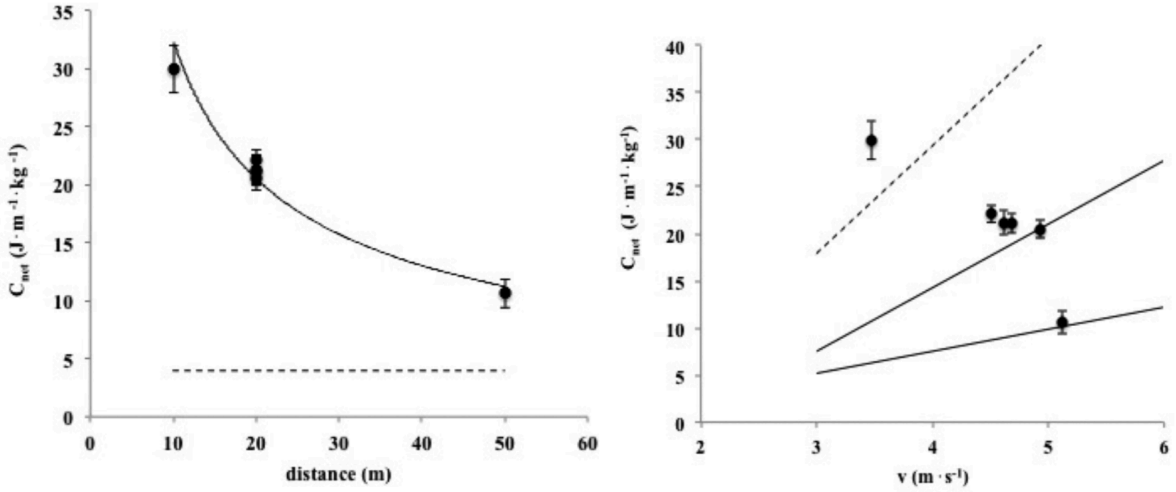

Figure 1. 23: Net energy cost of shuttle running as a function of the distance covered (left panel). The dashed line represents the energy cost of linear-constant-speed running as measured in the same subjects. On the right panel the net energy cost of shuttle runs is reported as a function of shuttle speed. The continuous lines represent the C-v relationship as determined by Buglione and di Prampero (2013) over the 20-m (lower line) and 10-m (upper line) distances, whereas the dotted line represents the C-v relationship determined over the 5-m distance by Zamparo et al., (2014). (Zamparo et al., 2015)

Sprints

The acceleration phase of a sprint is expected to be associated with a higher metabolic cost compared to running at the same (constant) average speed, as is the case for shuttle running. However, no studies are reported in the literature about this topic, essentially because of the difficulty of separating the acceleration phase from a (necessary and following) deceleration phase. A way to estimate the energy demands of sprint running was proposed by di Prampero and coworkers in 2005 and is based on the concept of 'equivalent slope'. These calculations allow to infer the metabolic cost of transport of level accelerated running (with constant acceleration) by considering it an analogue of running uphill at a constant speed, a condition in which the energy cost (C) as a function of the slope is known (e.g. Margaria 1938, Minetti et al. 1994, Minetti et al., 2002).

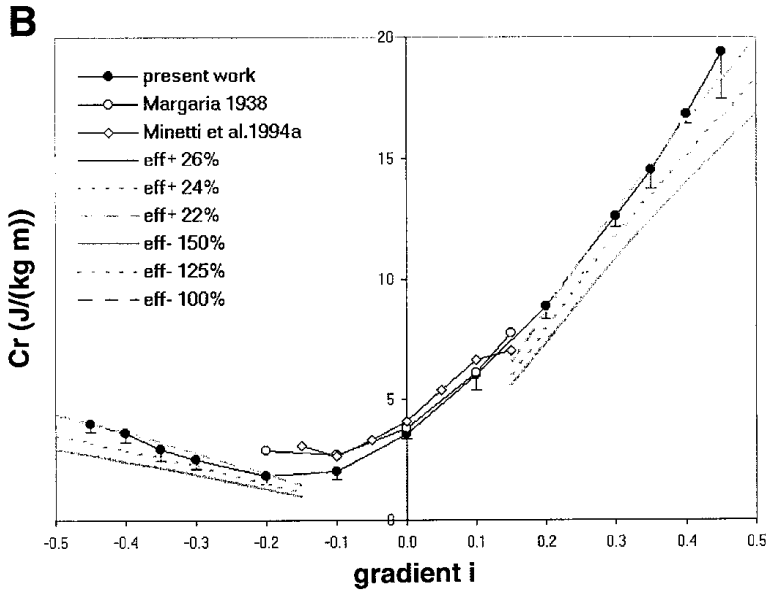

Figure 1. 24: energy cost of running as a function of gradient(full dots: data reported by Minetti et al. 2002; empty circles: data reported by Margaria 1938 and Minetti et al. 1994). The dotted lines represent values of efficiency for positive work (at positive slopes: 0.22-0.26) and negative work (at negative slopes: 1-1.5) (Minetti et al. 2002).

As proposed by Minetti et al. (2002) the relationship between C and the gradient (Figure 1.24) is well described by the following equation:

$$C = 155.4i^5 - 30.4i^4 - 43.3i^3 + 46.3i^2 + 19.5i + 3.6$$

where i is the (downhill: negative, uphill: positive) gradient (e.g. incline).

As proposed by di Prampero and coworkers (2005) i corresponds to the angle between the ground and the runner (see Figure 1.25) so that C, in sprint running could be calculated as:

$$C = (aES^5 - bES^4 - cES^3 + dES^2 + eES + 4.4)\,EM$$

where ES is the equivalent slope (a_f/g) and EM is the equivalent mass ($(a_f^2+g^2)^{0.5}/g$); thus, C can be estimated by knowing g (the acceleration of gravity) and a_f (the forward acceleration, a parameter that can be quite easily obtained from GPS data).

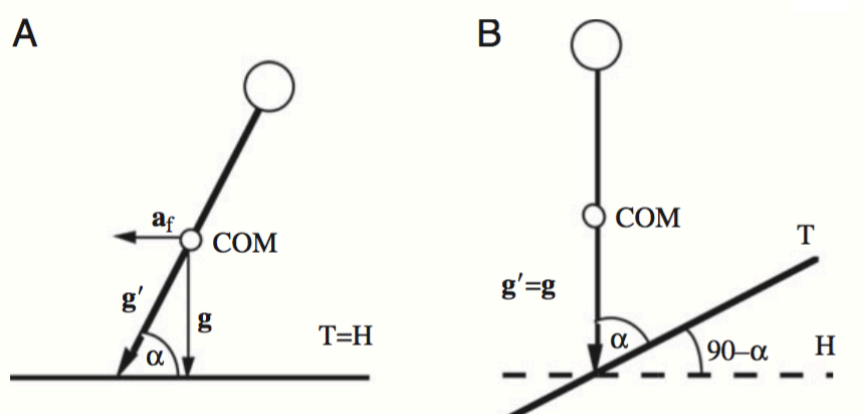

*Figure 1. 25: Simplified view of the forces acting on a runner. The subject is accelerating forward while running on flat terrain (A) or running uphill at constant speed (B); **af**=forward acceleration; **g**=acceleration of gravity; T=terrain; H=horizontal; α (=arctan **g**/**af**) is the angle between runner's body and T; the angle between T and H is α′=90–α. The equivalent slope refers to the angle between T and H (ES = 90- α). (di Prampero et al., 2005).*

The equation proposed by di Prampero et al. (2005) can be considered valid only within −0.45 < i < +0.45 (i.e. the gradient range of the metabolic experiments in the study of Minetti et al. 2002). Since the values of equivalent slope in maximal sprints fairly exceed these values, this model was mainly applied to analyse team sport data rather than to investigate the energetics of "pure maximal sprints".

More recently, Minetti & Pavei (2018), revisited the method proposed by di Prampero et al. (2005) based on data published by Giovanelli et al. (2016) on the energy cost of uphill running up to slopes of +0.84; with this new model is possible to predict the energy cost of sprint running with accelerations larger than 8 $m \cdot s^{-2}$:

$$C = 0.102 \cdot \sqrt{(af^2 + 96.2)} \cdot (4.03 \cdot af + 3.6e^{-0.408 \cdot af})$$

The equation proposed by Minetti & Pavei (2018), requires only the determination of the forward acceleration however, as in the case of the equation of di Prampero et al. (2005), it is not yet validated against direct measurements of energy cost.

Mechanics of non-steady running: sprints and shuttles

Whereas on flat terrain (and at constant speed) positive (W^+, concentric) and negative (W^-, eccentric) work ought to be the same (e.g. Cavagna & Kaneko, 1977), $W^+ > W^-$ when on a positive slope and $W^- > W^+$ when on a negative slope. As discussed by Minetti et al. (2002) the efficiency of uphill locomotion at very high slopes ought to be equal to that of "pure" concentric (positive) work (eff^+) whereas downhill, efficiency ought to become closer to that of "pure" negative work (eff^-). Since sprints and shuttles are characterized by accelerations and decelerations (and since these are

analogous to running on a positive or negative slope), when investigating the mechanics (as well as the efficiency) of unsteady locomotion is important to calculate both W^+ and W^- (and hence both eff^+ and eff^-). Moreover, quantifying the mechanics of non-steady locomotion with the "gold standard" methods requires expensive equipment, such as several force plates and/or a very larger number of cameras (to perform a 3D kinematic analysis. This because the entire movement should be recorded, whereas in constant-speed linear running is sufficient to analyse few steps (at constant speed) and the use of a treadmill largely favours the acquisition of these data.

Whereas, the energetics of shuttle running are known from (recent) literature, the mechanics of shuttle running are less known. The reverse is true for sprints were more is known about the mechanics than the energetics; in this latter case, however, data are reported for horizontal power only, a parameter that can be estimated by means of a simple 2D kinematic analysis.

Shuttles

Zamparo and co-workers (2016), using a motion capture system with 8 cameras were able to calculate the mechanical work generated during a shuttle over a (short) distance of 5+5 m. Data reported in that study indicate that external, internal the total mechanical work increase as a function of shuttle speed and reach values far larger than those reported during steady-state running at the same average running speed (compare data reported in Figures 1.21 and 1.26). These data furthermore show that internal work is a larger fraction of total mechanical work and could thus not be neglected.

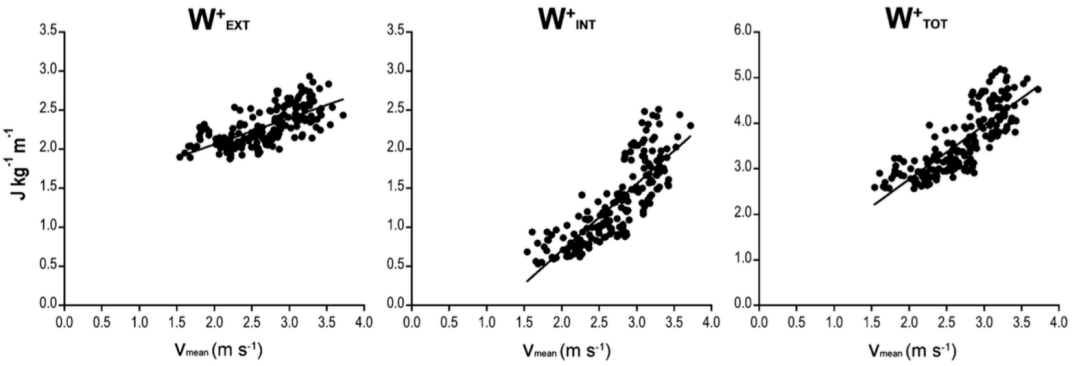

Figure 1. 26: external, internal and total (positive) mechanical work as a function of mean shuttle velocity over a 5+5 m distance (Zamparo et al., 2016).

An increase in (external) mechanical work with increasing speed during shuttle runs over the 5+5 m distance was also reported by Zago et al. (2018) but no studies analysed so far these matters on shuttle-runs over longer distances; to cover this gap is one of the aims of this thesis.

Sprints

The first paper that investigated the sprint running acceleration phase was published by Fenn in 1930 with the aim to quantify maximal power output in humans. Later on, Cavagna et al. (1971) partitioned the (external) mechanical work into its forward and vertical components to better describe the mechanical demands of sprint running. In his paper of 1971, however, Cavagna did not investigate the internal work and therefore, up to now, no data of total mechanical work are reported in the literature for the sprint running acceleration phase. As indicated above, internal work is an important component of total mechanical work in non-steady locomotion (shuttles) and thus, it is supposed to be important also in sprint running.

But for the paper of Cavagna et al. (1971) most of the methods used in the literature to investigate mechanical work in sprints stem for the paper of Samozino et al. (2015); these authors proposed a simple 2D kinematic analysis to calculate (only) the forward component of mechanical power output. Even so, this method provides a good basis for understanding the magnitude of power that need to be generated in sprinting. As proposed by these and other authors (e.g Chelly & Denis, 2001; di Prampero et al., 2005) data of horizontal running velocity can be fitted with a mono-exponential function:

$$v(t) = vmax \cdot (1 - e^{-t/\tau})$$

where v is the modelled running velocity, v_{max} the maximal velocity reached in the sprint and τ the time constant of the v vs. t relationship. The instantaneous forward acceleration and the running distance can then be calculated from the first derivative and integral respectively; force (F) and mechanical power (P) are then calculated as:

$$F = ((vmax - vmax \cdot (1 - e^{-t/\tau}))/\tau) \cdot m$$
$$P = (((vmax - vmax \cdot (1 - e^{-t/\tau}))/\tau) \cdot m) \cdot (vmax \cdot (1 - e^{-t/\tau}))$$

were m is the body mass of subject. With this method, the horizontal (forward) component of force and power are calculated (Figure 1.27). Vertical force can then be calculated as the product of body mass times the acceleration of gravity (mg).

Using this method, Slawinski et al. (2017) observed that (horizontal) power increases during the first second of a sprint and decreases thereafter and that maximal power output easily exceeds 2000 W in elite male runners. Large correlations were observed between maximal power output and sprint performance (running time/speed) but the strength of these correlations diminishes in

homogenous subsets of elite sprinters or when the analysed distance increases (Slawinski et al. 2017; Rabita et al., 2016).

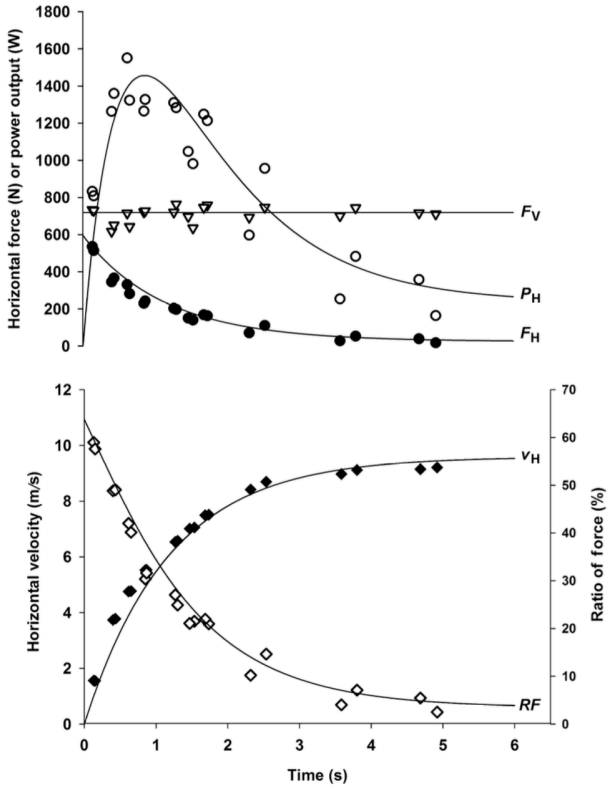

Figure 1. 27: horizontal velocity (vh), horizontal force (Fh), vertical force (Fv) and horizontal power output (Ph) during the sprint acceleration phase a function of time. (Samozino et al., 2015).

All these recent studies are based on the determination of external, horizontal, power only; since they do not take into consideration the vertical component of it, (or the internal power) in all these studies total power output is likely underestimated. To provide a comprehensive description of the work and power output in the sprint running acceleration phase, was another aim of this thesis.

"Apparent" mechanical efficiency of non-steady running: sprints and shuttles

Sprints

Since no data are reported in the literature about the energetics of sprint running and since also data of (total) mechanical power output are lacking for this motor task, no data of efficiency during sprint running are available either. Some estimates of sprint running efficiency were provided by Minetti & Pavei (2019) who suggested that (apparent) mechanical efficiency of (positive) work can reach maximal values of 0.80 when running on the level (equivalent slope = 0), as observed during (constant speed linear) running at maximal speeds (> 20 $km \cdot h^{-1}$) by Cavagna & Kaneko (1977). When the equivalent slope increases (e.g. when the runner accelerates), apparent efficiency decreases: an

efficiency of 0.25 is expected at (positive) equivalent slopes larger than 0.35 after which efficiency would not change with further increases in slope since only positive work is performed in these conditions (see Figure 1.28).

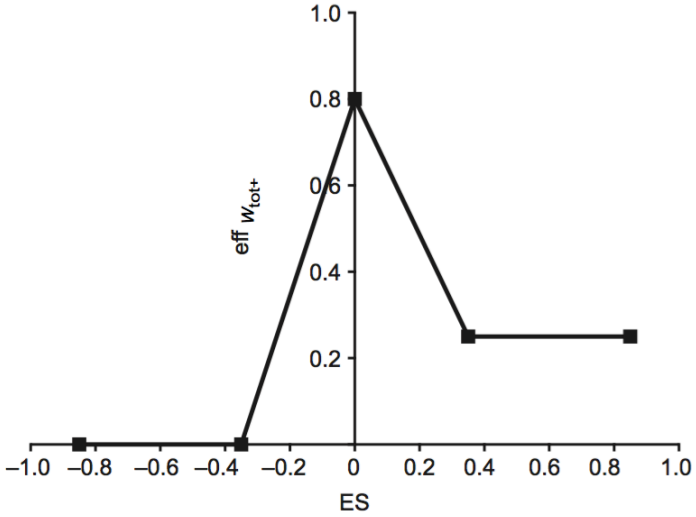

Figure 1. 28: mechanical efficiency of positive work as a function of the equivalent slope. Efficiency is highest when running at maximal (constant) speeds on the level (ES = 0); it reaches a value of about 0.25 when running uphill at ES > 0.35 and is nil downhill at ES > 0.35 (Minetti & Pavei, 2018).

Shuttles

In shuttle running, over a distance of 5+5 m, data of total (positive and negative, internal and external) mechanical work (W_{tot}) and of energy cost (C) were reported by Zamparo et al. (2016); based on these data positive "apparent" mechanical efficiency was calculated ($eff^{+} = W^{+}_{tot}/C$) and found to be lower than that observed during constant speed linear running at the same (average) speed (see Figure 1.29). This finding is coherent with the calculations of Minetti and Pavei (2018) that suggest a lower efficiency of positive work as accelerations (and hence ES) increases (Figure 1.28).

As discussed by Zamparo et al. (2016), the differences in positive efficiency between constant speed linear running and shuttle running could be attributed to differences in elastic energy reutilization. In fact, when humans run at steady speed tendons could play an important role as energy savers allowing this form of locomotion to be particularly efficient. In un-steady conditions (e.g. shuttle runs) "apparent" efficiency is much lower probably due to a different role of the tendon in these conditions.

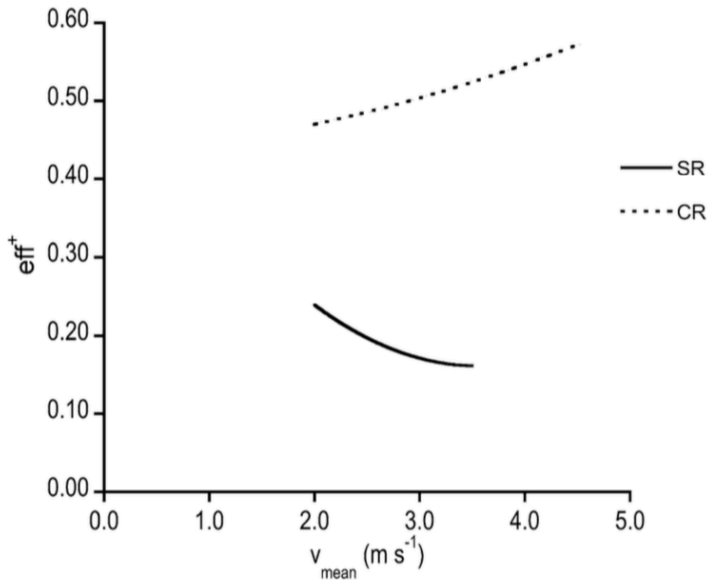

Figure 1. 29: "Apparent" mechanical efficiency of positive work as a function of speed in 5+5 shuttle runs (continuous line). Dotted line refers to running at constant speed. (Zamparo et al. 2016).

A detailed analysis of the implications of muscle-tendon interaction in human locomotion is provided in the next chapter. Briefly, the elastic elements are expected to promote body propulsion during the first meters of the sprint and then to shift their capability from a power amplification mechanism to an elastic energy saving mechanisms (Roberts & Azizi, 2011).

Summary

Investigating the energetics and mechanics of non-steady locomotion is far more complex than investigating these parameters during walking or running at steady speed. Moreover, whereas for the steady-state condition is sufficient to analyse just few representative steps, this is not the case for non-steady locomotion where the motion over the entire distance must be analysed. This represents a challenge both from a theoretical and methodological point of view. The findings of the few studies published on this topic point to the influence of tendon behaviour on elastic recoil, whole-body mechanics and metabolic requirements.

MUSCLE-TENDON INTERACTION: IMPLICATIONS FOR HUMAN LOCOMOTION

As summarized in the paper of Roberts & Azizi (2011), spring elements like tendons deform when a force is applied and recoil to their resting shape when the force is released. When springs and tendons deform, they also store energy in the form of elastic strain energy, and when they recoil this energy is released. Springs and tendons cannot produce mechanical energy, they can only return the energy loaded previously by an external source. The amount of energy stored depends on the stiffness of the spring and on its deformation. Compared to many biological tissues, tendon behaviour is determined by a single force-length relationship and cannot be modified or controlled directly.

As suggested by Roberts & Azizi (2011) the functional role of tendons can be categorized according to the directional flow of energy, with three possible patterns (Figure 1.30): (A) energy from the body or a body segment is temporarily stored in tendons, then returned to the body; (B) the mechanical energy produced by a muscle contraction is stored in a tendon, then released to increase mechanical energy of the body or a body segment; and (C) energy from the body or a body segment is temporarily stored in tendon, then released to do work on muscle, that is actively lengthened to absorb energy.

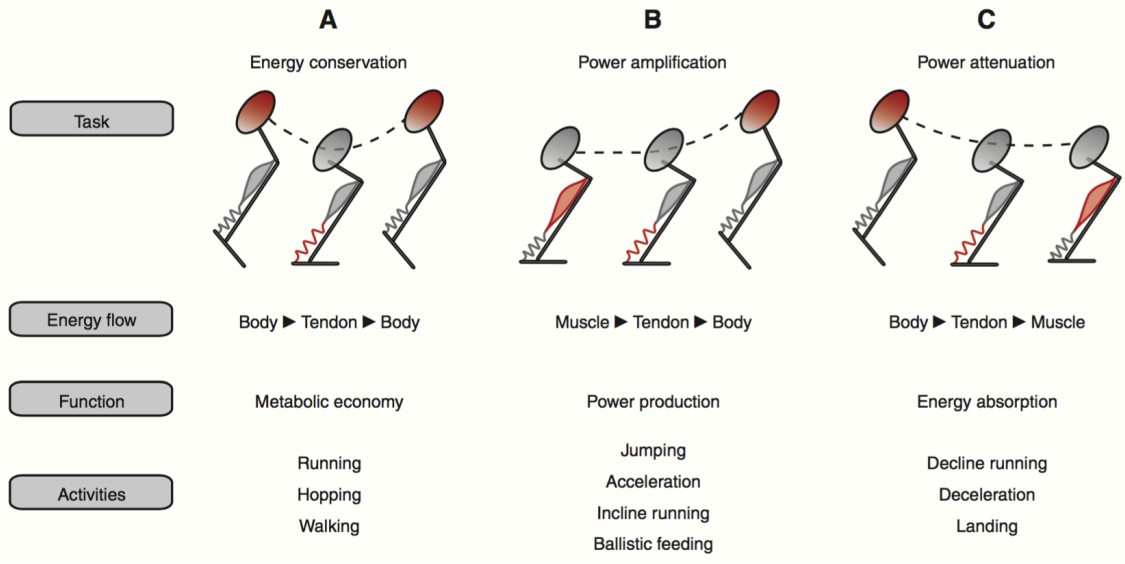

Figure 1. 30: Schematic illustrating how the directional flow of energy in muscle-tendon systems determines mechanical function. (A) Mechanical energy is conserved (i.e. muscle work is reduced) when elastic structures store and recover cyclic changes in the mechanical energy of the body or an appendage. (B) Tendons loaded directly by the work of muscle contraction can release that energy rapidly to the body. If the energy is released more rapidly than it is stored, muscle power can be amplified. (C) A rapid decline in the mechanical energy of the body or an appendage can be temporarily stored as elastic strain energy, followed by the release of this strain energy to do work on active muscles. This mechanism has the potential to reduce peak power input to muscles, thereby functioning as a power attenuator. (Roberts & Azizi, 2011).

Each functional role (tendon task) has its function: (A) energy conservation has the function to increase metabolic economy/efficiency; this mechanism occurs in walking, running and hopping on the level and at constant speed (steady locomotion); (B and C) power amplification and attenuation have the function to maximize power production and energy absorption, respectively, and are mechanisms that occur in accelerated and decelerated locomotion and in gradient locomotion (non-steady locomotion).

MUSCLE AND TENDON INTERACTION DURING STEADY-STATE RUNNING

The presence of tendons influences the actual working length of the muscle fibres, as well as its capability to generate force and power. Fukunaga et al. (2002) reviewed several studies on different types of locomotion, providing evidence that during walking (Fukunaga et al., 2001; Hof et al., 1983), ankle bending (Kubo et al., 2000a; Sakuma et al., 2011), jumping (Ishikawa et al., 2005) and running (Lichtwark et al., 2007), tendon compliance may be responsible for a shift of the working length of the sarcomeres to their optimum length (i.e. a shift in the plateau of the force-length relationship) (see Figure 1.31).

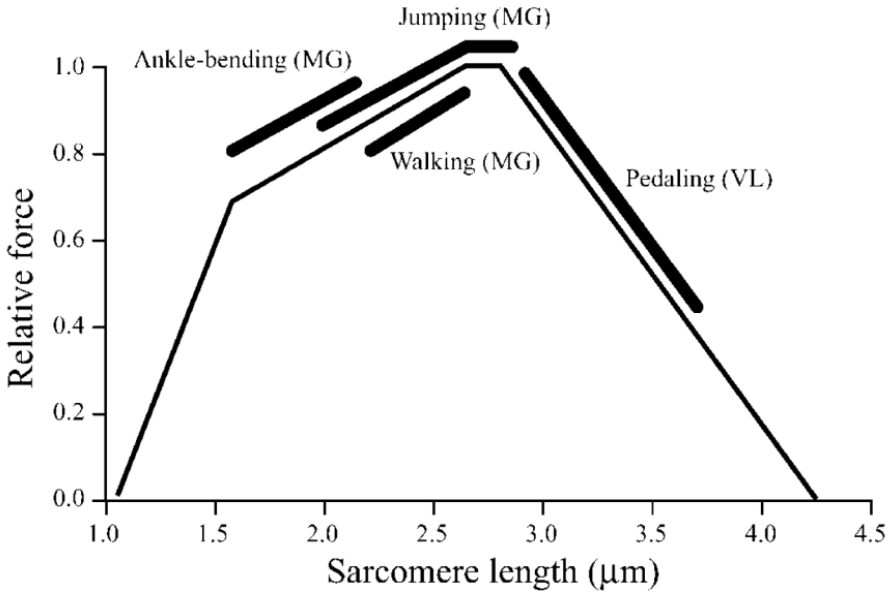

Figure 1. 31: F-L relationships of a sarcomere during different forms of locomotion: tendon compliance allows the muscle to operate close the optimal length. GM refers to the Gastrocnemius Medialis, whereas VL to the Vastus Lateralis (Fukunaga et al., 2002).

In the case of steady-state running, during the first phase of muscle contraction, the tendon is stretched due to its compliance. This induces a right shift of sarcomere working length on the ascending limb of the force-length curve, allowing the muscle fibres to contract nearly constantly around the plateau region (i.e. close to their optimum length). The force potential of the muscle fibres is thus enhanced during steady-state running due to the sarcomere F-L relationship (Fukunaga et al.,

2002; Hof et al., 1983).

The displacement and velocity of the muscle fibre shortening in the concentric phase is thus reduced, and this allows the muscle fibre to contract at a relatively lower shortening velocity compared to the velocity of the entire muscle-tendon unit. This mechanism represents an advantage for the force potential of the muscle, due to the F-V properties (Hill, 1938). As an example, Lichtwark et al. (2007) highlighted that, during the stance phase of running, the gastrocnemius medialis operates almost isometrically and with a low shortening velocity, and that this is always accompanied by an increase in the strain of the series elastic elements (Lichtwark et al., 2007).

In more general terms, elastic elements could play an important role in determining the mechanical and physiological demands of human running (Albracht & Arampatzis, 2013). As an example: for a given amount of muscle force required to run at a particular speed, the required level of activation can be minimized if the muscle is operating near its optimal length, due to the fact that muscle contraction at longer or shorter lengths than the optimal one results in less muscle force (Gordon et al., 1966; Ramsey and Street, 1940). Furthermore, the level of activation can be also minimized if the muscle can operate at a lower shortening velocity (Fletcher & MacIntosh, 2017). Hence, for a given muscle-tendon unit length, if the tendons accommodate the larger part of the total MTU length changes, the fascicles could operate more isometrically, with lower contraction velocity and close to their optimal length. This notion was recently verified by Bohm et al. (2019) who investigated muscle and tendon behaviour of the soleus muscles during running at 10 km/h. These authors showed that a low F-V potential (i.e. the fraction of maximum force, in the F-V relationships) of the soleus, is associated with a low metabolic power; this suggests that if muscle shortening velocity can be reduced, the metabolic demand of human running could be reduced as well.

Another important aspect of tendon mechanics during locomotion regards the possibility to store mechanical energy as elastic strain energy and then return it during the elastic recoil; the regained energy possibly contributing to the propulsion phase of the movement (Alexander, 1991; Hof et al., 1983; McNeil Alexander, 2002). Indeed, as indicated by Roberts and Azizi, see figure 1.30), during steady-state running tendons act as energy savers: part of the total mechanical energy is temporarily stored in the tendons and then returned to the body at each step (Cavagna & Kaneko, 1977). The obvious advantage of storing and releasing elastic energy in tendons is that work production is reduced for the muscle, even if muscles still have to generate force to provide tension for the tendons. When muscles perform less work, their energetic requirements are lower (Fenn, 1924); as a result, energy conservation by exploiting the elastic mechanism allows to improve the economy and the efficiency of human locomotion.

A typical example of energy conservation using elasticity are the "bouncing gaits", such as running at constant speed. In this case, kinetic and potential energy reach minimum values during the stance phase and maximal values during the flight phase (Novacheck 1998; Minetti & Saibene, 2003). Based on measurements of energy consumption and mechanical work in humans and animals, Cavagna et al. (1977) concluded that part of the kinetic and potential energy lost during ground contact must have been stored temporarily in elastic structures and subsequently returned, thereby improving the efficiency of locomotion (Cavagna et al. 1964, Cavagna et al. 1977).

Biewener et al. (1998), using direct measurements of tendon force and fascicle length in hopping wallabies, showed that distal hindlimb muscles do minimal positive work during a hopping cycle, and that the energy recovered from elastic tissue is on average 20 times greater than muscle work output. This basic mechanism of energy re-cycling using elastic elements elasticity has been confirmed later in humans by using ultrasound measurements to determine muscle fascicle and tendon behavior in running (Lichtwark et al. 2007, Lichtwark & Wilson 2006, Lai et al. 2015, Farris & Sawicki 2012). These studies demonstrated that muscle fascicles of the triceps surae muscles work nearly isometrically during the ground contact phase, and that elastic elements exhibited a stretch-shortening cycle during the stance phase.

MUSCLE - TENDON INTERACTION DURING NON-STEADY RUNNING

During sprint running or shuttle running, the energy expended per unit distance, as well as mechanical work production (at the whole-body level), is different (e.g. larger) than when running at constant speed. Also, the mechanical energy demands placed on human lower limb MTUs are fundamentally different. At variance with steady-state running, during maximal sprints the lower limb MTUs must operate in a motor-like manner, in order to generate net positive mechanical energy (Mero et al., 1983; Cavagna et al., 1971). A large amount of net positive mechanical energy can be achieved by minimizing the negative work done during early stance or by increasing the positive work done during late stance. Moreover, since elastic elements could not perform positive work, it is reasonable to presume that the work done by the muscle fascicles will be greater during a maximal sprint compared to running at a constant speed (Roberts & Scales, 2002). Indeed, during ballistic movements such as jumping, the fascicles of distal limb muscles shorten during the loading phase, while the MTU is lengthening. This phenomenon allows the tendons to store elastic strain energy and release it during the propulsion phase (Roberts & Azizi, 2011). However, this mechanism doesn't allow the tendon to reduce the energy demand of a muscle (Roberts & Azizi, 2011; Roberts, 2002; Anderson & Pandy, 1993). In fact, in this case, elastic elements operate as power or energy amplificatory, as shown in Figure 1.30.

To amplify power, the mechanical energy produced by muscle contraction is stored with a slow rate in the tendon and then released with a much higher rate. Peak power production (in muscles) occurs at 20-30% of the maximal shortening velocity (Askew & Marsh 1998, He et al. 2000) but in some movements, such as sprint running, joint movements exceed the optimal velocities for muscle power generation. In such fast movements, joint power can exceed what would be theoretically possible for the muscle (Sawicki et al. 2015) and this high power generation (exceeding muscle capacity) is called power amplification (Roberts and Azizi, 2011). This may occur when energy stored in the elastic tissues is rapidly released to power limb movement. Some animals (frogs, as an example) utilize an anatomical catch mechanism to allow muscle to stretch the tendon with a slow shortening velocity before the start of the movement. This is similar to the operation of a catapult and humans can use limb inertia and body mass to achieve the same mechanism without an anatomical catch (Farris et al. 2015). This mechanism is present in different human movements such as countermovement jumps (Kurokawa et al., 2001; Ishikawa et al., 2005) and sprints (Lai et al., 2016).

No studies investigated these mechanisms in shuttle runs, but Lai et al. (2016) exanimated the influence of muscle and tendon (in gastrocnemius medialis and soleus) during the acceleration phase of running by means of a musculoskeletal model. Lai and co-workers showed that the (positive) muscle fascicle work done by the plantar flexor muscles decreases as a function of sprint distance. Furthermore, they found that storage of tendon elastic strain energy in the ankle plantar flexors is just as vital at the start of a maximal sprint as it is at the end. At the start of a maximal sprint, tendon elastic strain energy allows the MTUs to increase the amount of mechanical work done (work amplification), whereas at the end of a maximal sprint, and when running at a constant speed, it acts to reduce muscle fascicle energy expenditure (energy conservation). The key distinction is the way in which the ankle plantar flexors utilize positive muscle fascicle work and negative MTU work to store elastic strain energy in the tendon during early stance.

Hence, during a sprint running acceleration phase, the ankle plantar flexors do have the capacity to vary their function from high-power, motor-like actuators (first steps of sprint running) to low-power, isometric struts (last steps of sprint running, similar to steady-state running) (Biewener & Roberts, 2000; Roberts & Azizi, 2011; Lai et al., 2016).

Summary

Tendon behaviour is expected to play an important role in determining the mechanical and physiological demands of human locomotion through its effects on muscle behaviour. Muscle-tendon interactions differ between steady (energy conservation) and non-steady speed running (power amplification and attenuation) but, while measuring muscle-tendon behaviour in steady state locomotion is relatively simple, this is not the case for non-steady locomotion. Investigating muscle and tendon architecture could also provide important information on the mechanical and physiological demands of human non-steady locomotion.

FINAL CONSIDERATIONS AND THESIS PERSPECTIVES

Humans can run at steady (e.g. constant speed along a linear path) or non-steady (e.g. with accelerations, decelerations and changes of direction) speed. Whereas, the primary aim when running at constant speed is to maximize the economy and the efficiency of locomotion, during accelerated and decelerated running the objective is that of maximizing force and power production (positive and negative, respectively) even at the expenses of economy/efficiency. Muscle and tendon behaviour differ in these two cases and the athletes specialized in steady speed running (e.g. long distance races) or non-steady speed running (e.g. short distance races) indeed show different morphological adaptations. The geometrical characteristics of muscles (such as fibre length, pennation angle and PCSA) indeed influence the force and/or the velocity of contraction while the morphological characteristics of tendons play an important role in the transmission of force from muscle to bone. Muscle-tendon interactions differ between steady (energy conservation) and non-steady speed running (power amplification and attenuation) and little is known about their role in determining the whole-body mechanics and the physiological demands in both cases.

Investigating the energetics and mechanics of non-steady locomotion is far more complex than investigating these parameters during walking or running at steady speed. Moreover, whereas for the steady-state condition is sufficient to analyse just few representative steps, this is not the case for unsteady conditions where the entire motion should be analysed. This represents a challenge both from a theoretical and methodological point of view.

For these reasons, investigating the role of muscle and tendon behaviour during steady and non-steady state running could provide important information about the underpinning mechanisms that determine the mechanical and energetic demands of human locomotion. For these reasons, this thesis focuses on two main topics (running at non-steady speeds and running at constant speed), each with its own specific aims.

RESEARCH AIMS

Non-steady speed running

To investigate the mechanical and energetic demands during non-steady locomotion using two different models: sprints (an acceleration phase) and shuttles (where an acceleration is followed by a deceleration and a change of direction). Given the difficulties in measuring muscle and tendon behaviour *in vivo* in these conditions, a further study was conducted to investigate the role of muscle architecture and Achilles tendon geometry (measured at rest) in determining the mechanical output during a sprint running acceleration phase.

The specific aims were:

1. To investigate the role of muscle and tendon geometry of the lower limb muscles in determining the force and the (horizontal) power during a sprint running acceleration phase.
2. To provide a detailed description of the mechanical power (internal and external) generated in the sprint running acceleration phase and to create an equation to predict internal mechanical power in these conditions.
3. To investigate the interplay between mechanics and energetics (e.g. locomotion efficiency) during non-steady locomotion, using as a model shuttle runs over different distances covered at different speeds.

Constant speed running

To provide a detailed description of muscle and tendon behaviour during running at constant (and increasing) speed, as well as to investigate the influence of the muscle-tendon unit components in determining the mechanical and energetic demands of running.

The specific aims were:

4. To describe the mechanical behaviour of different muscle-tendon units (and their components: muscle fascicles and tendons) at increasing running speeds.
5. To investigate the relative contribution of muscle fascicles and tendons in determining the physiological demands of running (energy cost and efficiency) at increasing speed.

RESEARCH STRATEGY

Five non-experimental, observational and correlational studies were conducted during the Ph.D. program, in order to answer to the aims of the thesis.

Study 1: This study was planned to answer to the first aim.

In this study we investigated the relationships between muscle-tendon parameters and average/peak values of horizontal velocity, force and power in the acceleration phase of sprint running (the first 20 m). Eighteen male sprinters performed two 20 m sprints on an athletic track during which the instantaneous values of horizontal velocity (v) were recorded by means of a radar; the instantaneous values of horizontal force (F) and power (P) were then calculated based on these data. Muscle thickness, fascicle length and pennation angle of knee extensors and plantar flexors, as well as Achilles tendon length and CSA, were measured by means of ultrasonography.

Study 2: This study was planned to answer to the second aim.

In this study we provide a more exhaustive description of the mechanical power output in the sprint running acceleration phase. Eighteen subjects performed two 20 m sprints in a gym. A 35-camera

motion capture system recorded the 3D motion of the body segments based on which the body center of mass (BCoM) trajectory was computed. The mechanical power to accelerate and rise the BCoM (external power, P_{ext}) and to accelerate the segments with respect to BCoM (internal power, P_{int}) were calculated. Furthermore, in this study we checked whether a predictive equation for P_{int} designed for steady state running was applicable to the sprint running acceleration phase.

Study 3: This study was planned to answer to the third aim.
In this study we calculated mechanical work and power (internal and external) and we estimated "apparent" efficiency during shuttle running. A 35-camera motion capture system recorded the 3D motion of the body segments while 20 athletes performed shuttle runs (with a 180° change of direction) at three paces (slow, moderate and maximal) and over four distances (5, 10, 15 and 20 m). Based on these data the BCoM trajectory was computed and external (P_{ext}) and internal (P_{int}) power were calculated. "Apparent" efficiency was then estimated based on values of energy cost reported in the literature (over the same shuttle distance and at corresponding speeds).

Study 4: This study was planned to answer to the fourth aim.
This study combines in-vivo ultrasound measurements of the Vastus Lateralis and Gastrocnemius Medialis muscles with electromyographic, kinematic (3D motion capture) and kinetic (force plates) measurements during treadmill running at different speeds (10, 13 and 16 $km \cdot h^{-1}$) to better understand the role of muscle and tendon behaviour in two functionally different muscle-tendon units (MTU): knee extensors and ankle plantar flexors. In addition, the Force-Length and Force-Velocity relationships of VL and GM were experimentally assessed by combining force (Cybex isokinetic dynamometer) and EMG data with ultrasound measurements.

Study 5: This study was planned to answer to the fifth aim.
In this study the influence of the tendon recoil in determining the mechanical and energetic demands of running was investigated. In-vivo ultrasound measurements of the Gastrocnemius Medialis were combined with electromyographic, kinematic (3D motion capture), kinetic (force plates) and metabolic measurements during treadmill running at different speeds (10, 13 and 16 $km \cdot h^{-1}$). Mechanical work production (external and internal) was calculated based on kinetic and kinematic data, and "apparent" efficiency was estimated from the ratio between mechanical and metabolic data (energy cost of running). An inverse dynamic approach was used to estimate the contribution of the Achilles tendon in determining the mechanical work of running.

CHAPTER 2

NON STEADY-STATE RUNNING: STUDY 1

CORRELATIONS BETWEEN MUSCLE-TENDON PARAMETERS AND ACCELERATION ABILITY IN 20 M SPRINTS

Authors: Andrea Monte, Paola Zamparo

Department of Neuroscience, Biomedicine and Movement Sciences, University of Verona, Italy

ABSTRACT

In this study we investigated the relationships between muscle-tendon parameters and average/peak values of velocity, force and power in sprint running focusing on the acceleration phase. Eighteen male sprinters (100 m PB: 10.66±0.51 s) participated to the study. Instantaneous values of horizontal velocity (v) were recorded by means of a radar and instantaneous values of force (F) and power (P) were calculated based on these data. Muscle thickness, fascicle length and pennation angle of knee extensors and plantar flexors, as well as Achilles tendon length and CSA, were measured by means of ultrasonography. In the first 20 m of the sprint average and peak speed were 6.31±0.59 and 8.88±0.98 $m \cdot s^{-1}$, respectively; force was highest at the start of the sprint (F_{peak} = 10.02±1.43 $N \cdot kg^{-1}$) and power peaked about 1 s after the start (26.64±5.99 $W \cdot kg^{-1}$). Muscle-tendon parameters showed stronger correlations with peak values of power (R range: 0.81-0.92), force (R range: 0.56-0.84) and speed (R range: 0.53-0.85) than with average values of velocity over the 20 m distance (R range: 0.41-0.61) (R <0.47=NS; R >0.71=P<.001). These data underline that the influence of muscle tendon parameters on sprint performance could be better appreciated when peak values of power can be calculated rather than by considering the simple measure of average velocity (e.g. distance/time).

Published in: Plos One, 14: e0213347. DO: 10.1371/journal.pone.0213347

INTRODUCTION

Sprint performance (e.g. in a 100 m race) is determined by the ability to accelerate rapidly, by the magnitude of maximal velocity and by the ability to maintain this velocity up to the end of the race (Ross et al., 2001); the ability to accelerate rapidly in the first steps of a sprint is what separates an elite sprinter from a merely good one (Hunter et al., 2005); indeed, best sprinters exert larger propulsive forces (relative horizontal impulses) in the sprint running acceleration phase (Morin et al., 2011; Zamparo et al., 2016; Morin et al., 2012). The ability to accelerate is a key parameter also in many team sports and the goal of many training programs.

The ability to generate large forward accelerations is thus related to the capability to produce high amounts of horizontal external force over the entire acceleration phase: the changes in velocity during a sprint running acceleration phase are indeed accompanied by changes in force production (Zamparo et al., 2016; Morin et al., 2012). As an example Rabita et al. (2015) have shown that, in the first 30 m of a 100 m race the increase in running velocity is mirrored by a decrease in horizontal force; as a result, power output, which is recognized to be the major determinant of sprint performance and acceleration ability (Morin et al., 2012; Rabita et al., 2016; Slawinski et al. ,2015), is maximal in the first steps of a sprint.

At the muscle level, force, velocity and power are influenced by fibre type distribution and architecture: i) fast contracting fibres can shorten up to 2-3 times faster than slow contracting ones; ii) muscles with larger cross sectional area (CSA) generate larger tensions and peak isometric forces (this is, as an example, the case of pennate muscles); iii) muscles with (relatively) longer fibres (e.g. fusiform, non-pennate, muscles) can contract more rapidly and generate peak power at a higher velocity (Cormie et al., 2011; Lieber, 1992; Lee & Piazza, 2009; Rossuer et al., 1000; Lai et al., 2016; Wilson & Lichtwark, 2011)..

For these reasons the relationship between sprint performance and muscle architecture was investigated in the literature. However, this was done in just few studies (to our knowledge) that related top running velocity, or personal best time in a 100 m event, with muscle-tendon characteristics. Kumagai et al. (2000), reported a significant negative relationship between 100 m best time and fascicle length of vastus lateralis (VL, $R = -0.43$, $P < .01$), gastrocnemius medialis (GM, $R = -0.44$, $P < .01$) and lateralis (GL, $R = -0.57$, $p < 0.01$) whereas Abe et al. (2000) reported a significant negative relationship between 100 m best time and fascicle length of VL ($R = -0.51$, $P < .01$) and GL ($R = -0.44$, $P < .05$) but not with GM ($R = -0.22$, NS). At the same time, Kumagai et al. (2000) demonstrated significant positive relationships between 100 m sprint time and pennation angle of VL ($R = 0.34$, $P < .05$), GL ($R = 0.46$, $P < .01$) and GM ($R = 0.37$, $P < .05$). More recently, Kubo et al. (2016), reported significant positive relationships between muscle thickness of knee extensors

(R = 0.616, P < .05) and 100 m race time while they found no relationship with tendon stiffness, and elongation, of the knee extensor muscles (R =0.194 and R =0.249, NS, respectively). Stafilidis & Arampatzis (2007) reported a negative relationship between maximal elongation of VL tendon and aponeurosis with 100 m sprint times (R = -0.57, P <0.01). Finally, Miyake et al. (2017) reported no relationship between 100 m best time and quadriceps CSA (R = 0.265, NS) while they found a significant positive relationship between 100 m best time and knee extensors moment arm (R = 0.614, P < .001); interestingly, stronger relationships were found, in Miyake's study [18], when correlating knee extensors moment arm with sprinting velocity (in the acceleration phase: R = 0.72) or maximal velocity (R = 0.62).

In conclusion, a strong correlation should be expected between muscle-tendon parameters and sprint performance (as was indeed the case in many of the cited studies). However, as indicated above, the capacity to exert force (and power) is an important determinant of performance in the first 20-30 m of a sprint; it is thus likely that muscle-tendon parameters will correlate better with measures of force (and power) in this phase than with measures of average speed (e.g. 100 m best time).

We thus decided to focus our attention on the acceleration phase (the phase of peak force and peak power production) and to investigate the correlations between muscle-tendon parameters (knee extensors, plantar flexors and Achilles tendon) and some of the parameters which determine sprint performance in this phase (power, force and velocity as well as the degree of curvature of the v vs. t relationship).

Our hypothesis was, therefore, that muscle-tendon characteristics would be more strongly related to peak rather than mean values of speed, force and power in the first 20 m of a sprint (as well as with the sprinter's 100 m PB) since it is in the acceleration phase that the sprinters have to provide the largest values of force (and power).

MATERIALS AND METHODS

Subjects

Eighteen male sprinters participated in this study (age: 24.36±5.0 years; body mass: 74.5±5.92 kg; stature: 1.78±0.06 m); they were free from any type of injury (this was verified by means of an interview) and were asked to abstain from training in the 24 hours before the testing session. The current personal best times over the 100 m distance (100 m PB) in these sprinters (10.66±0.51 s; range 10.02-11.44 s) were attained in the competitive season preceding the experiments. All participants received written and oral instructions before the study and gave their written informed consent to the experimental procedure. The experimental protocol was approved by the Ethical Committee of Verona University and performed in accordance with the Helsinki Declaration.

Experimental procedure

Muscle-tendon characteristics

Muscle-tendon parameters were measured in vivo using B-Mode ultrasound apparatus after 10 min of resting. The athletes remained in a supine position for the measurement of quadriceps muscles and in a prone position for the measurements of plantar-flexors muscle and Achilles tendon, with the muscles relaxed, the leg straight, (i.e. hip and knee extended) and the ankle flexed at 90°. A water-soluble gel was applied to the transducer to aid acoustic coupling and to reduce the deformations of the muscle and tendon. For each muscle, two images were captured and subsequently analysed with ImageJ software and Photoshop CS5 by the same operator, their average value was utilized in further analysis.

Muscle thickness of the knee extensors (vastus lateralis (VL), rectus femoris (RF), vastus intermedius (VI), vastus medialis (VM) was measured at mid distance between the lateral condyle of the femur and greater trochanter whereas muscle thickness of plantar flexors (gastrocnemius medialis (GM) and lateralis (GL) and soleus (SOL) was measured at 30% proximal between the lateral malleolus of the fibula and the lateral condyle of the tibia, as previously described (Kumagai et al., 2000; Abe et al., 2000; Abe et al., 2001), means of an ultrasound apparatus with a 6 cm, 8-10 MHz, linear-array probe (SIEMENS Acuson, P50). Briefly, the transducer was placed parallel to the longitudinal axis of the muscle. The distance between subcutaneous adipose tissue interface and inter-muscular interface was accepted as muscle thickness (Figure 2.1). The angles between the echo of the deep aponeurosis of the muscle and the interspaces among the fascicles of the muscles was taken as pennation angle. All measurements were analysed in the middle portion of the echographic image.

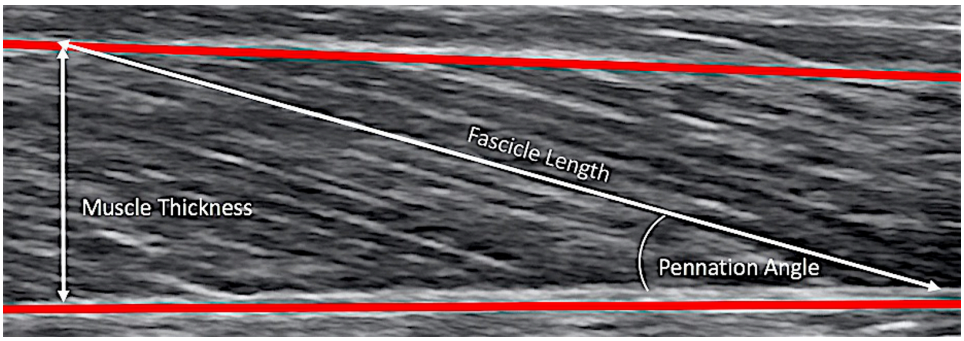

Figure 2. 1: Ultrasonographic (longitudinal) image for measuring muscle thickness, pennation angle and fascicle length in vastus lateralis.

The cross sectional area (CSA) of the Achilles tendon was captured in the transverse plane at 3 cm proximal to the insertion on the calcaneus; two images were captured with SIMENS software and subsequently analysed with ImageJ software and Photoshop CS5 by the same operator; their

mean value was utilized in further analysis.

Achilles tendon length was measured in the longitudinal plane between the calcaneal osteo-tendineous junction and the muscle-tendineous junction of gastrocnemius medialis, by combing multiple images (Silbernagel et al., 201; Kubo et al., 2016; Ryan et al., 2013).

The fascicle length across the deep and superficial aponeurosis was manually determined and the relative fascicle length for each muscle was calculated from the ratio of fascicle length and segment length (thigh or shank).

The mean coefficient of variation was 1.7% (range of: 1.65-1.79) for muscle thickness, 2.9% (range of: 2.81-3.00) for pennation angle, 3.5% (range of: 3.43-3.59) for relative fascicle length, 2.3% (range of: 1.94-2.37) for Achilles tendon CSA and 4.0% (range of: 3.89-4.08) for Achilles tendon length (a test-retest on 10 subjects performed by the same investigator).

Finally, the sum of muscle thickness, the mean of pennation angle and relative fascicle length by GL, GM and SOL were used as an indicator of plantar flexor (PF) characteristics, while the sum of muscle thickness, the mean of pennation angle and relative fascicle length by VL, VM, VI and RF were used as an indicator of knee extensor (KE) characteristics.

Velocity and kinetic variables analysis

After the muscle-tendon measurements, the athletes (who wore athletic spiked shoes) performed 20 min of warm-up (i.e. running, specific gaits and dynamic stretching) following which they were asked to perform 2 maximal sprints (with a standing start: 3-point start) over a 30 m distance (with 5 min of recovery between trials); a start signal was not provided and the sprinters started when they felt ready. Only the trial with the best acceleration phase (lower sprint time) was analysed.

We asked the subjects to sprint over a longer distance than that we wanted to analyse (30 m instead of 20 m) for two reasons: 1- to avoid the occurrence of a deceleration phase in the last steps of the run and 2- because to fit an exponential function it is necessary to know the amplitude of the signal (e.g. maximal speed). Indeed, the acceleration phase is generally not completed at 20 m but at a distance ≥ 30 m (Samozino et al., 2015).

Instantaneous running velocity (v) was measured at a sampling rate of 46 Hz with a radar system (Stalker ATS II System) over a distance of 30 m. The radar was placed on a tripod 10 m behind the starting line at a height of 1 m, corresponding approximately to the height of the great trochanter.

The data of running velocity were fitted with a mono-exponential function (Chelly & Denis, 2001; di Prampero et al., 2005) (the velocity onset was ≥ 0.2 $m \cdot s^{-1}$) with a customized Labview (v.10) program:

$$v(t) = vmax \cdot (1 - e^{-t/\tau})$$

where v is the modelled running velocity, v_{max} the maximal velocity reached in the 30 m sprint (i.e. measured by means of the radar gun) and τ the time constant of the v vs. t relationship.
The instantaneous forward acceleration (af) and the running distance (d) were calculated from the first derivative and integral respectively:

$$af(t) = ds/dt = (vmax - vmax \cdot (1 - e^{-t/\tau}))/\tau$$

$$d(t) = vmax \cdot t - (vmax \cdot (1 - e^{-t/\tau})) \cdot \tau$$

Finally, force (F) and mechanical power (P) were calculated as:

$$F = ((vmax - vmax \cdot (1 - e^{-t/\tau}))/\tau) \cdot m$$

$$P = (((vmax - vmax \cdot (1 - e^{-t/\tau}))/\tau) \cdot m) \cdot (vmax \cdot (1 - e^{-t/\tau}))$$

were m is the body mass of subject. The average and peak values of v, F and P were calculated in the acceleration phase only (from 0 to 20 m) (Figure 2.2). From the velocity, force and power-time curves the mean and peak values for each variable were calculated (v_{mean}: mean running velocity; F_{mean}: mean force; P_{mean}: meanpower; v_{peak}: peak running velocity; F_{peak}: peak force; P_{peak}: peak power). The values of force and power are reported in the paper normalized per kg of body mass.

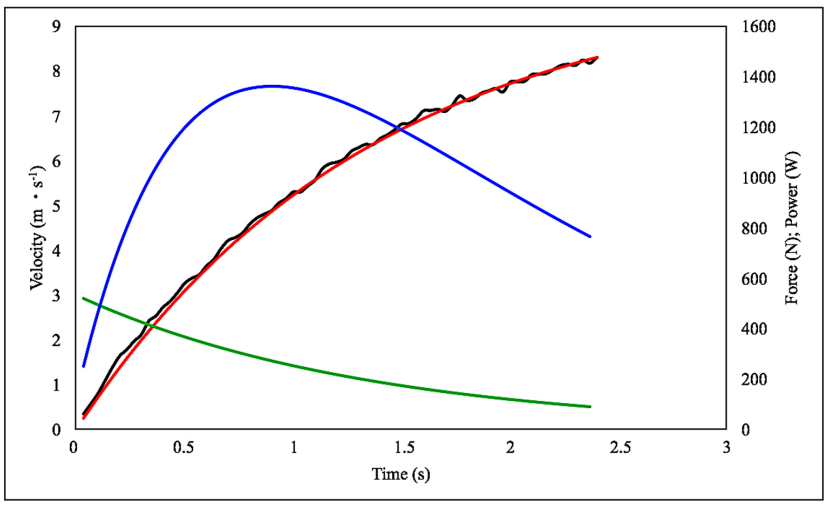

Figure 2. 2: Running velocity, force and power as a function of running time in a typical sprinter. Running velocity (black line); modelled running velocity (red line); force (green line) and power (blue line).

Statistical Analysis

All variables are expressed as mean ± standard deviations (SD). Relationships between muscle-tendon characteristics and running variables were examined using Pearson correlations. Significant level was set at $P< 0.05$ using SPSS 21.0.

RESULTS

The mean values and standard deviations of the muscle-tendon parameters are reported in Table 2.1.

	Thickness (cm)	Pennation angle (°)	Absolute fascicle length (cm)	Relative fascicle length
GL	1.81±0.11	12.0±1.1	7.47±1.09	0.20±0.03
GM	2.34±0.19	20.8±1.7	5.87±0.71	0.13±0.03
SOL	1.8±0.05	20.1±1.40	5.70±0.77	0.13±0.03
VL	2.8±0.13	17.4±2.0	8.19±1.26	0.23±0.03
VM	3.51±0.16	11.5±1.5	9.41±1.32	0.40±0.06
VI	1.9±0.14	9.0±0.6	8.89±1.22	0.29±0.05
RF	2.80±0.17	11.2±1.3	9.14±1.19	0.33±0.03
PF	5.99±0.33	17.6±1.3	6.35±0.87	0.15±0.05
KE	11.1±0.53	12.8±1.2	8.90±1.26	0.31±0.04

	CSA (mm^2)	Length (cm)
AT	72.4±8.7	20.3±4.1

Table 2. 1: Architectural characteristics of the analysed muscles. Data are means ± SD. For plantar flexor (PF) and knee extensor (KE) muscles, thickness is the sum of all muscles, while pennation angle and absolute/relative fascicle length are the average of all muscles. GL: gastrocnemius lateralis; GM: gastrocnemius medialis; SOL: soleus; VL: vastus lateralis; VM vastus medialis; VI vastus intermedius; RF: rectus femoris; PF: plantar flexors; KE: knee extensors; AT: Achilles tendon.

Muscle thickness of plantar flexors ranged from 1.64 to 2.66 cm, GM showing the largest muscle thickness (range: 2.01-2.66 cm). Pennation angle and relative fascicle length ranged from 10.5 to 23.1° and from 0.08 to 0.26 respectively, GM and GL showing the greater pennation angle and fascicle length (range: 18.4-23.1° and 0.16-0.24, respectively). Knee extensor muscles had a range of 1.77-3.78 cm for muscle thickness and 8.1-22° for pennation angle. VM and VL showed the greater thickness and pennation angle (range: 3.28-3.78 cm and 14.6-22.0°, respectively); the range of relative fascicle length in KE was 0.17-0.50; VM was the longest muscle. Finally, the CSA and length of Achilles tendon ranged from 61.7 and 88.9 mm^2 and from 13.5 to 26.3 cm, respectively.

Running velocity reached at the end of 20 m (8.88±0.68 $m \cdot s^{-1}$) was smaller than at the end of 30 m (9.78±0.71 $m \cdot s^{-1}$); thus, in the first 20 m of the sprint running velocity did not reach a steady-state (in all subjects) (v_{mean}: 6.31±0.59 $m \cdot s^{-1}$). The values of force were highest at the start of the

sprint (F_{peak}: 10.02±1.43 $N \cdot kg^{-1}$) and P reached its maximum value 0.97±0.1 s after the start (P_{peak}: 26.64±5.99 $W \cdot kg^{-1}$). The average values of force and power, over the entire 20 m distance, were 3.89±0.98 $N \cdot kg^{-1}$ (F_{mean}) and 18.23±5.03 $W \cdot kg^{-1}$ (P_{mean}). Significant relationships were observed between 100 m PB and v_{peak} (R = 0.50; P=0.045), F_{peak} (R = 0.54; P=0.042), P_{mean} (R = 0.65; P=0.0087), P_{peak} (R = 0.65; P=0.0087) and τ (R = 0.60; P=0.0091) but not with v_{mean} and F_{mean}.

The CV% values calculated based on data reported in Table 2.1 (CV% = SD/mean·100) indicate that the variability in the values of velocity (mean and peak over the 20 m distance) is lower (8-9%) than the variability in the mean and peak values of force ($N \cdot kg^{-1}$; 14-25%) and power ($W \cdot kg^{-1}$, 22-28%).

Relationships between variables

The correlation coefficients (R) of the relationships between muscle-tendon characteristics and running variables are reported in Table 2.2; statistical significance (P values) is indicated as well. The mean and peak values of v, F and P increase with muscle thickness and relative fascicle length (R = positive) and decrease with pennation angle (R = negative) for all muscles and AT. The opposite is true for the time constant (τ) R is negative for muscle thickness and relative fascicle length and positive for pennation angle.

	Thickness							
	PB	**v_{mean}**	**F_{mean}**	**P_{mean}**	**v_{peak}**	**F_{peak}**	**P_{peak}**	**τ**
GL	$-0.50^{(0.045)}$	$0.54^{(0.042)}$	$0.38^{(NS)}$	$0.80^{(0.000)}$	$0.85^{(0.000)}$	$0.78^{(0.000)}$	$0.92^{(0.000)}$	$-0.85^{(0.000)}$
GM	$-0.55^{(0.039)}$	$0.46^{(NS)}$	$0.28^{(NS)}$	$0.67^{(0.005)}$	$0.69^{(0.002)}$	$0.79^{(0.000)}$	$0.82^{(0.000)}$	$-0.83^{(0.000)}$
SOL	$-0.53^{(0.043)}$	$0.46^{(NS)}$	$0.52^{(0.044)}$	$0.78^{(0.000)}$	$0.64^{(0.009)}$	$0.70^{(0.002)}$	$0.82^{(0.000)}$	$-0.82^{(0.000)}$
VL	$-0.54^{(0.042)}$	$0.52^{(0.044)}$	$0.29^{(NS)}$	$0.68^{(0.003)}$	$0.71^{(0.000)}$	$0.67^{(0.005)}$	$0.78^{(0.000)}$	$-0.83^{(0.000)}$
VM	$-0.68^{(0.003)}$	$0.47^{(NS)}$	$0.25^{(NS)}$	$0.62^{(0.009)}$	$0.62^{(0.009)}$	$0.73^{(0.000)}$	$0.77^{(0.000)}$	$-0.81^{(0.000)}$
VI	$-0.56^{(0.035)}$	$0.41^{(NS)}$	$0.20^{(NS)}$	$0.52^{(0.044)}$	$0.53^{(0.043)}$	$0.56^{(0.035)}$	$0.64^{(0.009)}$	$-0.72^{(0.000)}$
RF	$-0.61^{(0.009)}$	$0.47^{(NS)}$	$0.27^{(NS)}$	$0.63^{(0.009)}$	$0.63^{(0.009)}$	$0.67^{(0.005)}$	$0.74^{(0.000)}$	$-0.88^{(0.000)}$
PF	$-0.52^{(0.044)}$	$0.44^{(NS)}$	$0.36^{(NS)}$	$0.76^{(0.000)}$	$0.76^{(0.000)}$	$0.81^{(0.000)}$	$0.89^{(0.000)}$	$-0.92^{(0.000)}$
KE	$-0.57^{(0.032)}$	$0.41^{(NS)}$	$0.28^{(NS)}$	$0.68^{(0.004)}$	$0.69^{(0.002)}$	$0.73^{(0.000)}$	$0.81^{(0.000)}$	$-0.91^{(0.000)}$
AT	$-0.59^{(0.027)}$	$0.51^{(0.044)}$	$0.41^{(NS)}$	$0.78^{(0.000)}$	$0.65^{(0.009)}$	$0.78^{(0.000)}$	$0.88^{(0.000)}$	$-0.90^{(0.000)}$

Pennation Angle

	PB	v_{mean}	F_{mean}	P_{mean}	v_{peak}	F_{peak}	P_{peak}	τ
GL	$-0.64^{(0.009)}$	$-0.57^{(0.032)}$	$-0.35^{(NS)}$	$-0.76^{(0.000)}$	$-0.74^{(0.000)}$	$-0.76^{(0.000)}$	$-0.88^{(0.000)}$	$0.88^{(0.000)}$
GM	$-0.70^{(0.002)}$	$-0.47^{(NS)}$	$-0.30^{(NS)}$	$-0.69^{(0.002)}$	$-0.62^{(0.009)}$	$-0.75^{(0.000)}$	$-0.83^{(0.000)}$	$0.91^{(0.000)}$
SOL	$-0.61^{(0.009)}$	$-0.52^{(0.044)}$	$-0.26^{(NS)}$	$-0.68^{(0.003)}$	$-0.65^{(0.009)}$	$-0.71^{(0.000)}$	$-0.82^{(0.000)}$	$0.83^{(0.000)}$
VL	$-0.33^{(NS)}$	$-0.52^{(0.044)}$	$-0.33^{(NS)}$	$-0.67^{(0.005)}$	$-0.64^{(0.009)}$	$-0.72^{(0.000)}$	$-0.80^{(0.000)}$	$0.66^{(0.005)}$
VM	$-0.50^{(0.045)}$	$-0.59^{(0.027)}$	$-0.33^{(NS)}$	$-0.74^{(0.000)}$	$-0.73^{(0.000)}$	$-0.75^{(0.000)}$	$-0.88^{(0.000)}$	$0.87^{(0.000)}$
VI	$-0.33^{(NS)}$	$-0.41^{(NS)}$	$-0.19^{(NS)}$	$-0.62^{(0.009)}$	$-0.69^{(0.002)}$	$-0.77^{(0.000)}$	$-0.80^{(0.000)}$	$0.89^{(0.000)}$
RF	$-0.47^{(NS)}$	$-0.57^{(0.032)}$	$-0.28^{(NS)}$	$-0.68^{(0.003)}$	$-0.60^{(0.009)}$	$-0.75^{(0.000)}$	$-0.82^{(0.000)}$	$0.85^{(0.000)}$
PF	$-0.69^{(0.002)}$	$0.52^{(0.044)}$	$-0.31^{(NS)}$	$-0.74^{(0.000)}$	$-0.80^{(0.000)}$	$-0.77^{(0.000)}$	$-0.88^{(0.000)}$	$0.86^{(0.000)}$
KE	$-0.60^{(0.009)}$	$0.51^{(0.044)}$	$-0.33^{(NS)}$	$-0.74^{(0.000)}$	$-0.82^{(0.000)}$	$-0.84^{(0.000)}$	$-0.90^{(0.000)}$	$0.73^{(0.000)}$
AT	/	/	/	/	/	/	/	/

Relative fascicle length and AT length

	PB	v_{mean}	F_{mean}	P_{mean}	v_{peak}	F_{peak}	P_{peak}	τ
GL	$-0.63^{(0.009)}$	$0.66^{(0.006)}$	$0.37^{(NS)}$	$0.80^{(0.000)}$	$0.75^{(0.000)}$	$0.80^{(0.000)}$	$0.90^{(0.000)}$	$-0.84^{(0.000)}$
GM	$-0.75^{(0.000)}$	$0.58^{(0.029)}$	$0.39^{(NS)}$	$0.75^{(0.000)}$	$0.64^{(0.009)}$	$0.75^{(0.000)}$	$0.86^{(0.000)}$	$-0.88^{(0.000)}$
SOL	$-0.53^{(0.042)}$	$0.53^{(0.042)}$	$0.19^{(NS)}$	$0.63^{(0.009)}$	$0.65^{(0.009)}$	$0.77^{(0.000)}$	$0.87^{(0.000)}$	$-0.88^{(0.000)}$
VL	$-0.66^{(0.006)}$	$0.49^{(0.044)}$	$0.29^{(NS)}$	$0.72^{(0.000)}$	$0.65^{(0.009)}$	$0.81^{(0.000)}$	$0.88^{(0.000)}$	$-0.88^{(0.000)}$
VM	$-0.68^{(0.003)}$	$0.58^{(0.029)}$	$0.39^{(NS)}$	$0.79^{(0.000)}$	$0.69^{(0.002)}$	$0.78^{(0.000)}$	$0.88^{(0.000)}$	$-0.85^{(0.000)}$
VI	$-0.73^{(0.000)}$	$0.48^{(0.049)}$	$0.35^{(NS)}$	$0.74^{(0.000)}$	$0.62^{(0.009)}$	$0.77^{(0.000)}$	$0.85^{(0.000)}$	$-0.80^{(0.000)}$
RF	$-0.68^{(0.003)}$	$0.58^{(0.029)}$	$0.34^{(NS)}$	$0.75^{(0.000)}$	$0.63^{(0.009)}$	$0.78^{(0.000)}$	$0.88^{(0.000)}$	$-0.85^{(0.000)}$
PF	$-0.62^{(0.009)}$	$0.57^{(0.032)}$	$0.31^{(NS)}$	$0.79^{(0.000)}$	$0.67^{(0.005)}$	$0.76^{(0.000)}$	$0.88^{(0.000)}$	$-0.84^{(0.000)}$
KE	$-0.66^{(0.006)}$	$0.53^{(0.042)}$	$0.35^{(NS)}$	$0.72^{(0.000)}$	$0.64^{(0.009)}$	$0.78^{(0.000)}$	$0.87^{(0.000)}$	$-0.80^{(0.000)}$
AT	$-0.70^{(0.002)}$	$0.48^{(0.049)}$	$0.32^{(NS)}$	$0.71^{(0.000)}$	$0.62^{(0.009)}$	$0.75^{(0.000)}$	$0.83^{(0.000)}$	$-0.88^{(0.000)}$

Tabella 2.2: GL: gastrocnemius lateralis; GM: gastrocnemius medialis; SOL: soleus; VL: vastus lateralis; VM vastus medialis; VI vastus intermedius; RF: rectus femoris; PF: plantar flexors; KE: knee extensors; AT: Achilles tendon; PB: 100 m personal best time; v: running velocity; F: force; P: power; τ: time constant of the v vs. t relationship; NS: no significant relationship; 0.000 = P < 0.001.

The effects of inter-subject differences in Achilles tendon CSA on v_{mean}, v_{peak} are reported in Figure 2.3 as an example of these relationships. This figure shows that a larger CSA of the Achilles tendon is associated with greater values of v_{mean} and v_{peak} and that the correlation coefficient (and the level of significance) of these relationships is lower for v_{mean} than for v_{peak}.

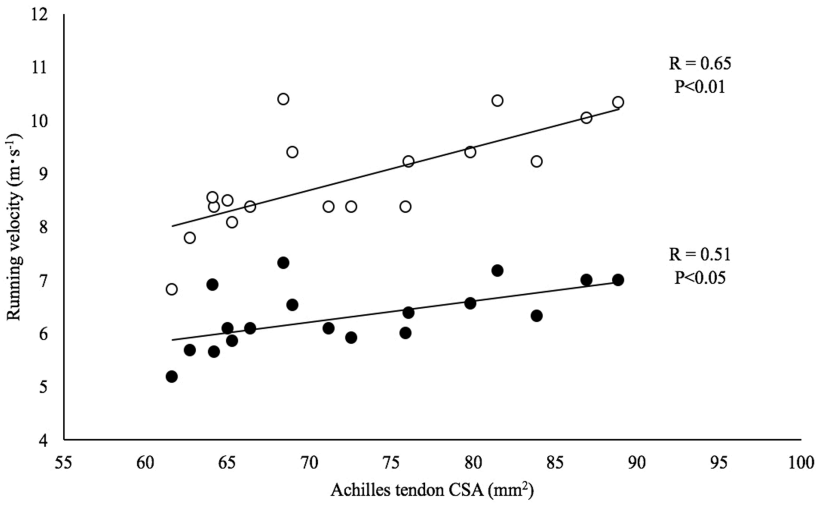

Figure 2. 3: Running velocity as a function of the Achilles tendon cross sectional area (CSA). Mean (full circles) and peak (open circles) running velocity.

Indeed, as can be seen by inspection of Table 2.2, correlations with v_{mean} are relatively weak compared to those with v_{peak} and τ ‖ better correlations (larger *R* and lower *P*) are observed between muscle-tendon characteristics and peak values of force and power than with the corresponding mean values. The strongest correlation between muscle-tendon proprieties and running variables is observed when considering peak power output (P_{peak}) or the time constant (τ).

DISCUSSION

In this study the relationship between muscle-tendon parameters and force/power production during the sprint running acceleration phase (in the first 20 m) was investigated; we observed that muscle thickness and relative fascicle length, as well as Achilles tendon CSA and length, are positively correlated with sprint running performance (with values of v, F and P) while pennation angle is negatively correlated with it.

Force and power were not directly measured but calculated based on values of horizontal speed. This is a limitation of this study (see critique of methods); however, this analysis allowed us to get a better insight on the determinants of sprint performance in comparison with previous studies where only the average (horizontal) speed over the 100 m distance was taken into consideration. Indeed, as indicated in the Introduction, relatively weak relationships (or no relationship) between muscle-tendon characteristics and best times over the 100 m distance were reported in previous studies (Lai et al., 2016; Kumagai et al., 2000; Abe et al., 2000; Miyake et al., 2017). Our findings indicate that the correlation coefficients of the relationships between muscle-tendon parameters and sprint performance largely improve when peak values of v, F and P in the acceleration phase are considered (R range: 0.62-0.92), peak power and τ being the parameters best correlated with muscle-

tendon proprieties (R range: 0.73-0.96). In this study we did not ask our sprinters to run the entire 100 m distance; their current 100 m PB times were utilized instead. This is a limitation of this study; however, these data confirm that the correlation coefficients are "weaker" in this case, and similar to those referring to v_{mean} in the acceleration phase: R range: 0.41-0.61).

In the following paragraphs the parameters investigated in this study will be discussed in comparison with the values reported in the literature.

Sprint variables

Running velocity increases as a function of time, while horizontal force production decreases, as previously reported in the literature (Morin et al.,2011; Samozino et al., 2015; Monte et al., 2016). Our P_{mean} values (1305±420 W; 18.23±5.03 $W \cdot kg^{-1}$) are similar to those reported by others during a sprint running acceleration phase (e.g. Slawinski et al. (2015): 15.3±03.3 $W \cdot kg^{-1}$; Monte et al. (2016): 17.2±3.63 $W \cdot kg^{-1}$). Moreover, our τ values (1.40±0.04 s) are close to those reported by others in subjects with similar characteristics (1.34±0.7 s, e.g. Samozino et al. (2015)).

Significant relationships were observed in this study between 100 m PB and v_{peak}, F_{peak}, P_{mean}, P_{peak} and τ but not with v_{mean} and F_{mean}. These results are in agreement with data reported by Slawinski et al. (2015) who indicate that 100 m personal best times are better related to the average power output (R = -0.69) in the first 20 m of a 100 m race than to the average running velocity over this distance (R = -0.29). The correlation coefficient reported in this study for P_{mean} (R = -0.65) is similar to the one reported by these authors.

Our results show that the variability (CV%) in the values of mean and peak velocity over the 20 m distance (8-9%) is lower than the variability in the mean and peak values of force and power (15-30%). This indicates that F and P are better indicators (than v) of the inter-subject variability in the acceleration phase of a sprint.

Muscle-Tendon variables

Our data of muscle thickness, pennation angle, fascicle length and Achilles tendon length and CSA are comparable to data reported in literature in subjects with similar characteristics (Kumagai et al., 2000; Kubo et al., 2016; Silbernagel et al., 2016; Ryan et al., 2013).

Our results suggest that muscle thickness is positively correlated with power production during sprint running in agreement with previous studies that highlighted a relationship between muscle thickness and power output (Shoepe et al., 2003) and in agreement with Kubo et al. (2016) who reported that muscle thickness of knee extensor and plantar flexors is significantly greater in sprinters than in controls. Miyake et al. (2017) reported no relationship between 100 m personal best

time and the quadriceps CSA; we suggest that this finding, rather than to a lack of relationship between CSA and sprint abilities, which should be expected on theoretical basis, could be attributed to the fact that "average speed", instead of power output, was taken into account.

An increase in muscle thickness (e.g. as a result of a strength training protocol) is associated to a greater force production capacity of the muscle (Lieber, 1992). Hence, a muscle with a larger muscle thickness is expected to exert a larger force on the ground; accordingly, the acceleration ability of the athlete is expected to improve, due to the positive relationship between force production and acceleration performance (Morin et al., 2012; Seitz et al., 2014).

Another important aspect of muscle architecture in relation to sprint running performance regards muscle length. As suggested by Abe et al. (2000), a greater fascicle length would confer greater velocity capacity, during identical tendon excursion, in the sprint acceleration phase. This because a fiber containing more sarcomeres in series would contract at a greater velocity than a fiber containing less sarcomeres in series; as a result, power production is expected to be greater in the former case, as well as sprint performance (Lieber, 1992). Our data support this theoretical background, in fact, we observed a strong positive correlation between (relative) fascicle length and mechanical power production (see Table 2), in agreement with other studies (Lieber, 1992).

Finally, because pennation angle "geometrically" depends on muscle thickness and fibre length, it is also expected to play an important role on sprint running performance. This was previously observed by Kumagai et al. (2000) who reported a positive relationship between pennation angle and 100 m PB; accordingly, we observed a negative relationship between pennation angle and sprint velocity. It is possible that a fiber with a greater pennation angle operates closer to its optimum length and, based on the length-tension relationship, is thus able to generate more force (Muhl, 1982). In fact, pennation affects the relative velocity of fibre shortening. To generate a given degree of shortening in the whole muscle, individual muscle fibres in a pennate muscle have to shorten further than those in a fusiform muscle (Azizi et al., 2008). Consequently, for any given velocity of whole muscle movement, the more pennate the muscle the closer to their maximum velocity the individual fibres are working. However, as suggested by Azizi et al. (2008) the fibre rotation that occurs during a contraction contributes to increase the shortening velocity of the whole muscle by allowing the muscle to function at a higher gear ratio. Therefore, this mechanism may potentially increase mechanical power production for a given overall muscle shortening speed in pennate compared to non-pennate muscle.

An important result of our study is the strong positive relationship between mechanical power output during a sprint and Achilles tendon CSA and length. Indeed, tendon morphological characteristics could influence its mechanical proprieties (e.g. its stiffness). As an example, Bohm et

al. (Bohm et al., 2015) showed that a higher stiffness and a larger CSA of the Achilles tendon could have a positive effect on running performance, influencing the stretch-shortening cycle and Lai et al. (Lai et al., 2016) showed, based on experimental data and computational modeling, that tendon elasticity plays an important role in enhancing power output at the start of a maximal sprint. A greater tendon CSA (e.g. as a result of training adaptation) should thus allow the runner to withstand a larger mechanical stress (allowing the sprinter to reach higher running speeds). Indeed, we observed that the faster runners are those with the greater Achilles tendon CSA, as previously reported by others (Ryan et al., 2013).

Critique of methods

Radar devices estimate the displacement of the body center of mass based on the displacement of the subject's lower back. During a sprint start, the BCoM position changes in relation to the lower back position; moreover, BCoM rises vertically while the radar or laser tripod height does not change (di Prampero et al., 2005). Therefore, based on these methods it is possible to calculate, using the fundamental laws of dynamics, horizontal force but not its vertical component; moreover, the fluctuations of velocity at each step (both along the vertical and horizontal axes) are not taken into account. Hence, even if the radar technology is considered a valid and reliable method for measuring sprinting speed (Simperingham et al., 2016), it is important to remember that force and power values determined with this method are underestimated compared to the real values.

It must be pointed out that, in a sprinting task, the aim is to cover in the shortest possible time a given horizontal distance; therefore, we think that the results of this study are meaningful and of interest even if the values of force were calculated (and not measured directly) in the forward direction only. Further studies should ascertain whether the strong correlations reported in this study between F and P and muscle-tendon characteristics still hold when F and P are directly measured (e.g. by means of force platforms).

CONCLUSIONS

The findings of this study improve our understanding of the interplay between muscle-tendon characteristics and sprint performance: the stronger correlations are observed between muscle-tendon parameters and peak power output and this suggests that considering/measuring this parameter: i) could allow to better understand the relationship between musculoskeletal morphometry and sprinting ability; ii) could allow to better understand the interplay between all these factors in determining sprint performance and iii) could increase the possibility to detect significant training induced changes.

These findings have implications not only for track and field sports but for all team sports involving sprinting that rarely cover more than 20 m in a straight line (e.g. rugby, soccer and football). This study provides information about how the architectural characteristics of knee extensors, plantar flexors and Achilles tendon contribute to power generation during a sprint running acceleration phase. These data show that the relationship between muscle tendon parameters and sprinting performance is particularly evident in the sprint acceleration phase were the largest forces are exerted and peak power is attained.

CHAPTER 3
NON STEADY-STATE RUNNING: STUDY 2

COMPREHENSIVE MECHANICAL POWER ANALYSIS IN SPRINT RUNNING ACCELERATION

Authors: Gaspare Pavei[1], Paola Zamparo[2], Norihisha Fujii[3], Takuya Otsu[3], Naoki Numazu[3], Alberto E. Minetti[1], Andrea Monte[2]

1 Department of Pathophysiology and Transplantation, University of Milan, Italy

2 Department of Neuroscience, Biomedicine and Movement Sciences, University of Verona, Italy

3 Faculty of Health and Sport Sciences, University of Tsukuba, Japan

ABSTRACT

Sprint running is a common feature of many sport activities. The ability of an athlete to cover a distance in the shortest time relies on his/her power production. The aim of this study was to provide an exhaustive description of the mechanical determinants of power output in sprint running acceleration and to check whether a predictive equation for internal power designed for steady locomotion is applicable to sprint running acceleration. Eighteen subjects performed two 20 m sprints in a gym. A 35-camera motion capture system recorded the 3D motion of the body segments and the body center of mass (BCoM) trajectory was computed. The mechanical power to accelerate and rise BCoM (external power, P_{ext}) and to accelerate the segments with respect to BCoM (internal power, P_{int}) were calculated. In a 20 m sprint, the power to accelerate the body forward accounts for 50% of total power; P_{int} accounts for 41% and the power to rise BCoM accounts for 9% of total power. All the components of total mechanical power increase linearly with mean sprint velocity. A published equation for P_{int} prediction in steady locomotion has been adapted (the compound factor q accounting for the limbs' inertia decreases as a function of the distance within the sprint, differently from steady locomotion) and is still able to predict experimental P_{int} in a 20 m sprint with a bias of of 0.70 ± 0.93 W kg^{-1}. This equation can be used to include P_{int} also in other methods that estimate external horizontal power only.

Published in: *Scandinavian Journal of Medicine and Science in Sports, 29: 1892-1900, 2019*

INTRODUCTION

Sprint running is a multifactorial skill composed of three phases: the acceleration, the maximum velocity and an eventual deceleration phase (Ross et al., 2001). The acceleration phase is one of the most important components in many sports, such as track and field events and football (e.g. the ability to accelerate in the first meters of a sprint allows a football player to catch the ball before the opponent). The ability to accelerate is related to the capacity to produce and apply high amounts of horizontal force and power (Hunter et al., 2005; Morin et al., 2011; Slawinsi et al., 2015; Rabita et al., 2015; Samozino et al., 2015; Monte et al., 2016). Sprint performance has been traditionally analysed with split times (e.g. with gates at known distance) or velocity (e.g. with GPS or radar systems) (Haugen et al., 2016). However, these methods/parameters do not investigate the mechanical determinants of that performance. Quantifying an athlete's sprint mechanics with force and power related parameters requires more complex and expensive equipment (e.g. force platforms or instrumented treadmills; Sawinski et al., 2015; Rabita et al., 2015; Cavagna, 1975). Although this approach seems inaccessible and impractical for many coaches, the improved understanding of sprint mechanics can be used to better inform performance and exercise selection during training.

The first pioneering attempts to quantify mechanical work and power during sprinting are from the beginning of the 19th century (Furusawa et al., 1927; Best, 1930; Fenn, 1930). In those papers the authors described the human capability to exert maximal power output. Since the 1960s a method for calculating mechanical work (or power) in locomotion emerged based on the König theorem. The work done to locomote is partitioned into the work performed to accelerate and lift the body centre of mass, and the work performed to accelerate the limbs with respect to the body centre of mass (Cavagna et al., 1963). Since then this method has been applied to many human and animal activities from walking to swimming (Minetti et al., 1994; Heglund et al., 1995) and has allowed the metabolic cost of several locomotion/tasks to be explained (Minetti et al., 1994; Heglund et al., 1995; Pavei et al., 2015; Zamparo et al., 2016). To date, this method has not been comprehensively applied to sprint running. Cavagna and colleagues (1971) did not examine the work done by the limbs, while Fenn focused exclusively on the maximal velocity phase. Consequently, relative to constant speed running, a detailed mechanical description of the acceleration phase is still lacking.

In the last decades researchers have focused their attention on lower limb dynamics to determine the amount of power generated by the different joints in sprint running, but only a few steps were analyzed in these studies (e.g. (Bezodis et al., 2014; Lai et al., 2016). Although this approach provides some insight of sprint performance by ranking joints according to the amount of power produced, it does not yet account for the athlete's entire power output. More recently, a new simpler method to calculate sprint running power output has been developed with the aim to be easily

computed and handled by coaches directly in the field (samozino et al., 2015; Cross et al., 2017; Mendiguchia et al., 2016). However, its current formulation involves only the progression (horizontal) velocity, without considering other crucial (and unavoidable) mechanical components that should be quantified and included. The purpose of these studies was to provide indexes of sprint power output rather than to quantify the whole power exerted by the sprinting or accelerating athlete. However, computing all the mechanical components of the sprint acceleration phase is necessary to give a precise estimation of the whole power that the athlete is able to exert (which is indeed the highest in the sprint running acceleration phase). These values of total mechanical power can then be used for comparing tasks or gaits even between different species. Moreover, mechanical power affects metabolic load, which can be better estimated when all the mechanical components are included.

Based on the aforementioned literature, the aims of this study were: i) to provide a comprehensive and detailed description of the mechanical determinants of the power output in the sprint running acceleration phase, similarly to other constant speed human gaits, and ii) to check whether a predictive equation for internal power designed for steady locomotion is also applicable in sprint running acceleration, so that it can be also implemented in new methods.

MATERIALS AND METHODS

Participants

Eighteen healthy male subjects were recruited for this study (22.7±1.8 years old, 66.9±11.4 kg body mass, 1.73±0.07 m height, mean±SD). They participated in different sports activities (athletics, tennis, soccer and handball) for 2.1±0.7 hours per day, 4.6±1.6 times per week, on average. The study was in agreement with the Declaration of Helsinki on human subjects and the ethical committee of the Department of Neuroscience, Biomedicine and Movement Sciences at the University of Verona approved the experimental protocol. All participants gave their written informed consent to the experimental procedure.

Experimental Protocol

Following a 10-minutes warm-up, participants ran two 20 m maximal sprints in a gym separated by three minutes recovery. Participants started from a semi-crouched position, with one foot on the starting line, the other freely behind and one hand touching a 0.3 m high cone; no starting blocks or spike shoes were used.

Data Analysis

Three-dimensional body motion was sampled by a 35-camera motion capture system (Vicon, Oxford Metrics, UK, composed of 13 T20s; 12 T20; 2 T10s; 8 T10 cameras) at 100 Hz. The spatial coordinates of 18 reflective markers located on the main joint centers of the limbs were captured (Minetti et al., 1993; Pavei et al., 2017). Marker positions were post-processed through a 'zero-lag' second-order low-pass Butterworth filter with a cut-off frequency (8±1 Hz) detected by a residual analysis on each marker coordinate (Winter,1979). The time-course of the body center of mass (BCoM) position was computed as a weighted mean from an 11-segment model (Minetti et al., 1993; Pavei et al., 2017) based on Dempster's inertial parameters of body segments (Winter, 1979). From the 3D BCoM trajectory, the time course of potential (PE) and kinetic (KE) energies were computed to obtain the total mechanical energy (TE =PE +KEx +KEy +KEz, where x is the antero-posterior axis, y the medio-lateral axis and z the vertical axis). Positive external power (P_{ext}, $W \cdot kg^{-1}$) was calculated as the summation of all increases in the TE time-course divided by time, and represents the power necessary to lift (Pv =PE+KEz) and accelerate (Pf =KEx) the BCoM (Cavagna et al., 1977). The power to accelerate the BCoM medio-laterally (Pl = KEy) was also calculated, despite a normally negligible contribution to straight line running (Cavagna, 1975). The power necessary to rotate and accelerate the limbs with respect to the BCoM (the internal power, P_{int}, $W \cdot kg^{-1}$, Pavei et al., 2015; Cavagna & Kaneko, 1977) was calculated from the movement of the segments with respect to BCoM as translational and rotational kinetic energy of each segment (Fenn, 1930; Pavei et al., 2015; Minetti et al., 1998) and was summed to P_{ext} to obtain the total mechanical power (P_{tot}, $W \cdot kg^{-1}$) (Cavagna & Kaneko, 1977). From kinematic data, mean velocity (v, $m \cdot s^{-1}$), stride frequency (SF, Hz) and duty factor (d), defined as the fraction of contact time within the stride duration, were calculated. These kinematic parameters were also used to compute predicted P_{int} according to Minetti's model equation (Minetti et al, 1998):

$$Pint = SF \cdot v^2 \cdot \left[1 + \left(\frac{d}{1-d}\right)^2\right] \cdot q$$

where q is a compound factor that accounts for the limb mass and for the spatial configuration of limb segments during locomotor phases: in constant speed human walking and running q = 0.1. Differently, locomotion is occurring at unsteady speed in the present investigation and q has been computed at each step by dividing the experimental P_{int} value by the other kinematic parameters. In order to build up a P_{int} predictive framework for sprint acceleration over different distances, which could be handy in field conditions, representative mean q for sub-distances ($q_{subdist}$) were obtained

by averaging step q values from the sprint start to each sub-distance. Then the relationship between $q_{subdist}$ and sub-distances was statistically fit by a power equation (see Results) so that, were P_{int} of whichever sprint running acceleration shorter than (or equal to) 20 m, it could be predicted by feeding all (measured and estimated) terms into the above equation.

To test the predictive procedure/equation, we randomly assigned the two trials of each subject to a 'model training' and a 'prediction testing' data set, respectively. The kinematic parameters and the experimental P_{int} values of the first data set were used to obtain $q_{subdist}$ as described above. The second data set was used to check the reliability of model equation for unsteady running by comparing, pairwise for each subject, experimental P_{int} to predicted P_{int}; the latter was computed for each sub-distance according to the measured kinematic parameters (v_{mean}, SF and d) and the inferred $q_{subdist}$ values (from the power regression of the first data set). Bland-Altman plots were used to explore the comparisons.

The agreement between experimental and predicted P_{int} was presented as a function of the whole sprint distance (20 m) and three sub-distances (0-5 m, 0-10 m and 0-15 m) in order to test the validity of the predictive equation also for shorter distances. Contact time, needed for defining duty factor, was calculated via the sagittal position and vertical velocity of the 5^{th} metatarsal marker because all the subjects showed a forefoot support during the entire stance phase. Vertical velocity and antero-posterior displacement of the 5^{th} metatarsal marker are null during stance (since the subject is moving overground and foot velocity falls to zero at each contact) and two distinct changes in the slope of both velocity and sagittal position vs. time can be detected at foot touchdown and take-off. Data were analysed with a custom written software (LabVIEW 10, National Instrument, USA).

Statistical analysis

Data were presented as mean ± standard deviation (SD). Pearson statistical test and the square of Pearson correlation coefficient (R^2) were used to examine the linear and power relationship between variables. Bland-Altman plot was used for comparison between predicted and experimental values of P_{int}. Statistical significance was set at $p<0.05$. Statistical analyses were performed with SPSS version 24 (IBM).

RESULTS

Mean 20 m velocity (of BCoM) was 5.81±0.43 $m \cdot s^{-1}$ and max velocity was 7.66±0.64 $m \cdot s^{-1}$. P_{ext}, P_{int} and P_{tot} increased linearly with velocity (Figure 3.1) and P_{ext} was the major determinant (59%) of P_{tot} (Figure 2).

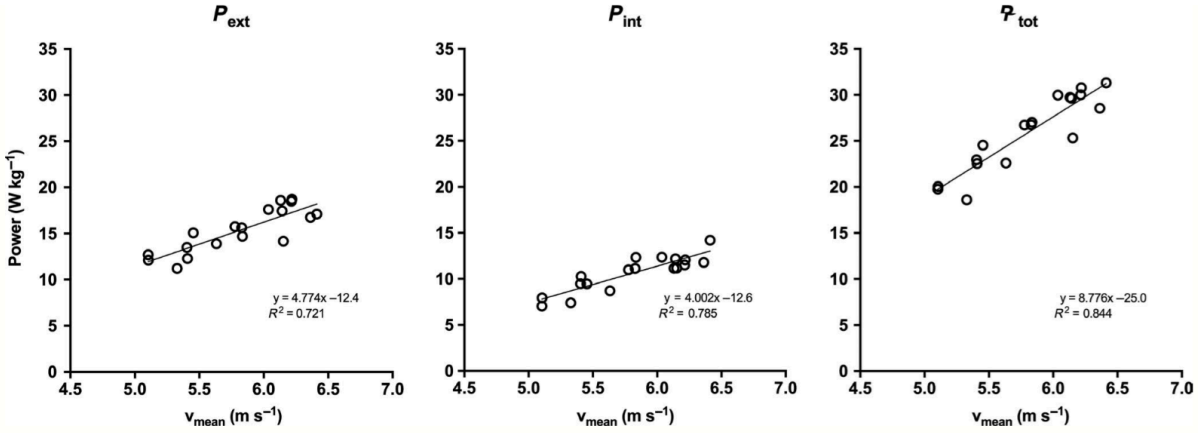

Figure 3. 1: Mechanical power (W kg-1) as a function of mean sprint velocity, the faster subjects show higher mean velocity (each point represents a subject and is the average value between the two trials).

P_{ext} was mainly composed of Pf with a 12% contribution of Pv (Figure 2); the contribution of Pl (not shown in Figure 3.2) was negligible (only 1%).

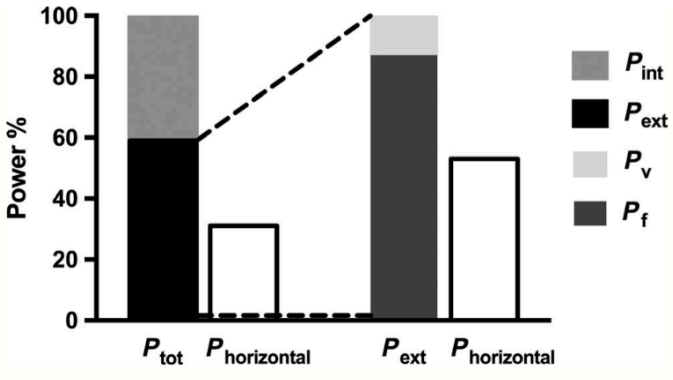

Figure 3. 2: The average mechanical power of the whole 20 m sprint acceleration has been partitioned in its components and represented as percentage of Ptot or of Pext. Ptot: total mechanical power; Pext: mechanical external power; Pint: mechanical internal power; Pf: mechanical power to accelerate the BCoM forward; Pv: mechanical power to lift the BCoM. Phorizontal the mechanical power calculated with the simple method (Samozino et al., 2015) is expressed as percentage of Ptot and of Pext in left and right histograms, respectively

In Figure 3.3, P_{ext}, P_{int} and P_{tot} are shown as a function of sprint time and distance: P_{tot} and P_{ext} peak within the first 5 meters then constantly decrease, whereas P_{int} reaches a plateau between 5 and 10 m from the start and then keeps its value constant.

Stride frequency did not change with sprint distance (Figure 3.4A), whereas duty factor and q decreased from the start to the end of the sprint (Figures 4B and C). The compound factor $q_{subdist}$ decreased with sprint distance with a power decay: $q_{subdist} = 0.255x^{-0.236}$, where x is sprint distance (m) (R^2=0.993; $p<0.001$, Figure 3.4D) and asymptotically approached 0.1 (as in constant speed running).

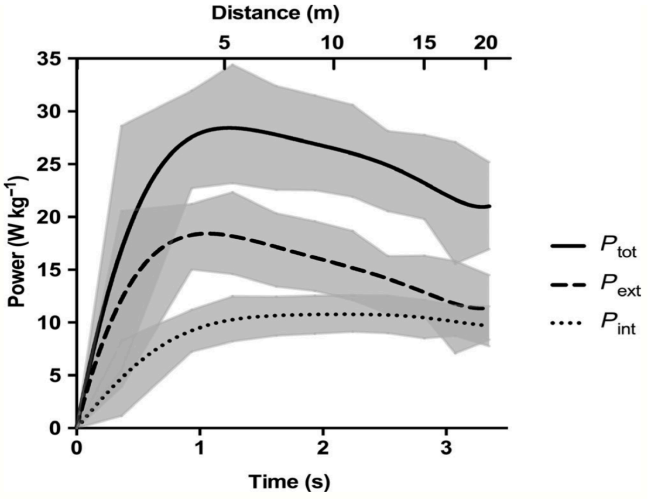

Figure 3. 3: Mechanical power (W kg-1) as a function of sprint time and distance (lines represents the average values of the subjects). Pext: mechanical external power; Pint: mechanical internal power and Ptot: total mechanical power. Gray area represents the standard deviation.

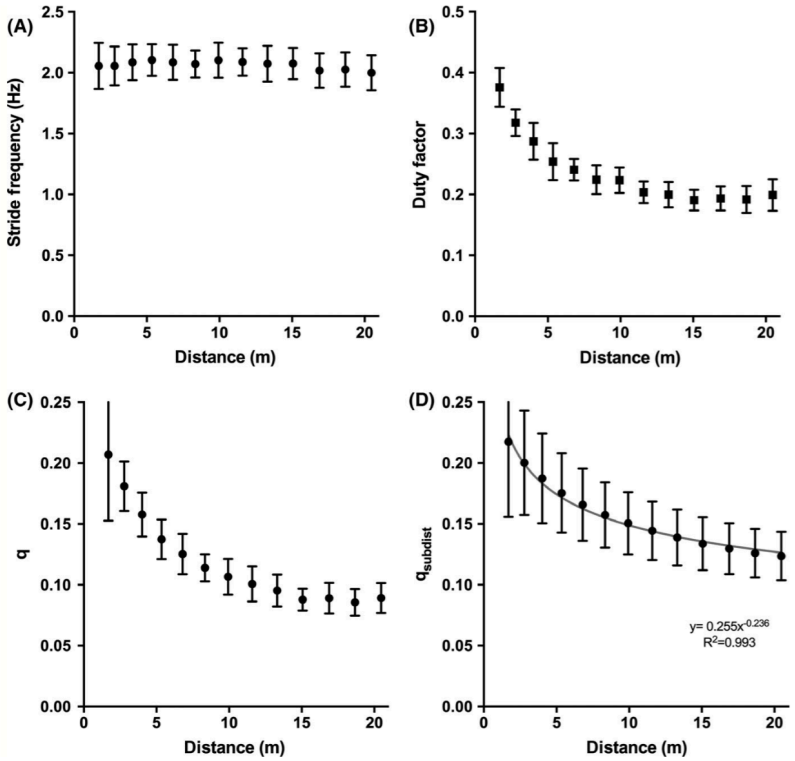

Figure 3. 4: Stride frequency (SF, Hz, A), duty factor (B), and the compound factor q (C) are shown as a function of sprint distance (m). Values are mean ± SD for each single step (all subjects) in the acceleration sequence. The $q_{subdist}$ the average of q values from the sprint start to each sub-distance, was calculated for half of the trials only and is shown in panel D. This factor has been used for the prediction of the mechanical internal power over the four distances (see text for details)

When individual SF, duty factor, v_{mean} and $q_{subdist}$ (per step, as in Figure 3.4) are used in Minetti's model (Minetti et al., 1998), the prediction of P_{int} at the different sprint distances is obtained. In Figure 3.5, Bland-Altman plots of P_{int} values for each subject are shown over the whole sprint

distance (0-20 m) and at the three sub-distances (0-5, 0-10 and 0-15 m). The mean difference between predicted P_{int} and experimental P_{int} was 0.17, 0.63, 0.83 and 0.70 $W \cdot kg^{-1}$over 0-5, 0-10, 0-15 and 0-20 m, respectively. A small uniform systematic error was present at the sub-distances; the random error was uniform without a tendency to over or underestimate P_{int} across the mean P_{int} values, and no significant trends were found in the regression lines for any sprint distance (0-5m y= -0.282x +2.805, R=0.39, p=0.11; 0-10m y= -0.053x +0.079, R=0.089, p=0.73; 0-15m y= 0.065x +0.123, R=0.141, p=0.58; 0-20m y= 0.113x -0.479, R=0.223, p=0.37).

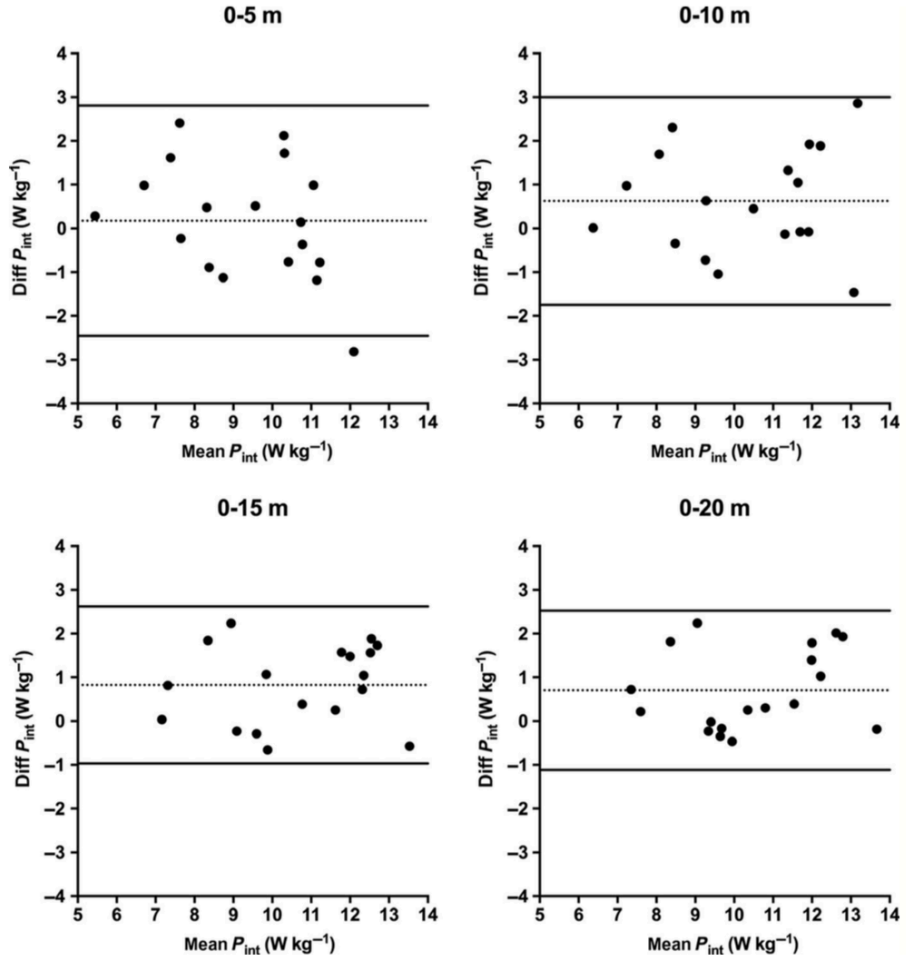

Figure 3. 5: Bland-Altman plots of predicted and experimental mechanical internal power (Pint, W kg−1) over 0-5, 0-10, 0-15 and 0-20 m. The label on the ordinate axis represents the difference between predicted and experimental mechanical internal power; positive values mean overestimation of the prediction. Dotted line and continuous lines represent mean difference and 95% limits of agreement respectively. Each point is the trial of a subject that was not used for the $q_{subdist}$ computation.

DISCUSSION

The whole mechanical power exerted during a maximal sprint over a 20 m distance can be partitioned into the power to accelerate the body forward (Pf) that accounts for 50% of the total power, the power to accelerate/rotate limbs with respect to BCoM (P_{int}) that accounts for 41% of the total power and the power to rise BCoM (Pv) that accounts for 9% of the total power. To our knowledge, this is the

first study that analyses mechanical power in such a detail, highlighting the relative contribution of the different components to mechanical power production. In a previous investigation, where P_{int} was not measured, Cavagna and colleagues (1971) used force plates to work out P_{ext} and its components (Pf and Pv) during sprint running. Their results are similar to those reported in the present study. Thus, inverse and forward dynamics, which often differ in their prediction in constant speed running (Pavei et al., 2017; Pavei et al., 2015) because of a bias localization of BCoM of the former methodology, concur to reveal the same dynamics in the acceleration phase of a sprint. As inverse dynamics is unable to account for the visceral mass oscillation in affecting BCoM position (Minetti et al., 1994; Cazzola et al., 2014), the similar mechanical results obtained by means of the methods suggests that visceral mass vertical oscillation excursion is decreased in the acceleration phase of sprint running due to a diminished 'bounciness' of the spring-mass system. By analyzing the BCoM vertical trajectory during our acceleration phase (especially at the beginning), we found an almost nil downward displacement of BCoM, whereas the upward displacement was always present. This monotonically ascending BCoM behaviour is similar to that reported in uphill constant speed running (Minetti et al., 1994) and likely prevents the spring loading at each footfall (an equal compression and restore of the spring is the typical bouncy characteristic of constant speed level running). Moreover, this BCoM behaviour reinforces the idea that acceleration running can be assimilated to constant speed running up on a gradient 'equivalent slope' (di Prampero et al., 2005; Minetti & Pavei, 2018).

With the exception of the quoted paper by Cavagna et al. (1971), a direct comparison of mechanical power with other sprint studies (e.g. Rabita et al., 2015; Nagahara et al., 2016)) is difficult. For example, Rabita et al. (2015) measured the instantaneous vertical, horizontal and mediolateral forces, and the resultant force. However, these data were averaged for each contact phase and consequently the values of mechanical power represent the mean power during the stance phase only. The mean mechanical (external) power output (P_{ext}) obtained in these sprint trials (15.3±2.4 $W \cdot kg^{-1}$) is in line with Margaria's et al. (1966) mechanical power values exerted during the run-up staircase test: 15.2±2.7 $W \cdot kg^{-1}$in an aged matched cohort of subjects. Margaria's test was designed to estimate the maximal anaerobic power (due to anaerobic alactic mechanisms) exerted mainly by the lower limbs (without considering P_{int}). The work done to accelerate limbs with respect to BCoM was already shown to be an important part of total work in accelerated locomotion, such as shuttle running (Zamparo et al, 2016; Zamparo et al., 2019), compared with steady locomotion (i.e. continuous running (Minetti, 1998). Our results support this evidence, with P_{int} reaching the 41% of P_{tot} (Figure 3.2) and 69% of P_{ext}, highlighting that P_{int} cannot be disregarded in all accelerative/sprinting activities when mechanical (and metabolic) power/work is computed. P_{int} can be calculated only with

the kinematic analysis of the limbs, however Minetti (1998) developed a model equation that estimates P_{int} values based on some simple kinematic parameters (SF, duty and a compound factor, q); this equation was verified in steady (human and animal) locomotion (walking and running/trotting/galloping). With the present data on sprint acceleration, we showed that the model is still able to predict P_{int} thanks to a speed/distance independency of stride frequency and an expected decrease in duty factor. The compound factor q has been adjusted in relation to sprint length because of its decay (distance dependent). This behaviour is different from constant speed locomotion, but could be expected because of the change in the limbs' configuration (Minetti & Saibene, 1992) from the start to the maximal speed (Nagahara et al., 2014) and the constant value of 0.1 is approached asymptotically. With this adjusted q factor ($q_{subdist} = 0.255x^{-0.236}$, R^2=0.993, where x is sprint distance (m), see Figure 3.4D) the new P_{int} predictive equation is:

$$P_{int} = SF \cdot v^2 \cdot \left[1 + \left(\frac{d}{1-d}\right)^2\right] \cdot 0.255 \cdot x^{-0.236}$$

($W \cdot kg^{-1}$). This equation can predict experimental P_{int} with a systematic error of 0.70±0.93 $W \cdot kg^{-1}$ on a 20 m sprint without a tendency to over- or under-estimate across mean power values (Figure 3.5). The proposed equation also showed good agreement on shorter sprint distances, with a small systematic overestimation and a uniform random error (Figure 3.5). This updated equation can be used to estimate and add P_{int} to the P_{ext} calculated by force plates or by other simpler methods (see below) that do not measure limbs displacement.

In recent years a simpler kinematic approach has been developed for power output computation during accelerated running (Samozino et al., 2015). It considers the time course of a runner's velocity that can be easily measured by laser-assisted or other time/gate devices (Samozino et al., 2015; Morin et al., 2016; Romero-Franco et al., 2017; Pantoja et al., 2016; Pantoja et al., 2018). From the time course of BCoM velocity of our subjects, we also computed the horizontal power as proposed by Samozino et al. (2015): i) by fitting the time course of the subject's velocity with a mono- exponential equation, which was ii) time differentiated to obtain acceleration and iii) by multiplying acceleration and velocity, mass-specific power was obtained ($W \cdot kg^{-1}$), iv) the mean of which was considered as horizontal power ($P_{horizontal}$) and compared with our values (Figure 3.6).

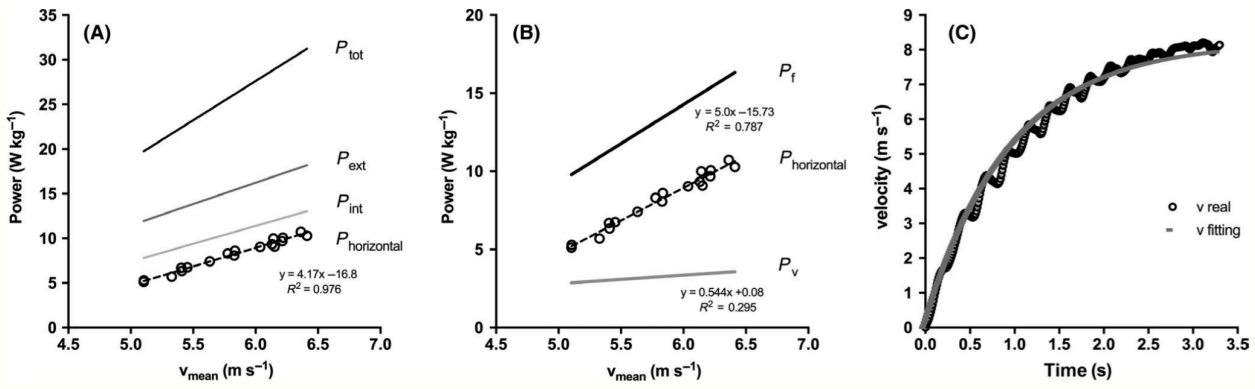

Figure 3. 6: Sprint variables. A, mechanical power (W kg^{-1}) as a function of 20 m sprint mean velocity. Black, dark gray and light gray lines refer to total mechanical power (Ptot), mechanical external power (Pext) and mechanical internal power (Pint) respectively; open circles with dashed line refer to the mechanical power calculated with the simple method (Phorizontal) (each point represents a subject and is the average value between the two trials). B, mechanical power (W kg^{-1}) as a function of 20 m mean sprint velocity. Black line represents the power to accelerate the BCoM forward (P_f), gray line represents the power to lift the BCoM (P_v), open circles with dashed line refer to $P_{horizontal}$ (each point represents a subject and is the average value between the two trials). C, typical time course of the forward velocity during the 20 m sprint. Open circles refer to measured velocity, gray line shows the mono-exponential fitting of measured velocity

This figure shows that since the proposed approach (Samozino et al., 2015) based on $P_{horizontal}$ does not consider limbs' movements, $P_{horizontal}$ values cannot reach our P_{tot} values (Figure 3.6A and Figure 3.2) as P_{int} is not included. $P_{horizontal}$ should approach P_{ext}, however, when comparing $P_{horizontal}$ with P_{ext} a remarkable difference was still present (~47%, Figure 6A and Figure 3.2). This occurs because $P_{horizontal}$ does not take into account the vertical rise of BCoM (i.e. Pv) at the beginning of the sprint acceleration and at each stance phase, where BCoM lowers its trajectory in the first half of the stance and has to be redirected upward for the next bounce in the second half (Cavagna et al., 1964). Furthermore, when $P_{horizontal}$ is compared with Pf (the power to accelerate BCoM in the forward direction), an underestimation (~39%, Figure 3.2) is still evident (Figure 3.6B). This discrepancy can be understood by analysing the time course of BCoM velocity (Figure 3.6C). The mono-exponential fitting used in $P_{horizontal}$ (the simple method proposed by Samozino et al., 2015) does not account for the velocity oscillation that occurs at each foot contact, where the foot touches the ground in front of BCoM causing a braking/decelerating action. This occurs because, differently from moving on wheels, humans expose their BCoM to deceleration/acceleration sequences at each foot contact in their rimless-spoked-wheel locomotion (Cavagna, 2010). During running, this causes a velocity oscillation along the mean (monotonically) increasing velocity of the subject that deviates from the mono-exponential fitting (Figure 3.6C). The difference between Pf and $P_{horizontal}$ can thus be considered to represent the power for accelerating BCoM forward at each stance; this power difference is greater at the beginning of a sprint and becomes negligible at the end of the acceleration phase (Figure 3.6C). Hence, $P_{horizontal}$ represents the minimum amount of mechanical power necessary to horizontally accelerate a mass equal to the athlete body mass, as when moving on wheels. It is

important to note that the Samozino's method was validated in comparison with the force plates method. However, as previously said, the authors compared the radar gun method with the force plates by using the average values of force during the stance phase and not the whole force time-course. Therefore, as for the velocity time course presented in Figure 3.6C, an underestimation of the real power values is expected when using average forces. Our data suggest that, in addition to $P_{horizontal}$, other mechanical components are needed to accelerate during a sprint, such as BCoM vertical displacement and P_{int} (that can be implemented with the aforementioned equation), and should be accounted for.

At the end of this complete dissection of mechanical power during sprint acceleration, we can conclude that the power to accelerate and rise BCoM is the major determinant of the total power output (59%) and the power to accelerate the limbs with respect to BCoM (41%) is also an important determinant that cannot be disregarded when computing the total mechanical power output needed to sprint.

CONCLUSIONS

This whole description of mechanical power partitioning during a 20 m sprint highlights the determinants of sprint performance and could be used to better estimate the athlete's training load and to check possible imbalances in the partitioning of the power output. The power to accelerate the limbs can also now be computed in the acceleration phase of sprint running based on simple kinematics parameters, without the need of an expensive and cumbersome motion capture setup, by employing the adapted form of Minetti's model equation proposed here. The simple method commonly used to quantify and test an athletes' mechanical power during sprint can be improved by considering internal power and velocity fluctuations in order to obtain a more precise estimate that can also be compared to power output from other human and animal gaits.

CHAPTER 4
NON STEADY-STATE RUNNING: STUDY 3

MECHANICAL WORK IN SHUTTLE RUNNING AS A FUNCTION OF SPEED AND DISTANCE: IMPLICATIONS FOR POWER AND EFFICIENCY

Authors: Paola Zamparo[2], Gaspare Pavei[1], Andrea Monte[2], Francesca Nardello2, Takuya Otsu[3], Naoki Numazu3, Norihisha Fujii[3], Alberto E. Minetti[1]

1 Department of Pathophysiology and Transplantation, University of Milan, Italy
2 Department of Neuroscience, Biomedicine and Movement Sciences, University of Verona, Italy
3 Faculty of Health and Sport Sciences, University of Tsukuba, Japan

ABSTRACT

Biomechanics (and energetics) of human locomotion are generally studied at constant, linear, speed whereas less is known about running mechanics when velocity changes (because of accelerations, decelerations or changes of direction). The aim of this study was to calculate mechanical work and power and to estimate mechanical efficiency in shuttle runs (as an example of non-steady locomotion) executed at different speeds and over different distances. A motion capture system was utilised to record the movements of the body segments while 20 athletes performed shuttle runs (with a 180° change of direction) at three paces (slow, moderate and maximal) and over four distances (5, 10, 15 and 20 m). Based on these data the internal, external and total work of shuttle running were calculated as well as mechanical power; mechanical efficiency was then estimated based on values of energy cost reported in the literature. Total mechanical work was larger the faster the velocity and the shorter the distance covered (range: 2.3–3.7 J m^{-1} kg^{-1}) whereas mechanical efficiency showed an opposite trend (range: 0.20–0.50). At maximal speed, over all distances, braking/negative power (about 21 W kg^{-1}) was twice the positive power. Present results highlight that running humans can exert a larger negative than positive power, in agreement with the fundamental proprieties of skeletal muscles in vivo. A greater relative importance of the constant speed phase, associated to a better exploitation of the elastic energy saving mechanism, is likely responsible of the higher efficiency at the longer shuttle distances.

Published in: Human Movement Science; 66: 498-496; 2019

INTRODUCTION

The majority of the studies on human or animal locomotion are conducted at steady/constant speed (e.g. treadmill locomotion or ground locomotion along a linear path) even if, in real life, human's and animal's gaits very often occur at variable/non-steady speed (Minetti et al., 2001; Minetti et al., 2013; Wilson et al., 2013; Wilson et al., 2015). As an example, during hunting, a predator combines speed, agility and endurance to maximize capture success; during these manoeuvres accelerations and deceleration phases, as well as turns and changes of direction are performed by both pray and predator in a race for survival (e.g. Wilson et al., 2013; Wilson et al., 2015). Besides a general interest in describing the fundamental aspects of non-steady legged locomotion in humans, the interest in these matters is driven by the need to understand the mechanics and energetics of activities typical of team sports where human's movement resemble indeed those of prey and predator, e.g. in the attempt to catch and keep possession of a ball (or to avoid that someone else gets hold of it). Indeed, in football, soccer or rugby large accelerations and decelerations can be observed, as well as turns and sudden changes of directions (e.g. di Prampero et al., 2015; Osgniach et al., 2010; Taylor et al., 2017).
Shuttle runs (SR) are a good model of unsteady locomotion: they are characterized by an acceleration phase (where mainly positive power is exerted), a deceleration phase (where mainly negative power is exerted) and a change of direction (CoD: a 180° turn) and can be performed at different speeds and over different distances.

The energetics of shuttle running has been only recently investigated (e.g. Bucheit et al., 2011; Buglione & di Prampero, 2013; Stevens et al., 2015; Zadro et al., 2011; Zamparo et al., 2014; Zamparo et al., 2015; Zamparo et al., 2016) because the energy expenditure during a single SR does not reach a steady state and thus cannot be easily determined. These studies have shown that the energy cost (C, J m^{-1} kg^{-1}), the energy expended per unit distance) in SR increases with shuttle velocity and decreases with shuttle distance (e.g. Buglione & di Prampero, 2013; Zamparo et al., 2014) and is far larger than the values of C generally reported during linear, constant speed running, a condition in which C is rather unaffected by the speed (e.g. Cavagna & Kaneko, 1977; di Prampero et al., 2015; Saibene & Minetti, 2003).

Shuttle running thus implies a significant increase in energy expenditure compared to running at constant-linear speed mainly because of the accelerations and decelerations phases but also because of the changes of direction; turns are indeed associated with additional energy expenditure relative to straight line walking or running (McNarry et al., 2017; Minetti et al., 2011; Zamparo et al., 2014; Wilson et al., 2013).

The mechanics of SR has received less attention so far. Only a recent study (Zamparo et al., 2016) reports data of mechanical work (W_{tot}, J m^{-1} kg^{-1}) in SR and only over a distance of 5 + 5 m.

The results of this study indicate that W_{ext} (the work to raise and accelerate the body center of mass - BCoM- within the environment) in SR is about twice that of linear, constant speed running and that W_{int} (the work to accelerate and decelerate the limbs in respect to the BCoM) accounts for 50% of total mechanical work when the shuttle velocity is high. In that study the energy cost of SR was also determined with the aim to calculate mechanical efficiency in SR (eff = W_{tot} /C); efficiency was found to be much lower than that reported for linear running (e.g. as reported by Cavagna & Kaneko, 1977) probably due to: i) lower elastic energy reutilization given the short distance covered, ii) more muscle co-activation required to stabilize the body (during turns) and iii) muscle fascicles probably working at less favourable lengths and velocities in SR than during constant linear running.

The aims of this study were: i) to obtain a comprehensive description of SR mechanics as a function of shuttle distance and velocity (mechanical data are reported only for a short shuttle distance, 5 + 5 m); ii) to investigate the implications that SR mechanics have on mechanical efficiency in non-steady speed conditions (available data suggest a lower elastic energy reutilization compared to linear running). In particular, we hypothesized that: i) total mechanical work per unit distance would increase as a function of velocity for each shuttle distance but, at any given velocity, it would decrease with the shuttle distance (as is the case for the energy cost of shuttle running); ii) mechanical efficiency would be larger the longer the distance covered (e.g. the smaller the time spent in the acceleration/deceleration phases).

A further purpose of this study was to compare positive and negative power production during the acceleration and deceleration phases of shuttle runs covered at maximal speed since no data in the literature are reported regarding the power that can be expressed by humans when decelerating (whereas the acceleration phase is quite extensively investigated in the literature, e.g. Nagahara et al., 2018; Slawinski et al., 2017).

MATHERIALS AND METHODS

Subjects

Experiments took place at the Biomechanics Facility of the University of Tsukuba (Japan). Twenty healthy Japanese (16 males and 4 females) were recruited for this study (22.3 ± 1.17 years of age, 67.0 ± 11.8 kg of body mass, 1.73 ± 0.07 m of stature); they were practicing different sports activities (athletics, tennis, judo and team sports such as basketball, soccer, volleyball and handball) 2.1 ± 0.9 h per day and 4.6 ± 1.6 times per week, on the average. Of these athletes, 13 declared to be familiar with the CoD. Informed consent was obtained from each participant in accordance with the approval of the Institutional Review Board of the Department of Neurosciences, Biomedicine and Movement Sciences of the University of Verona (Italy) (Agreement No. 5818, 2017). The study was in

agreement with the Declaration of Helsinki for the study on human subjects.

Technical setup and instrumentation

A motion capture system (Vicon MX, Oxford Metrics, UK) was utilised to record the 3D body motion; 35 cameras were utilised (13 T20s; 12 T20; 2 T10s; 8 T10) to cover the entire volume; kinematic data were acquired at a sampling rate of 100 Hz (see Fig. A.1 in Supporting Information). The coordinates (x: antero-posterior; y: medio-lateral, z: vertical) of 18 reflective markers located on the main joint centres were recorded so that the body was considered composed by 12 segments (trunk: greater trochanter/gleno-homeral axis; head: gleno-homeral axis/vertex; thigh: greater trochanter/femoral condyle; shank: femoral condyle/lateral malleolus; foot: calcaneous/tip toe; upper arm: gleno-homeral axis/elbow axis; forearm: elbow axis/ulnar styloid). The mass of each segment and the radius of gyration were determined according to Ae, Tang, and Yoki (1992) inertial parameters in order to calculate the 3D trajectory of the body center of mass (BCoM).

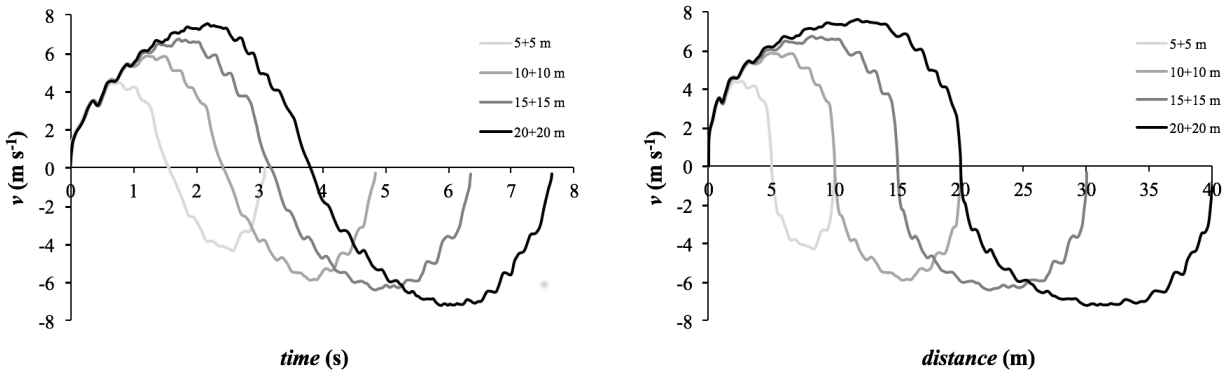

Figure 4. 1: BCoM horizontal velocity (m s-1) as a function of shuttle time (s, left panel) or distance (m, right panel) during shuttle runs over different distances: 5+5 m (light grey line); 10+10 m (grey line); 15+15 m (dark grey line) and 20+20 (black line).

Experimental design and procedure

The design of the study is non-experimental, descriptive and correlational.

All participants were requested to perform shuttle runs over a distance of 5 + 5 m, 10 + 10 m, 15 + 15 m and 20 + 20 m (with a 180° change of direction, CoD) at different self-selected paces (slow, moderate and maximal), during which kinematic data were recorded. Each subject performed 2 trials in each condition. An initial warm-up (i.e. running, specific gaits and CoD) was proposed to each athlete to familiarise with the procedures. The subjects used their own sport shoes and the pavement floor of the indoor Gym was in PVC (see Fig. A.1 in Supporting Information).

Subjects were requested to position the right foot over the starting line and to touch, with their right hand, a 30 cm tall cone positioned at their side; they were then requested to reach (and touch) a

second cone (positioned at a distance of 5, 10, 15 or 20 m) and to change direction a first time; after that they were requested to reach (and touch) the cone positioned at the starting line, to change direction again and then to stop, after one or two steps. No further indications were given so that the subjects freely chose when to stop the acceleration phase and start to decelerate.

The profile of horizontal velocity of the BCoM as a function of time or distance covered (at maximal velocity) is reported in Fig. 4.1 for a representative subject: this figure shows that each SR is composed by two acceleration and two deceleration phases; negative values of velocity are observed in the second half of the SR because of the change of direction. This figure also shows that, when shuttle distance increases the duration of the acceleration phase also increases so that larger values of velocity can be attained before the deceleration phase starts. This figure also indicates that the acceleration phase lasts more than the deceleration phase, over all shuttle distances.

Data analysis

Mechanical work calculations

Based on BCoM position data the time course of potential (Ep) and kinetic (Ek) energies was computed in order to obtain total mechanical energy (Et = Ep + Ekx + Eky + Ekz). The profiles of Et, Ep and Ek (in the x, y and z axes) as a function of the shuttle distance (at maximal velocity) are reported for a representative subject in Figure 4.2. This figure shows that Et increases in the acceleration phase and decreases in the deceleration phase over all distances and that Ekx contributes most to Et, followed by Ep, whereas the contribution of Eky and Ekz is negligible over all distances.

Positive external work (W^{+}_{ext}, J m^{-1} kg^{-1}) was calculated based on the summation of all increases in E_T time course (Cavagna & Kaneko, 1977); conversely, the summation of all decreases in E_T time course gives the negative external work (W^{-}_{ext}, J m^{-1} kg^{-1}) (Minetti et al., 1993). The work necessary to rotate and accelerate the limbs with respect to BCoM (the positive internal work, W^{+}_{int}, J m^{-1} kg^{-1}) was calculated according to Cavagna and Kaneko (1977) and Minetti et al. (1993). Finally, total mechanical work (W^{+}_{tot}, J m^{-1} kg^{-1}) was calculated as the sum of W^{+}_{int} and $W^{+}ext$ (as previously proposed for walking and running at constant, linear speed). Data of W^{+}_{int}, W^{+}_{ext} and $W^{+}tot$ are reported in the paper normalized per shuttle distance (e.g. expressed in J m^{-1} kg^{-1}). Data were analysed with a custom written software (LabVIEW 10, National Instrument, USA).

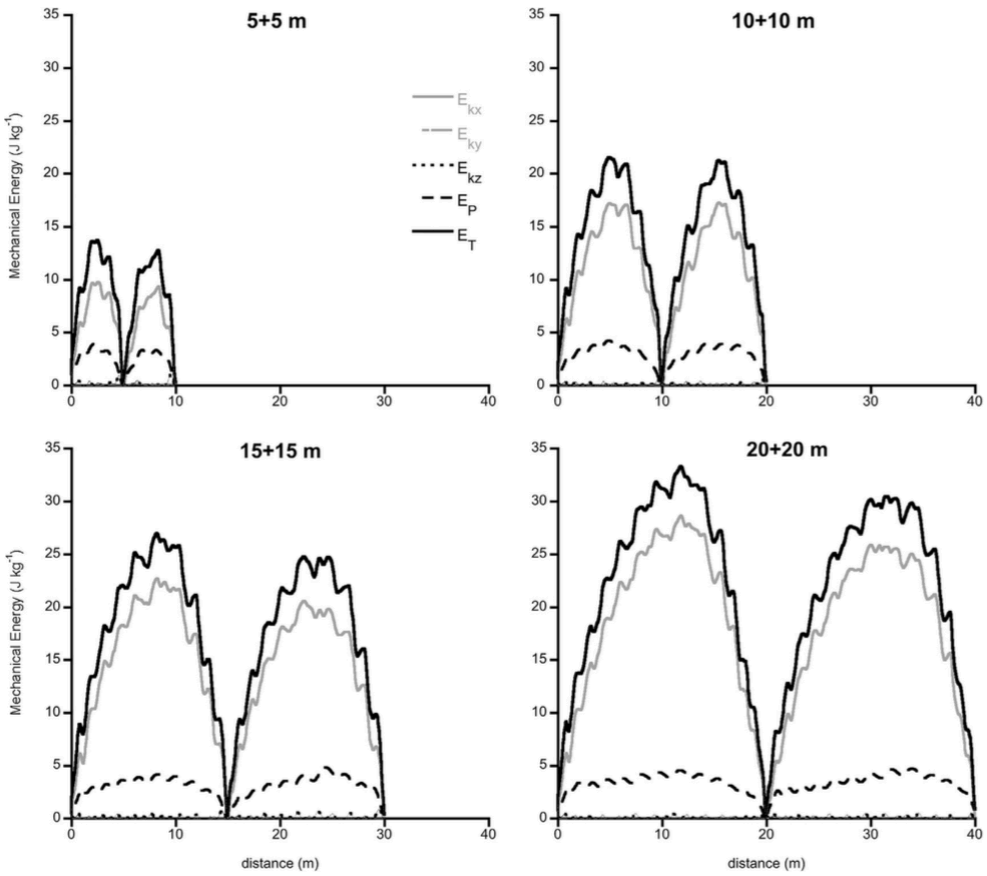

Figure 4. 2: Time course of BCoM kinetic (Ekx,: dark grey continuous line; Eky, dark grey dashed line; Ekz; black dotted line), potential (Ep, light grey continuous line) and total (ET, black continuous line) energies (J kg-1) as a function of shuttle distance during 5 + 5 m (top-left panel), 10 + 10 m (top-right panel), 15 + 15 m (bottom-left panel) and 20 + 20 m (bottom-right panel) shuttle runs.

Mechanical efficiency calculations ("apparent" efficiency)

In several studies referring to constant speed-linear walking or running, mechanical efficiency is calculated as $W^{+}_{tot} \cdot C^{-1}$, where

W^{+}_{tot} is calculated as described above and C is the net energy cost of walking/running (e.g. Cavagna & Kaneko, 1977; Pavei & Minetti, 2016; Saibene & Minetti, 2003; Willems et al., 1995, Peyré-Tartaruga & Coertjens, 2018). This efficiency is some- times defined as locomotion efficiency or "apparent" efficiency since it can assume values that exceed those of "pure" muscle efficiency (e.g. larger than 0.25–0.30). As an example, in constant speed linear running, "apparent" efficiency can be as large as 0.5–0.6 (Cavagna & Kaneko, 1977) and this indicates that mechanical work could result from elastic recoil of muscle tendon- structures, other than muscular work per se. In those forms of locomotion where no or little stretch occurs (e.g. cycling and swimming), the work generated by the muscles force almost entirely flows into the mechanical work measured at the whole-body level so that "apparent" efficiency is close to, or lower than, 0.25–0.30.

Thus, mechanical (or "apparent ") efficiency is not a measure/indication of muscle efficiency per se, since an increase in its values does not indicate that the muscles work in a more efficient way (as pointed out by Ettema, 2001); this efficiency is, however, calculated in locomotion studies to obtain insight into the mechanisms of conversion of metabolic energy into mechanical work (at the whole-body level) because it can help to understand whether work has be "recycled" via storage and release of elastic energy (e.g. an energy saving mechanism, as suggested by Alexander, 1991).

It goes without saying that the values of mechanical ("apparent") efficiency, for a given metabolic input (e.g. C), depend on the methods adopted to define, measure or calculate mechanical work in all its components (internal and external, positive and negative, see Discussion). In this study we adopted the methods described above, to be able to compare our efficiency data with those already reported in the literature for running (e.g. Cavagna & Kaneko, 1977) and shuttle running (Zamparo et al., 2016). In our previous work we reasoned on the differences between SR and constant speed linear running and we concluded that, since in SR braking can be substantial, also negative work (W^-_{tot} in both its components: W^-_{ext} and W^-_{int}) should be taken into account in the computation of efficiency whereas its metabolic counterpart is already included in the measured C. In that paper we show that, since negative and positive work ought to be the same ($W^+_{tot} = W^-_{tot}$, as is the case when running on the level), by assuming a constrained ratio between positive and negative work efficiency of 1:5 (compatibly with previously reported data from muscle physiology, e.g. Woledge et al., 1985), efficiency of positive work in SR can be calculated as: $eff^+_{tot} = 6/5\ W^+_{tot} \cdot C^{-1}$. The 6/5 term thus corrects eff^+_{tot} for the presence of negative work (internal and external) (for further details see Zamparo et al., 2016).

In this study, the efficiency in SR was thus estimated/calculated, based on the values of W^+_{tot} (at a given average shuttle velocity, e.g. v_{mean}) and on data of net energy cost of shuttle running (C) at the very same velocity as obtained by applying the C vs. v_{mean} relationships reported in the literature for shuttle runs over the 5 + 5 m distance ($C = -12.82 + 11.94 \cdot v_{mean}$; Zamparo et al., 2015), 10 + 10 m distance ($C = -12.72 + 6.75 \cdot v_{mean}$; Buglione & di Prampero, 2013) and 20 + 20 m distance ($C = -1.83 + 2.34 \cdot v_{mean}$; Buglione & di Prampero, 2013); as discussed in detail in these papers, these values of C are calculated by taking into account the anaerobic (lactic and alactic) contribution. No metabolic data are reported in the literature for the 15 + 15 m distance; hence efficiency was not estimated/calculated in this specific case.

Mechanical power calculations

In shuttle runs over all distances, but only at maximal velocity, average mechanical power (P, W kg^{-1}) was calculated in the deceleration phase preceding the first CoD (negative power, P^-)and in the

acceleration phase following it (positive power, P^+) from the ratio $\Delta Et/\Delta t$, where Δt (s) is the duration of the acceleration or deceleration phases. These calculations were performed in two intervals: i) over the entire acceleration/deceleration phase: ΔEt (J kg^{-1}) = $E_{Tmax} - E_{T0}$, from v_{max} to v = 0 (before the CoD) and from v = 0 to v_{max} (after the CoD); ii) by considering a "cut off" in the total energy time course (ΔEt = 5 J kg^{-1}) common for all distances ($\Delta Et = Et5 - Et0$, before and after the CoD). In the former case power is calculated over a different number of steps (depending on the shuttle distance) whereas in the latter case the cut off corresponds, with good approximation, to the first/last running step before and after the CoD (over all shuttle distances).

Finally, in shuttle runs over all distances, but only at maximal velocity, the average values of acceleration (acc) and deceleration (dec) were calculated over the entire acceleration/deceleration phase: from v_{max} to v = 0 (before the CoD) and from v = 0 to v_{max} (after the CoD).

Statistical analysis

Data are reported as averages ± SD. A two-way ANOVA was performed to investigate the effects of shuttle distance and of the method employed to calculate power on the values of P^-, P^+ and the P^-/P^+ ratio (at maximal velocity only). A Bonferroni post hoc test was used to determine the possible differences between groups according to speed or distance. A one-way ANOVA was performed to investigate the effects of distance (at maximal velocity only) on the values of acc, dec and the dec/acc ratio. Statistical analyses were performed with SPSS version 20 (IBM). Statistical significance was set at α-value of < 0.05.

RESULTS

The average values of v_{mean} and v_{max}, of W^+_{ext}, W^+_{int} and W^+_{tot} at the three velocities and over the four shuttle distances are reported in Table 4.1. The individual values of W^+_{ext}, W^+_{int} and W^+_{tot} are reported in Figure A.2 and A.3 (Supporting Information) as a function of the average shuttle speed for each shuttle distance. In Figure A.4 (Supporting Information) the partitioning of the total work in its internal and external components is reported, as well as the partitioning of the external work in its "vertical and horizontal" components as a function of shuttle distance and speed.

distance m	*pace*	v_{mean} $m \cdot s^{-1}$	v_{max} $m \cdot s^{-1}$	W_{ext}^{+} $J \cdot kg^{-1} \cdot m^{-1}$	W_{int}^{+} $J \cdot kg^{-1} \cdot m^{-1}$	W_{tot}^{+} $J \cdot kg^{-1} \cdot m^{-1}$
	S	2.02±0.2	2.83±0.3	1.90±0.2	0.64±0.1	2.54±0.2
5+5	M	2.53±0.2	3.52±0.3	1.99±0.2	0.89±0.12	2.88±0.2
	max	3.08±0.3	4.22±0.3	2.28±0.2	1.39±0.26	3.67±0.5
	S	2.68±0.3	3.44±0.3	1.73±0.1	0.65±0.07	2.38±0.2
10+10	M	3.32±0.3	4.39±0.4	1.80±0.2	0.88±0.11	2.68±0.2
	max	3.90±0.3	5.45±0.4	2.06±0.1	1.38±0.22	3.45±0.4
	S	3.05±0.4	3.90±0.5	1.65±0.1	0.67±0.07	2.32±0.1
15+15	M	3.67±0.3	4.82±0.5	1.67±0.2	0.86±0.12	2.53±0.2
	max	4.44±0.3	6.21±0.5	1.97±0.2	1.41±0.23	3.37±0.4
	S	3.25±0.4	4.09±0.5	1.60±0.1	0.68±0.06	2.28±0.1
20+20	M	3.98±0.4	5.10±0.6	1.62±0.1	0.87±0.11	2.49±0.2
	max	4.86±0.4	6.75±0.6	1.88±0.2	1.43±0.21	3.31±0.4

Table 4. 1: Average (± SD) values of shuttle velocity and mechanical work at different paces and over different distances. S: slow shuttle velocity; M: moderate shuttle velocity; max: maximal shuttle velocity; v_{mean}: average velocity of the shuttle run; v_{max}: maximal velocity of the shuttle run; W^{+}_{ext}: positive external mechanical work; W^{+}_{int}: positive internal mechanical work; W^{+}_{tot}: positive total mechanical work.

Figure 4.3 reports the average values of total mechanical work (W^{+}_{tot}, upper panel) and mechanical efficiency (eff^{+}_{tot}, lower panel) as a function of shuttle distance for each shuttle speed.

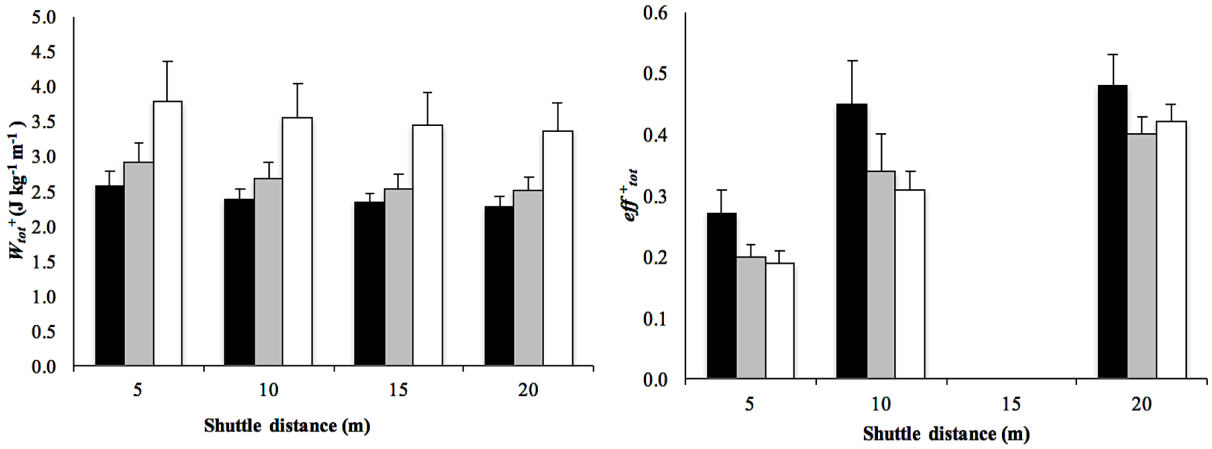

Figure 4. 3: Total mechanical work (upper panel) and mechanical efficiency (lower panel) as a function of shuttle distance at slow (black columns), moderate (grey columns) and maximal (white columns) velocities. Data are means ± SD.

This figure shows that total mechanical work increases with shuttle speed and decreases with shuttle distance (Figure 4.3, upper panel). The increase in W^{+}_{tot} with speed (for a given distance) is larger than its decrease with distance (for a given speed): W^{+}_{tot} is about 30% larger at maximal than at slow speed (average over all distances) and about 10% lower at 20 vs. 5 m (average at all speeds). Mechanical efficiency decreases with shuttle speed and increases with shuttle distance (Figure 4.3, lower panel). The difference in eff^{+}_{tot} between 5 and 10 m is larger than the difference in eff^{+}_{tot} between 10 and 20 m; about 40% and 15%, respectively (average at all speeds).

Positive and negative power were calculated at maximal velocity only, before and after the CoD; these data are reported in Table 4.2. On the average (both methods and all distances) P^- amounts to 21.2 ± 4.2 J $kg^{-1}$and P^+ to 11.7 ± 2.3 J kg^{-1}; the former is thus about twice than the latter. The differences between P^+ and P^- depend essentially on differences in the time spent in the acceleration and deceleration phases (t_{acc} and t_{dec}) since total mechanical energy changes are about the same in these two phases (before and after the CoD).

	distance	t_{acc}	t_{dec}	ΔE^-_T	ΔE^+_T	P^-	P^+
	m	s	s	J·kg^{-1}	J·kg^{-1}	W·kg^{-1}	W·kg^{-1}
ΔE_{Tmax}	**5+5**	0.96±0.1	0.58±0.09	10.7±1.3	10.89±1.3	18.9±4.0	11.4±2.0
	10+10	1.56±0.21	0.87±0.16	16.9±2.4	17.05±2.4	19.9±4.3	11.3±2.6
	15+15	2.04±0.28	1.05±0.18	21.6±2.8	21.7±2.8	21.0±4.1	10.9±2.3
	20+20	2.51±0.31	1.23±0.16	24.8±4.3	24.9±4.3	20.4±4.5	10.2±2.4
$\Delta E_T = 5\ J \cdot kg^{-1}$	**5+5**	0.38±0.07	0.23±0.06	4.7±0.2	4.8±0.1	21.9±5.1	13.0±2.4
	10+10	0.38±0.06	0.21±0.05	4.5±0.5	4.6±0.5	22.3±4.4	12.2±2.1
	15+15	0.39±0.07	0.21±0.04	4.6±0.3	4.7±0.2	22.4±3.7	12.4±2.1
	20+20	0.41±0.10	0.21±0.06	4.6±0.3	4.7±0.2	22.9±6.7	12.1±2.4

Table 4. 2: Average (± SD) values referring to the deceleration/ acceleration phases (before/after the CoD) during shuttle runs at maximal velocity. Data were calculated during the entire acceleration or deceleration phases (ΔE_{Tmax}) or by considering a cut off of 5 J·kg^{-1}, corresponding to the last/first step before/after the change of direction (ΔE_T = 5 J·kg^{-1}). See text for details. CoD: Change of direction; t_{acc}: duration of the acceleration phase; t_{dec}: duration of the deceleration phase; ΔE^+_T: total energy changes during the acceleration phase; ΔE^-_T: total energy changes during the deceleration phase; P^+: positive power output; P^-: negative power output (braking power).

The 2-way ANOVA indicates that power output is affected by the method utilized to calculate it (main effect, df = 80; F = 12.5; $p < 0.001$) but that the P^-/P^- ratio is not (df = 80; F = 9.8; p = 0.527). P^+ was found to decrease with the distance covered (main effect, p = 0.019) while P^- is not influenced by it (df = 20; F = 10.6; p = 0.553) as a consequence the P^-/P^+ratio increases as a function of shuttle distance (main effect: df = 10; F = 11.2; $p < 0.001$): is about 20% larger at 20 + 20 m than at 5 + 5 m (see Fig. 4). No significant interactions were observed (method × distance) for any of these three parameters.

Finally, the average acceleration and deceleration values were calculated at maximal velocity only, before and after the CoD. Average acceleration (acc) decreased (df = 20; F = 12.6; $p < 0.001$) as a function of the distance covered: 4.00 ± 0.62 m s^{-2} (5+5m), 3.35 ± 0.58 m s^{-2} (10+10m), 2.89 ± 0.46 m s^{-2} (15+15m) and 2.55 ± 0.42m·s^{-2} (20+20m) and the values of average deceleration (dec) followed a similar trend ($P < 0.001$): 6.82 ± 1.64 m s^{-2} (5 + 5 m), 5.73 ± 1.19 m s^{-2} (10 + 10 m), 5.06 ± 1.22 m s^{-2} (15 + 15 m) and 4.43 ± 0.89 m s^{-2} (20 + 20 m). The ratio dec/acc (1.75 ± 0.39) is similar

to the P^- / P^+ratio (1.94 ± 0.46) calculated over the same time interval even if the former does not change as a function of shuttle distance (df = 20; F = 2.9; p = 0.979) as the latter (see Figure 4.4).

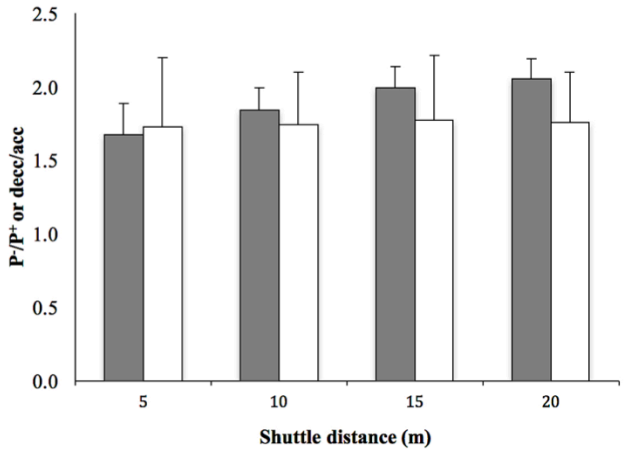

Figure 4. 4: The ratio of negative to positive power (P-/P+; grey columns) and the deceleration/acceleration ratio (dec/acc; white columns) in shuttles over different distances covered at maximal speed. Data are means ± SD.

DISCUSSION

In this study we investigated mechanical work and power during accelerated and decelerated running in humans by using, as an experimental model, shuttle runs over different distances and at different speeds. Indeed, shuttle runs are characterized by an acceleration phase, a deceleration phase and a change of direction (a 180° turn) and larger accelerations (and decelerations) could be attained either by increasing the velocity or the distance of the shuttle.

Internal, external and total mechanical work

Data of mechanical work reported in this study are based on the analysis of the time course of potential and kinetic energy of BCoM (W^+_{ext}) and on the computation of the translational and rotational kinetic energy of the body segments (W^+_{int}). We applied these methods in order to compare our data with previously published data on human running and because they have been widely used in human as well as in animal locomotion (Ahn et al., 2004; Cavagna & Kaneko, 1977; Genin et al., 2010; Griffin & Kram, 2000; Pavei et al., 2017; Pellegrini et al., 2014; Saibene & Minetti, 2003; Willems et al., 1995). At variance with constant speed linear running, a certain amount of work needs to be performed to rotate the body along its vertical axis during the turns, this work was not taken into account in this paper, and this is a limitation of our study. However, this "additional" mechanical work is performed once in a SR and is expected to have a little influence on the total mechanical wok that is expressed per unit distance. Indeed, no major differences were observed when com- paring energy expenditure in SR without turns (only deceleration and acceleration phases in the same

direction) or with different turning angles (0, 45, 90 and 180°) (Zamparo et al., 2014).

As hypothesized, and previously found for the energy cost of shuttle running, we observed that total mechanical work (W^+_{tot}): i) increases as a function of velocity for each shuttle distance; ii) at any given velocity is lower the longer the shuttle distance. The largest values of W^+_{int}, W^+_{ext} and W^+_{tot} are indeed observed at maximal velocity and do not greatly differ with shuttle distance (see Fig. 3). Interestingly, the lowest values of W^+_{tot} (at slow speed over the 20 + 20 m distance) are close to those assessed during constant speed, linear running (e.g. Cavagna & Kaneko, 1977) and the same is true for the values of W^+_{int} and W^+_{ext}.

Mechanical work data reported in this study over the shorter shuttle distance (5 + 5 m) are in line with those reported by Zamparo et al. (2016) over the same distance: in agreement with the previous study our data underline that W^+_{int} is a strong determinant of W^+_{tot} and that this parameter could not be neglected, especially during high velocity shuttle running (over all shuttle distances).

Mechanical efficiency (eff^+_{tot})

As indicated in the methods section, the efficiency calculated in this study (eff^+_{tot}) is sometimes defined as locomotion efficiency or "apparent" efficiency and does not correspond to the efficiency that can be calculated at the muscle level. Measuring it can help to understand whether mechanical work has been "recycled" via storage and release of elastic energy (e.g. Full, 1991; Lai et al., 2014; Minetti et al., 1999) thus indicating the presence of an energy saving mechanism (Alexander, 1991). Data of eff^+_{tot} reported in this study over the shorter shuttle distance (5 + 5 m) are in line with those reported by Zamparo et al. (2016); this finding encouraged us to attempt to calculate/estimate mechanical efficiency also over the other distances (no efficiency data are reported in the literature about shuttle runs over longer distances) even if the fact that the energy cost was not directly measured is a limitation of this study.

The large range in eff^+_{tot} (from about 0.20 to 0.50, Fig. 3, lower panel) suggests the crucial role of the partitioning between acceleration (pure muscle efficiency ≈0.25–0.30 e.g. Woledge et al., 1985) and "almost" constant speed ("apparent" efficiency ≈0.5–0.6 Cavagna & Kaneko, 1977) phases during the shuttle run. It is likely that a greater relative importance of the constant speed phase, associated to a better exploitation of the elastic energy saving mechanism, is responsible of the higher "apparent" efficiency at the longer shuttle distances. Moreover, in the acceleration/deceleration phases (especially over the shortest shuttle distances) muscles could contract at sub-optimal length and/or velocity conditions, with a potentially negative influence on their efficiency.

The method to calculate efficiency utilized in this study is based on the ratio between total mechanical work and metabolic energy cost. Total mechanical work estimation is still debated in the

literature, as also acknowledged for some aspects by the original authors (Willems et al., 1995). In absence of a closed-form solution in the literature, despite some really knowledgeful attempts (Aleshinsky 1986 a, b, c, d, e) we kept on adding W_{int} and W_{ext} to approximate W_{tot} by considering as only energy transfer the one within body limbs segments. The only components left behind with our approach are the rotational work over the twist axis at change of direction and the internal friction in body tissues, which could affect the total mechanical work done. It has to be considered that efficiency, which is output divided by input, cannot include in the numerator the effects of isometric muscle contraction and co-contraction although their metabolic counterparts are already included in the denominator.

Mechanical power output

Human and animal locomotion at constant average speed and on the level utilizes equivalent and counterbalancing phases of positive and negative work to maintain an average energy level (e.g. Daley & Biewener, 2003; Rubenson et al., 2004; Saibene & Minetti, 2003). Positive and negative work, in both level and non-level gaits, depend on the work generated by muscles or dissipated by muscles and other anatomical structures through either shortening (concentric) or lengthening (eccentric) contractions. During running on the level push time is larger than brake time (at least at speeds lower than 4 $m \cdot s^{-1}$, as in the present study), whereas total mechanical energy changes ($\Delta E^{+}t$ and $\Delta E^{-}t$) are about the same (e.g. Cavagna, 2010). This difference in time is generally attributed to the greater muscular force exerted during the eccentric phase. Our data extend these considerations to un- steady locomotion (albeit at maximal velocity only): the time spent in the acceleration phase is larger than that spent in the deceleration phase, over all shuttle distance, whereas positive and negative mechanical energy changes during a SR are essentially the same (see Table 4.2). To our knowledge these are the first data on braking power in human running reported so far in the literature; indeed, whereas the mechanics of accelerated running (sprints) has been investigated in humans (and animals), braking power received far less attention.

Only data at maximal speeds were considered in these calculations because force (and power) in submaximal runs can be voluntary modulated by the subjects whereas, at maximal speeds, they had to exploit all their muscle force (and power). Our athletes, however, were free to select the "pacing strategy" when covering at top velocity the entire shuttle distance: they preferred to spend more time during the acceleration phase and less time during the deceleration phase probably because in the deceleration phase they could exert greater (eccentric) muscular forces.

The maximal values of (average) acceleration and deceleration were observed over the shortest shuttle distance; over longer distances these values tend to decrease. This could also be

appreciated by inspection of Fig. 4.1 where the slope of the v vs. t curves is a measure of the acceleration/deceleration of the runner. The ascending/descending limbs of the v vs. t curves show the same profile (and at a given time/distance are superimposable) for all shuttle distances and this highlights that runners exploit the same movement pattern when asked to perform at maximal velocity. However, the time to reach maximal velocity is different and this relates to different values of acceleration and deceleration over different shuttle distances.

Finally, our data show that the dec/acc ratio (in SR covered at maximal speed and over all distances) is not far from the P^-/ P^+ ratio (as measured in the same time interval); this ratio likely depends on the fundamental properties of skeletal muscles in vivo (larger values of force and power in eccentric than in concentric conditions) in agreement with the F vs. v relationship of isolated muscle.

CONCLUSIONS

Data reported in this study confirm and extend to longer shuttle distances our knowledge about the mechanics of shuttle running (an example of non-steady locomotion in humans): external, internal and total work increase as a function of shuttle speed but decrease as a function of shuttle distance. In addition, data reported in this study indicate that running humans can exert a larger negative than positive power (and a larger deceleration than acceleration) in agreement with the fundamental properties of skeletal muscles in vivo. Finally, the larger values of mechanical efficiency observed at the longer shuttle distance suggest a better exploitation of the elastic energy saving mechanism (i. e. these values are close to those reported for linear running at constant speed) whereas this mechanism seems impaired when the shuttle distance decreases (i.e. where accelerations and decelerations, e.g. non- steady conditions, play a more important role).

CHAPTER 5

STEADY-STATE RUNNING: STUDY 4

GASTROCNEMIUS MEDIALIS AND VASTUS LATERALIS *IN VIVO* MUSCLE-TENDON BEHAVIOUR DURING RUNNING AT INCREASING SPEED

Authors: Andrea Monte[1,2], Vasilios Baltzopoulos[2], Costantinos Maganaris[2], Paola Zamparo[1]

[1] *Department of Neurosciences, Biomedicine and Movement Sciences, University of Verona, Italy*

[2] *Liverpool John Moores University, Research Institute for Sport and Exercise Sciences (RISES), United Kingdom*

ABSTRACT

This study combines *in vivo* ultrasound measurements of the Vastus Lateralis (VL) and Gastrocnemius Medialis (GM) muscles with electromyographic, kinematic and kinetic measurements during treadmill running at different speeds (10, 13 and 16 $km \cdot h^{-1}$) to better understand the role of muscle and tendon behaviour in two functionally different muscle-tendon units. In addition, the Force-Length and Force-Velocity relationships of VL and GM were experimentally assessed by combining dynamometry and EMG data with ultrasound measurements. With increasing running speed, the operating length of the fascicles in the stance phase shifted towards smaller lengths in the VL ($P<0.05$) and longer lengths in the GM ($P<0.05$). However, both muscles contracted near-isometrically, close to their optimal length L_0, where isometric force is maximal. The GM and VL series elastic element (SEE) showed similar values of strain and recoil, but whereas the length of VL SEE did not change as a function of speed, GM lengthened and shortened more at higher speeds. With increasing running speed, the contribution of elastic strain energy to the positive power generated by the MTU increased similarly for GM (from 0.75 to 1.56 $W \cdot kg^{-1}$) and VL (from 0.62 to 1.02 $W \cdot kg^{-1}$). These results indicate that VL and GM have similar muscle and tendon behaviours during running at increasing speeds and that the primary function of both muscle-tendon units is to enhance the storage and recovery of elastic strain energy.

Submitted to: *Scandinavian Journal of Medicine and Science in Sports (under review)*

INTRODUCTION

In the past two decades, advancements in ultrasonographic techniques have made it possible to investigate *in vivo* the behaviour of human muscles and tendons during locomotion (Fukunaga et al., 2001; Ishikawa et al., 2007; Lichtwark et al., 2007). Combining *in vivo* scanning with more standard biomechanical measurements, such as inverse dynamics techniques, has allowed studying the link between loading during an activity and the muscle-tendon behaviour (Lai et al., 2014; Farris & Sawicki, 2012). Most studies have focused on the calf muscles (Fukunaga et al., 2001; Ishikawa et al., 2007; Lichtwarl et al., 2007; Lai et al., 2014; Lai et al., 2018; Farris & Sawick, 2012; Werkhausen et al., 2019). For instance, it has been shown that the triceps surae muscle group (i.e. soleus, gastrocnemius medialis and gastrocnemius lateralis) produces forces up to 12 times the body weight during running (Komi, 1990) and is the main force producer amongst all the major lower-limb muscle groups (Roberts, 2002). When running speed increases, the plantar flexor muscles must generate force over an increasingly shorter period of time, and this requires more forceful and rapid contractions. To achieve this and meet the energy demands for sustaining running, the muscle-tendon units (MTUs) (Roberts & Azizi, 2011) of the ankle plantar flexors work in a highly complex and tightly integrated manner (Ishikawa et al., 2007; Roberts, 2002). Due to their unique design, with short muscle fibres and a long Achilles tendon, the ankle plantar flexors can exert high levels of power with minimal energy demands, as the tendon's mechanical behaviour allows the muscle to operate more isometrically, accommodating the behaviour of the MTU throughout a large tendon displacement (Lai et al., 2014; Farris & Sawicki, 2012). This mechanism has a favourable effect on contractile force generation and the associated metabolic cost Lai et al., 2014; Farris & Sawicki, 2012, Roberts & Azizi, 2011). Modelling studies have, indeed, demonstrated that tendon strain can optimize the region where muscle fibres operate on their Force-Length (F-L) and Force-Velocity (F-V) relationships during running at increasing speed Lai et al., 2014; Farris & Sawicki, 2012). Furthermore, these studies have shown that the stretching and subsequent recoiling of the Achilles tendon during running allows storing and releasing substantial amounts of elastic strain energy, which increase as a function of running speed, thus contributing more to the mechanical work done by the MTU of the ankle plantar-flexors Lai et al., 2014; Farris & Sawicki, 2012). For example, Farris & Sawicki, 2012 as well as Lai et al. (2014) showed that the relative contribution of the Achilles tendon elastic strain energy to the positive power done by the MTU is about 65-75% at low running speeds and increases as a function of speed. It has, therefore, been postulated that this increasing elastic strain energy contribution with speed allows the muscle to undergo an increasingly smaller length change during contraction (Alexander, 2002). However, only few studies have so far investigated the *in-vivo* operating length and velocity of the ankle plantar flexor muscles, as well as the relative contribution

of the elastic strain energy, during running at increasing speeds.

To fully understand the complex interplay between muscle and tendon behaviour during running, the contribution of other contributing MTUs with different characteristics to those of the plantar flexors should also be considered. The knee extensor muscles are of particular interest as they have longer fascicles and a stiffer tendon compared to the ankle plantar flexors (O'Brien et al., 2010; Arampatzis et al., 2005), implying that the quadriceps muscle may undergo substantial length changes during locomotion (Sawicki et al., 2009). Consistent with this notion are the findings of modelling studies, showing large fascicle length changes in the vastus lateralis (VL) during running, leading to hypothetical large shifts of the F-L and F-V relationships (Arnold et al., 2013; Santuz et al., 2017). However, a more recent in-vivo study showed that the VL fascicles operate close to their optimum working length and quasi-isometrically when running at 10 $km \cdot h^{-1}$(Bohm et al., 2018). As a consequence, the large displacement of the VL MTU was primarily associated with changes in the length of the patellar-quadriceps tendon complex. However, no studies have so far quantified the operating length and velocity of VL or the relative contribution of its tendon complex in determining mechanical power production during running at increasing speed.

Therefore, the present study combines *in vivo* ultrasound measurements of VL and gastrocnemius medialis (GM) muscle behaviour with electromyographic and kinetic measurements during treadmill running in order to investigate the behaviour of these two functionally different MTUs at different running speeds. In particular, we experimentally investigated 1) the operating length and velocity of muscle fascicles and 2) the relative contribution of muscle fascicles and series elastic element (SEE) to the mechanical power done by the whole MTU, to better understand how they change as a function of running speed in the two MTUs.

Based on recent literature, we hypothesised that both muscles would demonstrate small fascicle length changes, close to their optimal length, allowing the muscles to operate at a high force potential during running at increasing speed. Therefore, we expected that the SEE would accommodate the larger part of the MTU displacement at each running speed for both GM and VL. We also expected that, for both MTUs, power would be enhanced at faster running speeds as elastic strain energy would contribute a greater proportion of MTUs positive work during the stance phase of running.

MATHERIALS AND METHODS

Subjects

Fifteen men (years: 24±2.4 years; body mass: 74±2.8 kg; height: 1.77±0.04 m) accustomed to endurance running participated in this study. The participants did not report any type of

neuromuscular injury in the six months before the experiments.

Experimental design

Each subject participated in two experimental sessions. In the first session, the Force-Length (F-L) and Force-Velocity (F-V) relationships of VL and GM were experimentally assessed by means of maximal isometric (MVC) and isokinetic tests of the knee extensors and plantar flexors, respectively. During these experiments, an ultrasound apparatus was utilised to record the fascicle length of VL and GM. The force applied to the patellar and Achilles tendon was calculated from the knee/ankle joint moment and the tendon lever arms. Finally, during each contraction mode test (isometric or isokinetic) the EMG activity of VL or GM was measured as well as that of the corresponding antagonist muscle: biceps femoris or tibialis anterior.

In the second session, the fascicle length of VL and GM, the kinematics of the body segments, the dynamics (ground reaction forces) and the EMG activity of the above two muscles were measured during running at three different speeds: 10, 13 and 16 $km \cdot h^{-1}$.

Data collection

Assessment of the F-L relationship

For the knee extensors measurements, the participants were secured on a dynamometer (Cybex NORM, USA), fixed with a trunk and pelvic strap and the arms positioned crossed in front of the chest. For the plantar flexor measurements, the participants were secured to the same dynamometer in a prone lying position with the right knee in the anatomical position and the foot of the dominant leg fixed to the dynamometer footplate.

The F-L relationship was calculated from MVCs at various joint angles. For the knee extensors: the hip joint angle was set at 85° (0° refers to supine position) to reduce the contribution of the rectus femoris to the resultant moment of the knee extensors (Bohm et al., 2018; Herzog et al., 1990); for the plantar flexors: the legs were fully extended in the anatomical position. For the knee extensors, eight MVCs of the right leg were performed from 90° to 20° of knee joint angle (0° = knee fully extended), whereas for the plantar flexors five MVCs were performed from 20° plantarflexion to 20° dorsiflexion (0° = foot at right angles to the shank) at 10° intervals.

The actual knee and ankle angles during the MVCs were measured in 2D to obtain the leverage of both muscle groups. Two dimensional kinematics were recorded on the basis of five markers for the leg [iliac spine and greater trochanter of the opposite side; lower portion of the patella (patellar tendon origin); upper anterior surface of the tibia (patellar tendon insertion); tibiofemoral contact point (considered to represent the knee centre of rotation)] and seven markers for the foot

(tibiofemoral contact point, heel, toe, medial malleolus, insertion of Achilles tendon and markers at 5 and 10 cm proximal to the calcaneal insertion). The marker positions were recorded by means of video analysis (Casio Exilim Camera) at 200 Hz and analysed with a video processing software (Tracker v4.0). The camera was positioned on the left side of the subject, at right angles to the longitudinal axis of the thigh. To eliminate any radial distortion, a rectilinear filter was applied during marker tracking on the video frames. The resultant marker trajectories were smoothed using a forward and reverse pass second order low pass Butterwoth filter (cut-off 15 Hz).

During the MVC, fascicle length changes were captured by B-mode ultrasound imaging with a 6 cm linear array probe operating at 60 Hz (Philips EPIQ 5). For VL and GM, the probe was attached to the skin approximately at 50% of the femur length and at 30% of the distance between the popliteal crease and the malleolus, respectively. In both cases, the ultrasound probe was located on the muscle belly and corrected with respect to the superficial and deeper aponeurosis, in order to have a clear image of the perimysial connective intramuscular tissue, that it is indicative of the muscle fascicle structure. *In vivo* muscle fascicle length and pennation angle were calculated from the ultrasound videos (see Data Analysis).

Finally, the EMG activity of the VL and GM and the corresponding antagonist muscle, were recorded during the knee extensor and plantar flexor MVCs, respectively. Two bipolar Ag-AgCl electrodes were placed in the central region of the muscles after skin preparation (including shaving, gentle abrasion and cleaning with an alcohol-based tissue pad). The raw EMG data were recorded at 1000 Hz with a Biopac System (MP100, Biopac System, Santa Barbara, USA).

The dynamometer data (angular velocity, moment and position) and the EMG activity of the muscles were collected synchronously at 1000 Hz with the Biopac System. All the instrumentation used in the procedures were synchronised with an external manual trigger (5 V).

Assessment of the F-V relationship

To obtain the F-V relationship, maximum isokinetic torque was recorded at the angular velocities of 30, 90, 150, 180 and 210 $deg \cdot s^{-1}$ for the plantar flexors and 45, 90, 150, 210 and 250 $deg \cdot s^{-1}$ for the knee extensors. The range of motion used during the MVC was also used during the isokinetic trials and data were analysed only in the isokinetic phase of the contraction. After a familiarization trial, the subjects performed three consecutive contractions at each velocity with two min of recovery in between. Also in these cases, the tendon force was calculated by taking into account the tendon lever arm and the influences of the antagonist muscle were subtracted, as described in the next section. All instrumentation was synchronised with an external manual trigger as above (5 V).

Running trials

Each athlete ran at three different constant speeds (10, 13 and 16 $km \cdot h^{-1}$) for 6 min using a self-selected step frequency and step length. All participants were forefoot runners. Small retroreflective markers (14 mm diameter) were placed at specific anatomical locations on the participants' trunk, arms, and lower limbs. The marker set used in this study was the same proposed by Lai et al. (2018). However, we added other ten markers (four on the right and left knee and the other six on the right shank/foot) to measure the tendon lever arm during running as described by Rasske et al. (2017) (see Data Analysis). The 3D marker trajectories were recorded using 12 Vicon cameras (Vero 2.2, Oxford Metrics, UK) sampling at 250 Hz. Ground reaction forces (GRFs), the resultant GRF, the centre of pressure and the free moment vectors were recorded using two force plates embedded in the instrumented treadmill (M-GAIT, MOTEK) sampling at 1500 Hz.

Moreover, a B-mode ultrasound scanner (Telemed Echo Blaster 128, Vilnius, Lithuania) was used to record images at 60 Hz with a depth and width of 60 mm. Ultrasound data were recorded from the right VL and GM of each participant (in two separate running trials and in a randomized order) with the ultrasound probe positioned in the same location utilised during the dynamometric measurements. Fascicle length and pennation angle were calculated with the software and procedures mentioned in the dynamometric measurements and described in the data analysis.

Finally, EMG signals from Ag-AgCl bipolar electrodes were collected simultaneously with the ultrasound, kinematic and kinetic signals using a wireless system (Biopac System) sampling at 1000 Hz. The location of the electrodes was the same used in the dynamometric measurements. All experimental data were synchronised by a digital output generated by the ultrasound scanner that triggered all instrumentation (the Vicon cameras, the treadmill ground reaction forces and the EMG signals).

Data Analysis

Dynamometric measurements

The total moment generated by the knee extensor and plantar flexor muscles was corrected for the gravitational force effects (determined during a passive joint rotation driven by the dynamometer) and the joint and the dynamometer axes were aligned visually during contraction. Finally, the EMG-moment relationships of the antagonist muscles (biceps femoris and tibialis anterior) were determined to estimate and account for the contribution of the antagonistic moment to the net joint moment, as described in detail previously (Kellis & Baltzopoulos, 1998).

To calculate the force applied to the tendon (patellar or Achilles), the joint moment measured with the dynamometer was divided by the tendon lever arm using a 2D approach. For the knee

extensor, the lever arm was measured as the perpendicular distance from the tendon's line of action to the centre of rotation of the knee, based on the position of three markers (origin and insertion of the patellar tendon and the tibiofemoral contact point that was considered to represent the knee centre of rotation). The location of each of those three markers was determined by ultrasound scanning. Particularly, the marker on the tibiofemoral contact point was positioned in the mid space between the femur condyle and tibia plateau. This "geometric method" (see Tsapoulos et al., 2006 for details) uses the tibio-femoral contact point to represent the knee centre of rotation and was used in different conditions and locomotion tasks (Kellis & Baltzopoulos, 1998; Baltzopoulos, 1995) . In the case of plantar flexors, the lever arm was measured as the perpendicular distance from the tendon's line of action to the centre of rotation of the ankle based on the position of four markers (medial malleolus representing the ankle centre of rotation, insertion of Achilles tendon, and markers at 5 and 10 cm proximal to the calcaneus to represent the Achilles tendon line of action), as suggested by Rasske et al. (2017). The location of each marker was determined by ultrasound scanning as previously suggested by Rasske et al. (2017), in order to place the markers on the correct anatomical positions.

By knowing the maximum force applied to the patellar/Achilles tendon during the MVCs and the corresponding muscle fascicle length, the F-L relationship was determined for each subject based on a second-order polynomial fit. Based on this relationship, the maximal isometric force applied to the tendon (F_{max}) and the optimal shortening length (L_0, the length at which this peak occurs) were determined.

The F-V relationship was determined based on the force and fascicle velocity values during the isokinetic test and these values were fitted using the following exponential equation (Hill, 1938):

$$v = \left(e^{-\frac{P}{b}} - e^{-\frac{P_0}{b}}\right) a$$

where v is the fascicle velocity ($m \cdot s^{-1}$), P is the force value, $P0$ the maximal isometric force recorded during the MVC and extrapolated by the polynomial fit and a and b are experimentally determined constants. Constants a and b were obtained from the intercept (a/b) and slope ($1/b$) of the linearized Hill's plot of $(P_0 - P)/V$ *vs.* P, where P is the torque developed at different velocities of shortening, V is the angular velocity of shortening and P_0 is the maximal force of contraction (isometric, as obtained from the F-L curve) (Ferri et al., 2003; Csapo et al., 2010). Finally, the intercept value on the abscissa was taken as the maximal fascicle shortening velocity (V_{max}).

For the ultrasound measurements, the length of muscle fascicles was defined as the distance between the deep and superficial aponeuroses. Pennation angle (α) was defined as the angle between the collagenous tissue and the deep aponeurosis. A validated automatic tracking algorithm was used to quantify the muscle fascicle length and pennation angle frame by frame (Gillet et al., 2013). At the end of the auto-tracking, every frame of the tracked fascicle lengths and pennation angles was visually

examined to check the algorithm accuracy. Whenever the fascicle length or pennation angle was deemed inaccurate, the two points defining the muscle fascicles were manually repositioned. For the dynamometry measurements, only the fascicle length was taken into consideration.

The raw EMG signal during the isometric contractions was filtered with a band-pass third order Butterworth filter at 20-500 Hz, whereas the onset of muscle activity was detected by a threshold that was defined as the baseline activity plus three times its standard deviation. Finally, the root-mean-square of the signal was calculated.

Running measurements

In the last minute of each running trial, kinematics, kinetics, EMG and ultrasound data were analysed for ten stance phases for each participant. This timing was chosen to coincide with the determination of oxygen uptake. Data of each instrument were interpolated at 200 sample points. Each subject repeated the runs at 10, 13 and 16 $km \cdot h^{-1}$ twice, once for scanning the GM muscle and a second time to scan the VL muscle.

During running, based on the kinematics and kinetics variables, a 2D inverse kinematics and inverse dynamics approach were used to compute ankle/knee joint angles and net joint moments, respectively (Lai et al., 2018). Finally, joint powers were calculated by multiplying the net moment at each joint by the corresponding angular velocity, at each time interval. Net joint moments and joint powers were finally normalised to body mass. The calculations were performed with a custom written LabView program (v.10).

For the EMG data collected during running, the same noise reduction and onset identification procedure used for the MVC was applied. Moreover, a linear envelope of the EMG signal was calculated using the root-mean-square of a moving window (100 ms). Each muscle's linear envelope was then normalised to the peak magnitude of the respective linear EMG envelope measured during MVC and thus expressed in %RMS at MVC.

For the running measurements the MTU length of VL and GM were computed, at each instant, using instantaneous joint angles as proposed by Hawkins and Hull (1990). The SEE length, representing free tendon and aponeurosis for each MTU, was calculated as the difference between MTU length and the ultrasound-measured muscle fascicle length, taking into account the influence of pennation angle (Fukunaga et al., 2001). MTU, muscle fascicle and SEE lengths were then normalised to their resting length (during static standing); velocities were then computed by differentiating the normalised lengths of each component with respect to time[4]. A reliability and sensitivity study of the ultrasound-based measurement of the VL and GM fascicle behaviour and MTU behaviour throughout the entire stance phase revealed very good reliability between single trials

at all investigated speeds, the coefficient of multiple correlations (CMC) ranging from 0.90 and 0.98. Moreover, the average root mean square differences (RMSD) values were of about 5-7 mm for GM and VL fascicle lengths and of about 3-4 mm for the corresponding MTUs lengths (see Supplementary Material).

The following parameters were calculated (both in GM and VL): i) average MTU length during the stance phase (upper panels in Figure 5.1); ii) fascicle shortening in the stance phase, taken as the peak (negative) value of the fascicle length during shortening (middle panels in Figure 5.1); iii) SEE strain, taken as the peak (positive) value in the stance phase; iv) SEE recoil, calculated as the mean of the maximum and minimum strain values in the late stance phase (from the maximum value of strain to the end of the stance phase; bottom panels in Figure 5.1).

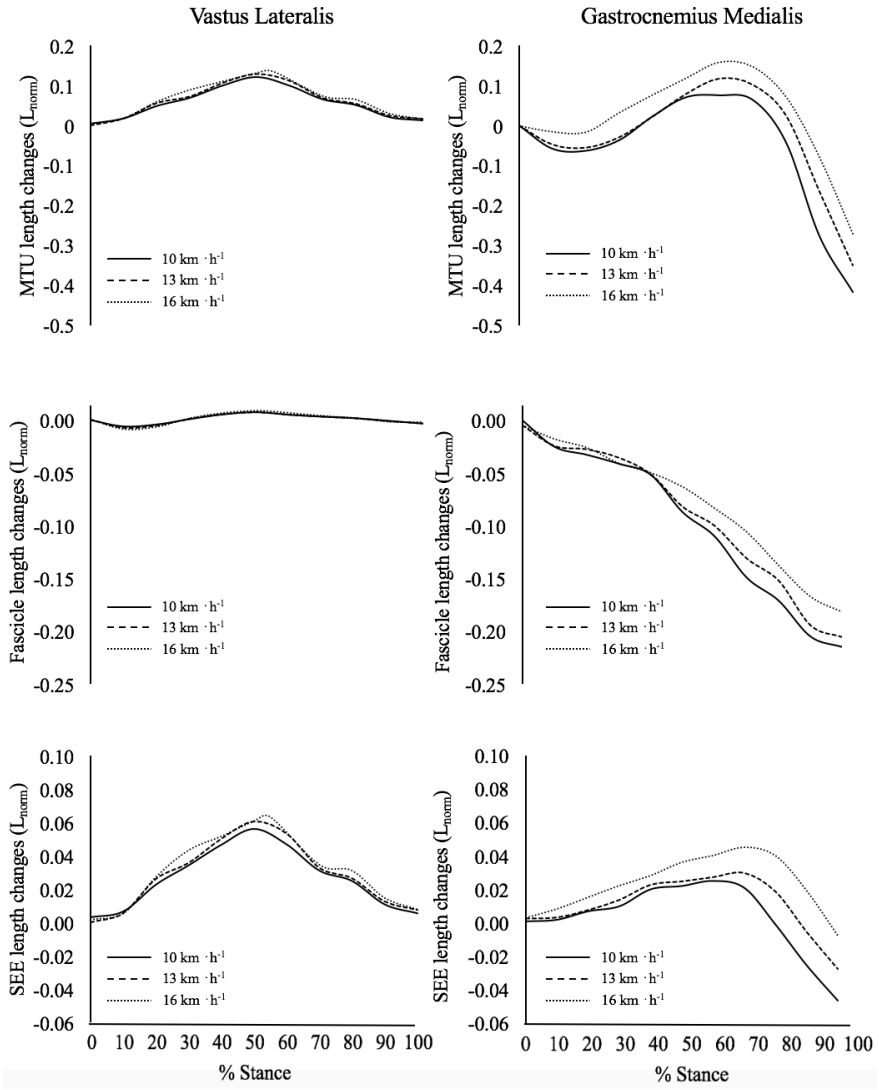

Figure 5. 1: Mechanical behaviour of Vastus Lateralis (left panels) and Gastrocnemius Medialis (right panels) muscle-tendon unit, muscle fascicle and series elastic elements during the stance phase while running at three steady-state speeds: solid line: 10 km·h^{-1}; thick dashed line: 13 km·h^{-1}; thin dashed line: 16 km·h^{-1}. MTU, muscle fascicle and SEE lengths were normalised to their corresponding resting lengths during static standing. Negative and positive length values denote shortening and lengthening, respectively.

Achilles and patellar tendon forces were calculated as the net ankle or net knee moment

divided by the tendon lever arm, where the moment arm was estimated as suggested by Rasske et al. (2017). The contribution of the antagonist moment (biceps femoris and tibialis anterior) to the net joint moment, was taken into account (as described above) and subtracted to that of the agonist muscles.

As proposed by Farris & Sawicki, 2012 the force attributable to GM and VL series elastic elements (F_{SEE}) can be estimated by multiplying "overall" tendon force by the relative PCSA of these muscles which, according to the literature, amounts to 15.9% of the PCSA of plantar flexors for GM and to and 34% of the PCSA of the knee extensors for VL (Kurokawa et al., 2001; Bekenecker et al., 2019). To estimate the force acting along the GM and along the VL muscle fascicles, the corresponding F_{SEE} was divided by the cosine of their pennation angle, as proposed by Lichtwark & Wilson (2006). Finally, the MTU force was assumed to be equal to F_{SEE}, as suggested by Farris & Sawicki, 2012.

The power output of the GM and VL MTU, of the GM and VL muscle fascicles and of the GM and VL SEE was then calculated as the product of their respective forces and velocities, where the velocity was the first derivative of the length changes (Farris & Sawicki, 2012); the positive power (during the propulsive phase) was then estimated for each running trial: positive power for the fascicle (P_{fas}^{+}), for the SEE (P_{SEE}^{+}) and for the MTU (P_{MTU}^{+}). The interplay between these power values is indicative of the fascicle and tendon interaction[5] where the most efficient scenario corresponds to $P_{fas}^{+} = 0$, a condition in which the fascicles are contracting isometrically and all P_{MTU}^{+} is supplied by P_{SEE}^{+} (i.e. by SEE recoil).

Force and velocity variations with fascicle operating length of GM and VL during the active state of the stance phase (at the three running speeds) are plotted in Figure 5.2 over the F-L and F-V curves as obtained during the dynamometric measurements. Fascicle length and fascicles velocity values were obtained from the analysis of the ultrasound scans. As proposed by Bohm et al. (2018), force was normalised to the maximum force obtained during the maximal isometric knee extension and plantar flexors contractions (F/F_{max}); fascicle length and fascicle velocity were normalized to the experimentally determined optimal fascicle length (L/L_0) and maximum shortening velocity (V/V_{max}), respectively. Therefore, the estimated forces corresponding to the fascicle lengths and velocities measured during running represent values at the activation level the contracting muscles exhibited during each running task.

Statistical analyses

A one-way ANOVA for repeated measures was conducted to test the possible differences among running speeds. The following outcome measures were tested (during the stance phase): mean length

of MTU; fascicles shortening; SEE strain and recoil; average EMG activity (linear envelope); mean values of fascicle operating length, F_{max} and V_{max}; the mechanical power production of each component in both muscles (VL and GM). When significant main effects were found, a post-hoc pairwise comparison using Fisher's least significant difference was used to determine the effect of speed. The alpha level was set to $P < 0.05$ and statistical analysis was performed with SPSS (v24.0). All data extracted for statistical analysis were normally distributed (Shapiro-Wilk normality test, $P > 0.05$).

RESULTS

F-L and F-V relationships

The F-L and F-V curves as obtained during the dynamometric measurements are reported in Figure 5.2. The values of L_0, F_{max} and v_{max} derived from these relationships were 9.57±1.66 cm, 5107±882 N and 122.3±14.5 cm·s^{-1} for the VL and 5.37±1.01 cm, 1019±177 N and 107.4±11.3 cm·s^{-1} for the GM, respectively. The operating length of the fascicles, the force and the velocity of GM and VL during the active state of the stance phase (at the three running speeds) are also plotted in Figure 5.2 over the F-L and F-V curves. The average length of both muscles during the stance phase changed significantly as a function of running speed (Figure 5.2A: VL, Figure 5.2C: GM) (main effect: $P<0.001$).

However, the length changes (L) in the muscles occurred in opposite directions: in respect to their corresponding optimal length (L_0,), VL fascicle length increased significantly (main effect: $P<0.01$) while GM fascicle length decreased significantly (main effect: $P<0.001$) with running speed. For each muscle, the comparisons revealed significant differences between all running speeds. However, at all speeds, both muscles operated close to their optimal length, the relative values (L/L_0) being 1.03±0.05, 1.06±0.06 and 1.1±0.06 for VL and 0.92±0.05, 0.88±0.07, 0.83±0.07 for GM, at 10, 13 and 16 km·h^{-1}, respectively.

Contraction velocity of VL and GM fascicles showed significant differences as a function of running speed (Figure 5.2B: VL, Figure 5.2D: GM) (main effect: $P<0.001$). Contraction velocity decreased for VL when the speed increased (main effect: $P<0.05$), whereas it increased for GM (main effect: $P<0.01$). Similar to fascicle length changes, the comparison of velocities for each muscle between running speeds showed significant differences ($P<0.05$) between all conditions. For both muscles, contraction velocity (V) was lower than their corresponding maximum values, with the relative values (V/V_{max}) being: 3.1±3, 1.8 ±3.5, -2.8±3.8 % for VL and 5±4.8, 8.1±6.7, 12±7 % for GM, at 10, 13 and 16 km·h^{-1}, respectively.

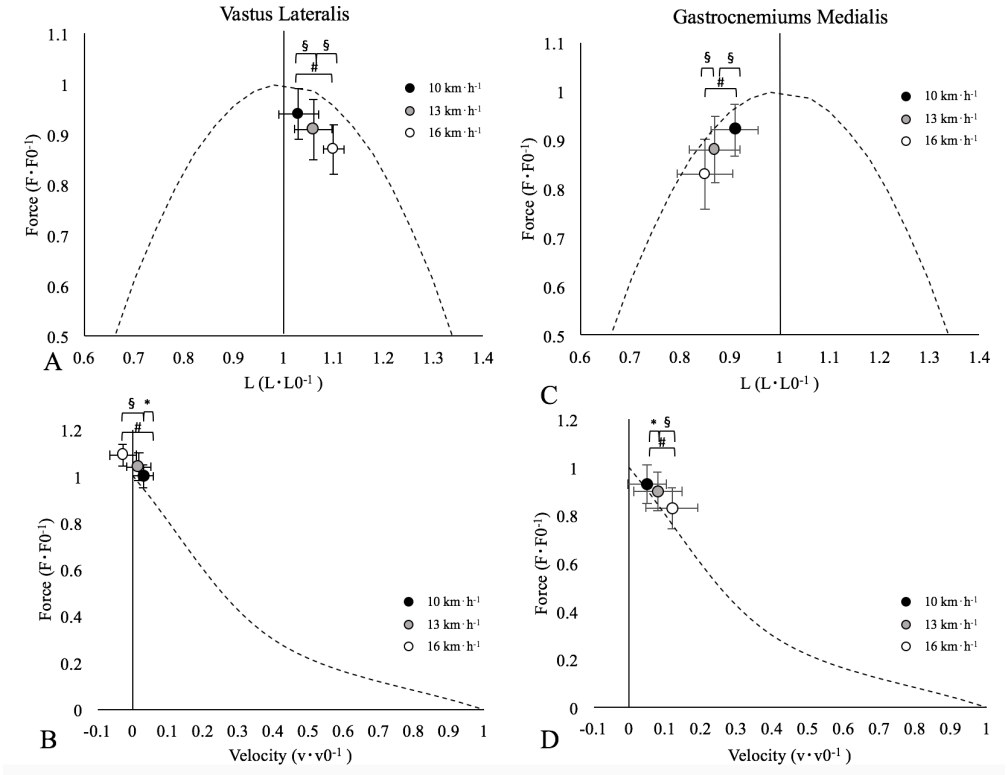

*Figure 5. 2: Operating length (upper panels) and velocity (lower panels) of Vastus Lateralis (left) and Gastrocnemius Medialis (right) muscle fascicles (mean and standard deviation) during the stance phase of running onto the normalised F-L and F-V. Force is normalised to the maximum force obtained during the maximal isometric knee extension and plantar flexors contractions; fascicle length and fascicle velocity are normalized to the experimentally determined optimal fascicle length and maximum shortening velocity, respectively. Black dots: 10 km·h^{-1}; grey dots: 13 km·h^{-1}; white dots: 16 km·h^{-1}; * P < 0.05; § P < 0.01; # P < 0.001.*

Muscle and tendon parameters during running

Figure 5.3 shows the mean MTU length values, the fascicle shortening, the SEE strain and recoil for both muscles in each running trial. VL MTU length, as well as VL SEE strain and recoil, showed no significant differences between running speeds, whereas an increase in VL fascicle shortening (main effect: $P < 0.001$) was observed at each speed. The average length of the GM MTU increased with running speed (main effect: $P < 0.001$). The same was the case for the GM fascicle shortening (main effect: $P < 0.001$) and GM SEE strain and recoil (main effect: $P < 0.001$), with significant differences between all three speeds for the latter.

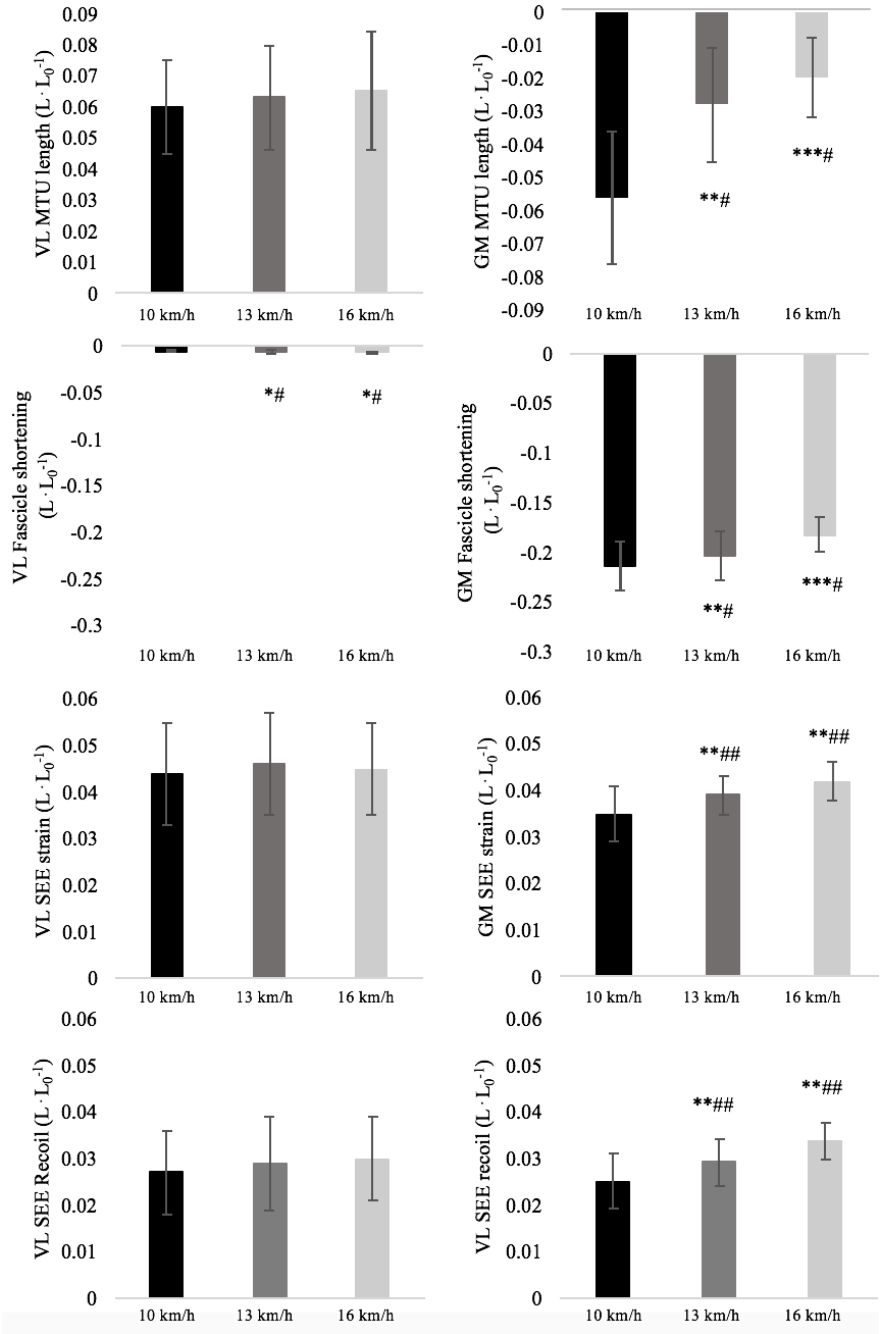

Figure 5. 3: Average change of MTU, fascicle shortening, SEE strain and SEE recoil values for Vastus Lateralis (left panels) and Gastrocnemius Medialis (right panels) as a function of running speed. Values are means ± SD and are dimensionless (relative lengths, normalised for the condition of static standing). Black column: 10 km·h^{-1}; dark grey column: 13 km·h^{-1}; light grey column: 16 km·h^{-1}. Significantly different from 10 km·h^{-1} (: P<0.05; **: P<0.01; ***: P<0.001); significant difference between 13 and 16 km·h^{-1} (#: P<0.05; ##: P<0.01; ###: P<0.001).*

EMG activity

Figure 5.4 shows the average EMG values of VL and GM in all running conditions during the stance phase. The mean EMG values of VL and GM showed significant differences as a function of speed (main effect: P<0.001 and P<0.01 for GM and VL, respectively), with significant differences found for each muscle between all running speeds.

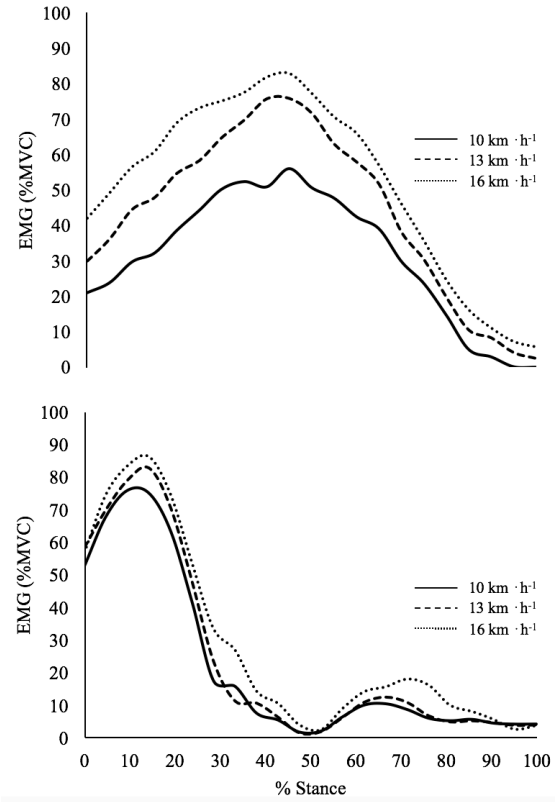

Figure 5. 4: EMG linear envelope for Gastrocnemius Medialis (upper panels) and Vastus Lateralis (lower panels) measured in the stance phase when running at three steady speeds (solid line: 10 km·h^{-1}; thick dashed line: 13 km·h^{-1}; thin dashed line: 16 km·h^{-1}). EMG activity was normalised to the peak EMG activity measured during the MVC.

Kinetic parameters

Figure 5.5 shows the average joint power at the level of knee and ankle during the stance phase at each running velocity (upper panels). Joint power parameters could be divided into two different phases: negative (absorption) or positive (propulsion). During the absorption phase the mean values of knee joint power were -6.25±0.88, -6.43±0.81, -6.53±0.77 W·kg^{-1}, whereas during the propulsion phase were 2.3±0.45, 3.29±0.51, 3.39±0.54 W·kg^{-1}, at 10, 13 and 16 km·h^{-1}, respectively. Significant differences were observed between all running speeds ($P<0.05$ and $P<0.01$ for negative and positive phase, respectively). The mean absorption values of ankle were -3±0.23, -4.51±0.37, -7.12±0.44 W·kg^{-1}, whereas during the propulsion phase were 5.40±0.88, 7.38±0.96, 9.72±0.91 W·kg^{-1}, at 10, 13 and 16 km·h^{-1}, respectively. Significant differences were observed between all running speeds ($P<0.001$ for both stance phases).

Increasing running speed from 10 to 16 km·h^{-1} resulted in an increase in average positive power produced by the MTU (P_{MTU}^{+}) in both muscles (middle panel of Figure 5.5) (VL: $P<0.05$ and GM: $P<0.001$) and significant differences were observed among speeds. P_{SEE}^{+} increased in GM as a function of speed ($P<0.01$), whereas no significant difference was observed for VL. For both muscles, P_{fas}^{+} showed significant differences as a function of speed ($P<0.05$).

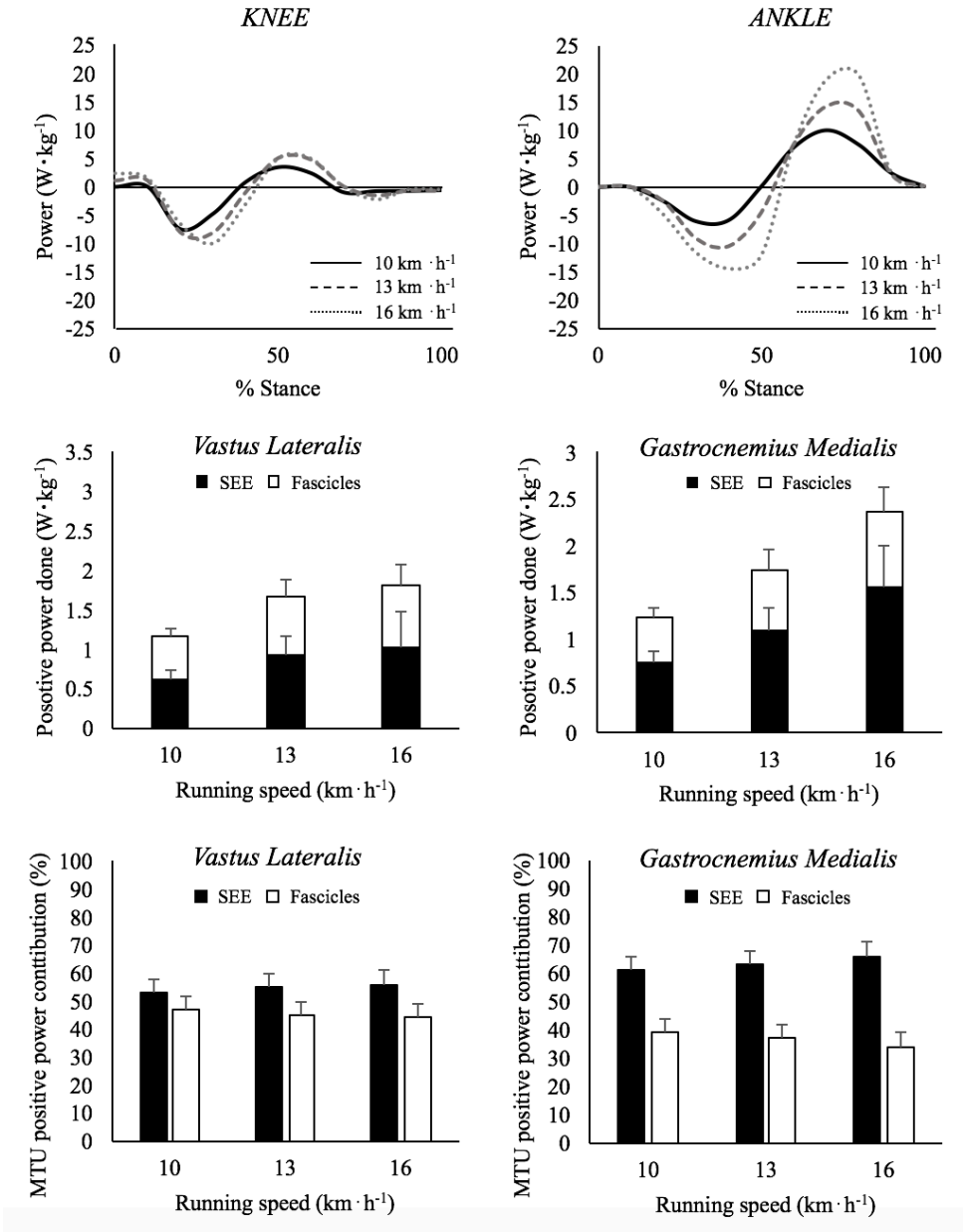

Figure 5. 5: Upper panels: average net joint power (normalised to body mass) calculated at the knee (left) and ankle (right) level when running at three steady speeds (solid line: 10 km·h^{-1}; thick dashed line: 13 km·h^{-1}; thin dashed line: 16 km·h^{-1}). Middle panels show the absolute value of the mechanical power done by the SEE (black columns) and by the muscle fascicles (white columns) for VL (left panel) and GM (right panel). The sum of the two components represent the total mechanical power of the MTUs. Lower panels show the relative contribution of the SEE (black columns) and muscle fascicles (white columns) in determining the mechanical power done by the MTU for VL (left panel) and GM (right panel).

The relative contribution of the fascicles in determining P_{MTU}^{+} was different between muscles (lower panel in Figure 5.5). For VL, 45% of the P_{MTU}^{+} could be attributed to the fascicle behaviour (no significant changes among speeds), whereas for GM, only 35% of the positive power was generated by the fascicle (no significant changes among speeds). As a consequence, tendon elastic power contributed 55% and 65% to the positive power done by the MTU for VL and GM, respectively (as an average, at all investigated speeds).

DISCUSSION

In the present study, the fascicle and SEE behaviours of two functionally different MTUs (Vastus Lateralis and Gastrocnemius Medialis) were analysed during running at increasing speed. As hypothesised, VL and GM fascicles were able to retain a high force-generating potential as they remained quasi-isometric at each running speed; the quasi isometric behaviour of both muscles could be attributed to the contribution of the SEE, which accommodated the larger part of the MTU displacement. Therefore, our results confirm the hypothesis of a similar fascicle and tendon behaviour for the two MTUs. We also expected to find an increase of the SEE strain and recoil with running speed in the two MTUs, but our data showed that this was the case for the GM only. Therefore, our second hypothesis is only partially confirmed.

As suggested previously (Lai et al., 2018; Bohm et al., 2018), tendon elastic strain energy would contribute a greater proportion of the positive work done by the MTU with increased running speed, in both muscle groups, enhancing the performance of the muscle fibres by allowing them to operate close to isometric conditions. Data reported in this study confirm the findings of the modelling study of Lai et al. (2014) and the hypothesis formulated by Bohm et al. (2018) for the GM MTU and extend these considerations to the *in vivo* VL MTU behaviour at different running speeds.

As shown by our data, increasing running speed affected differently the mechanical output of the two muscles. Contrary to our second hypothesis, the mechanical power provided by the SEE during the propulsive phase of running increased as a function of speed in the GM only, while it remained relatively constant for VL. On the other hand, the relative contribution of tendon elastic strain energy to the positive work done by the MTU was found to be rather constant as a function of speed in both muscles and to amount to about 65% for GM and 55% for VL.

A likely explanation for the lack of length changes in VL SEE at faster speeds (and therefore greater loading) is the high stiffness of the patellar-quadriceps tendon complex (O'Brien et al., 2010; Arampatzis et al., 2005; Stafilidis et al., 2005) in combination with the anatomical position of this structure distally to the point of ground reaction force application. These characteristics are consistent with a SEE suited more for effective contractile force transmission distally and joint position control, rather than elastic strain energy storage and release (Ker et al., 1998). Furthermore, the architecture of the knee extensor MTU (longer muscle fascicles compared to the in-series shorter tendon) is suited more for dissipation of the mechanical energy during the first instant of the shock-absorption phase (see Figure 5.5). Indeed, when the speed increased, the ankle plantar flexors absorbed most of mechanical power, allowing the knee extensors to work with little energy changes as a function of speed (see Figure 5.5). Therefore, the small changes in the negative phase of power may not have

been sufficient to further increase the elongation and consequent recoil in the VL SEE. Indeed, as indicated by several authors (Lai et al., 2014; Dorn et al., 2012; Arnold et al., 2013; Santuz et al., 2017) during the first part of stance VL absorbs mechanical energy whereas in the second phase of stance (propulsion phase) its function is to stabilize the body. In the propulsion phase, the back thigh muscles (especially the hamstrings) play the most important role in force development (e.g. Farris & Sawicki, 2012). Therefore, it can be expected that the contribution of VL in force production decreases as a function of speed, allowing the hip and the hamstrings to provide more force as running speed increases.

The important differences in the SEE behaviour between GM and VL MTUs result in a different mechanical output for the MTU. During the energy absorption phase of running, both MTUs store elastic strain energy, but as showed by Figure 5.5, the power generated by GM is far larger than that of VL. Consequently, it is possible that the SEE of VL absorbs and dissipates mechanical power, where the SEE of the GM works more as an energy saving mechanism. One other possible contributor mechanism for the SEE behaviour of GM is proximal-distal power transfer between joints, since this is a bi-articular muscle (Prilutsky & Zatsiorsky, 1994). Therefore, further studies should include multiple levels of analysis for the SEE.

VL muscle-tendon behaviour

This is the first study that experimentally investigated the operating length and velocity of the human VL fascicles during level running at increasing speed. Our data provide evidence that the VL fascicles operate close to their optimum working length (L_0) with small length changes during the stance phase, where the muscle is active and generates force and power. Furthermore, the same muscle fascicle behaviour was observed with increasing speed.

As highlighted by our data, at increasing speed, the VL muscle was activated in the initial stance phase, and this is associated with the function of the muscle to decelerate and support the body mass (Dorn et al., 2012). In agreement with Bohm et al. (2018), during the active state, the MTU showed the largest elongation (Figure 5.1), whereas the fascicles operated with significantly smaller changes around their optimal length (L_0). Indeed, as shown by Figure 1, the main length changes of the VL MTU were primarily associated with changes of the series-elastic elements of the VL (patellar and quadriceps tendon complex). This SEE behaviour, allows the fascicles to take advantage of the high force-length-velocity potentials during the active phase of the stance phase where the VL muscle generates force (Bohm et al., 2018; Nikolaidou et al., 2017).

With increasing running speed, the VL fascicles operate at longer lengths (see Figure 5.3), however, the favourable fascicle length conditions (isometric behaviour during stance) seem to be

the result of adjusted muscle activation. In all running conditions, VL muscle increased the EMG activity in the first part of the stance phase where the MTU is lengthened. This coordinated time course between EMG activity and MTU elongation provides evidence that time-adjusted muscle activation contributes to the minimisation of fascicle length changes during running at increasing speed. As a consequence, the MTU could operate at a high force-generating potential and absorb substantial power during the first phase of the stance, due to SEE strain (Figures 5.2 and 5.5, upper panel). On the contrary, during the propulsion phase the activation of VL muscle is much lower (10-20% of the EMG activity at MVC) (Figure 5.4), but sufficient to allow the VL muscle fascicles to remain quasi-isometric also in the second part of the stance phase. It is possible that the SEE recoil allows the muscle to maintain a rather constant length, while the SEE accommodates the larger part of the MTU displacement. This speculation is supported by the pattern of mechanical power production during the propulsion phase in our tests, which show that about half of the positive power provided by VL is derived from the SEE and that VL SEE elongation did not change significantly among speeds (Figure 5.5, lower panel).

Therefore, the favourable fascicle operating conditions observed in the present study may have functional importance for human running at increasing speed, because less active muscle volume would be required for a certain mechanical demand, allowing a reduction in metabolic cost during locomotion (Lai et al, 2014; Roberts, 2002; Fletcher & MacIntosh, 2017). Since during the propulsion phase the VL does not contribute to the positive power generated (Figure 5.5, upper panel), the knee extensors do not need to provide additional energy and a simple energy exchange within the MTU close to the optimal length (L_0) of the muscle fascicles may allow for a minimisation of the activation level and duration of muscle activity during the stance phase, which improves the economy of muscle force generation (Bohm et al., 2018; Hill, 1938).

GM muscle-tendon behaviour

This is the first study experimentally investigating the operating length and velocity of the human GM fascicles during level running at increasing speed. The results of the present study indicate that the GM fascicle length remained quasi-isometric throughout the period of high force development, irrespective of running speed, as was also the case for the VL muscle.

A previous modelling study investigating the behaviour of the GM MTU during running at increasing speed found similar results to ours, with the fascicles operating isometrically, at smaller lengths as a function of running speed[6]. Furthermore, GM fascicle length change has also been observed to be small during running in experimental studies but at lower running speeds (Lichtwark et al., 2007; Farris & Sawicki, 2012; Cornin & Finni, 2013). In the present study, the GM fascicles

shortened relatively little during the stance phase of running, but more than those of VL (see Figures 2 and 3). Thus, similar to the VL fascicles, the GM fascicles operated quasi-isometrically and close to their optimal length (L_0, see Figure 5.2) allowing the GM muscle to develop large contractile forces. These muscle forces increase the stretch and recoil of the tendon, thereby facilitating greater storage and recovery of tendon elastic strain energy.

We found that the GM elastic strain energy provided a greater relative contribution to the positive work done by the MTU compared to the positive work provided by the muscle fascicles and that this contribution increased as a function of speed in absolute terms but remained almost constant in relative terms (Figure 5.5). This result is consistent with previous studies suggesting that muscle fibres in distal limb muscles, such as the ankle plantar-flexors, contract isometrically to facilitate greater storage and recovery of tendon elastic strain energy at fast locomotion speeds (Tijs et al., 2015).

The greater storage and recovery of elastic strain energy, however, is coupled with an unfavourable shift of the muscle fascicles on their force-length relationship. In fact, although the GM muscle fascicles work with small and almost isometric changes, their operating regions shift down on the ascending limb of the F-L curve. It is likely that the observed increase in EMG activity with increasing running speeds reflects a greater volume of active muscle recruited in an effort to counteract these unfavourable conditions.

Regarding the contribution of the SEE in the GM MTU, our data are in agreement with those of previous studies that estimated the relative contribution of tendon elastic strain energy to the positive work done by the MTU for the ankle plantar-flexors during running (Farris & Sawicki, 2012): SEE strain energy was found to contribute 60% to the MTU positive work for the gastrocnemius when running at 7.2 km/h. Our data confirm these findings and extend them to a wider range of speeds supporting the idea that elastic strain energy contributes a greater proportion of the MTU propulsive power developed by the ankle plantar flexors compared to their muscle fascicles during running.

Limitations

There are certain limitations to the *in vivo* ultrasound and inverse dynamics approach used in this study that require consideration. Firstly, we did not directly measure or calculate the individual forces generated by the GM and VL MTUs during running. Instead, our interpretation regarding the function of the two muscles was based on the measured length changes of the MTU, muscle fascicles and SEE, as well as on the net moments and powers generated by the muscles spanning the knee and ankle, computed from inverse dynamics. Secondly, we assumed negligible inter-muscular force transmission between the individual muscles comprising the ankle plantar flexor and knee extensor

groups. In support of this assumption are the findings of Tijs et al. (2015), who have shown that non-myotendinous forces are likely to have a minimal effect on the overall function of muscles. Thirdly, the geometric approach used in this study modelled the MTUs with individual SEEs rather than with a common Achilles or patellar tendon. Finally SEE, length changes were indirectly calculated, rather than measured, using MTU and *in vivo* fascicle measurements. Such SEE length estimates represent all connective tissue structures in-series with the muscle fascicles, including the aponeurosis and free tendon.

CONCLUSIONS

The series elastic components of the ankle plantar-flexors have historically been considered to be more compliant than the knee extensor ones, and this consideration leads to speculate that these two MTUs should have a different functional role. However, this study shows that muscle and tendon behaviours of VL (knee extensor) and GM (ankle plantar-flexor) are quite similar. For both MTUs elastic strain energy provides the majority of the positive power done by the MTU and the increased utilization of SEE strain energy at increasing running speed is linked with a quasi-isometric muscle fascicle behaviour. These two mechanisms indicate that the series elastic components accommodate the majority of the MTU displacement. Therefore, by minimising the force-length and force-velocity changes during active muscle contraction, the SEE allows the muscle to contract quasi-isometrically and close to L_0, thus producing high forces economically. In addition, the SEE behaviour is consistent with the provision of strain elastic energy, which is expected to further reduce metabolic cost requirements. Data reported in this study indicate that, when speed increases, tendon elongation increases and muscle fascicle elongation diminishes for both the VL and GM MTUs, and this behaviour is consistent with a reduction in the energy demand of running. Future studies should investigate the link between muscle-tendon behaviour during running and the associated metabolic cost.

CHAPTER 6

STEADY-STATE RUNNING: STUDY 5

THE INFLUENCE OF ACHILLES TENDON BEHAVIOR ON LOCOMOTION EFFICIENCY DURING HUMAN RUNNING

Authors: Andrea Monte[1,2], Costantinos Maganaris2, Vasilios Baltzopoulos[2], Paola Zamparo[1]

[1] *Department of Neurosciences, Biomedicine and Movement Sciences, University of Verona, Italy*

[2] *Liverpool John Moores University, Research Institute for Sport and Exercise Sciences (RISES), United Kingdom*

ABSTRACT

We investigated the role of elastic strain energy on the "apparent" efficiency of locomotion (AE), a parameter that is known to increase as a function of running speed (up to 0.5-0.7) well above the values of "pure" muscle efficiency (about 0.25-0.30). In-vivo ultrasound measurements of the Gastrocnemius Medialis (GM) muscle tendon unit (MTU) were combined with kinematic, kinetic and metabolic measurements to investigate the possible influence of the Achilles tendon mechanical behaviour on the mechanics (total mechanical work, W_{TOT}) and energetics (net energy cost, C_{net}) of running at different speeds (10, 13 and 16 $km \cdot h^{-1}$); AE was calculated as: W_{TOT}/C_{net}. GM fascicles shortened during the entire stance phase, the more so the higher the speed, but the majority of the MTU displacement was accommodated by the Achilles tendon. Tendon strain and recoil increased as a function of running speed ($P<0.01$ and $P<0.001$ respectively). The contribution of elastic energy to the positive work generated by the MTU also increased with speed (from 0.09 to 0.16 $J \cdot kg^{-1}$). Significant negative correlations ($P<0.01$) were observed between tendon work and metabolic energy at each running speed (the higher the tendon work the lower the metabolic demand) and significant positive correlations were observed between tendon work and AE ($P<0.001$) at each running speed (the higher the tendon work the higher the efficiency). These results support the notion that the dynamic function of tendons is integral in reducing energy expenditure and increasing the "apparent" efficiency of running.

Paper under review

INTRODUCTION

Human locomotion entails the motion of the body through an environment: air in terrestrial locomotion whilst in contact with the ground, and water in aquatic locomotion. The minimum required work that has to be done to maintain the motion of any object in its surrounding environment, is given by the product of the resistance offered by the environment and the distance covered during the motion. The efficiency of the locomotor apparatus can thus be expressed as the ratio between the work necessary to maintain motion and the chemical energy transformed by the muscles. This "locomotion" efficiency (i.e. work done as a proportion of metabolic cost), has been investigated in several forms of terrestrial and aquatic locomotion, such as swimming (e.g. Zamparo et al. 2002), cycling (e.g. Minetti et al. 2001), walking and running (e.g. Cavagna and Kaneko 1977; Lejeune et al. 1988; Williams et al. 1987).

In the above mentioned studies, "locomotion" efficiency was, actually, calculated as the ratio between (total) mechanical work per unit distance (W_{TOT}) and net energy cost (C_{net}, the metabolic energy expended per unit distance); in turn, C_{net} was calculated as the ratio between net oxygen uptake and locomotion velocity ($\dot{V}O_{2net}$ /v) and W_{TOT} was calculated as the sum of two components: W_{EXT} (the work done to raise and accelerate the body centre of mass within the environment) and W_{INT} (the work associated with the acceleration of body segments with respect to the centre of mass). As calculated, "locomotion" efficiency approximates "pure" muscle efficiency values (about 0.25-0.30, as reported by Woledge et al. 1985) in the forms of locomotion where elastic recoil is negligible (e.g. swimming or cycling, as reported by Zamparo et al. 2002 and Minetti et al. 2001) whereas in the case of running, the efficiency calculated in this manner can reach far larger values (e.g. up to 0.5-0.7, as reported by Cavagna and Kaneko 1977).

"Locomotion" efficiency is, therefore, often referred to as "apparent" efficiency because an increase beyond pure muscle efficiency values does not indicate that the muscles work in a more efficient way (Ettema 2001). Rather, these increased efficiency values are an indication of the conversion of metabolic energy into mechanical work at whole-body level. As suggested by Alexander (1991), measuring "apparent" efficiency can thus help in understanding whether mechanical work is "recycled" via storage and release of elastic energy (an energy saving mechanism).

As an example, when running at steady-state speed, tendons stretch and recoil; through this succession of stretch-shortening cycles, tendons could play an important role as energy savers allowing this form of locomotion to be particularly efficient (Roberts and Azizi 2011). In these conditions, indeed, "apparent" efficiency ($AE = W_{TOT}/C_{net}$) increases linearly with speed because W_{TOT} increases whereas C_{net} does not show appreciable changes when the velocity increases (e.g.

Cavagna and Kaneko 1977). In other conditions (e.g. shuttle running or uphill running) AE is much lower due to the different role of the tendon, which acts more as a power amplifier (Roberts and Azizi 2011). As an example, during shuttle running, AE is lowest over short shuttle distances covered at maximal speed (e.g. when the accelerations and decelerations are larger and elastic recoil supposedly lower) and highest over long shuttle distances (e.g. in conditions that approximate those of constant speed, linear, running where elastic recoil is supposedly larger) (Zamparo et al. 2019). A further example is that of running on sand where AE is lower relatively to running on a hard surface and this could be attributable to a decrease in "muscle-tendon efficiency", the sand acting as a damper which reduces the energy that can be recoiled from the stretched tendon (Lejeune et al. 1988). Taken together, these findings suggest a link between the capability to exploit the elastic energy mechanisms in tendons and the values of "apparent" efficiency in human running.

The dynamic function of tendons is indeed integral to reduce the energy expenditure of steady-state running: energetic savings may occur by shifting the operating regions of the muscles on their force-length and force-velocity curves (Ramsey and Street 1940), by reducing muscle work (Biewener and Roberts, 2000), or by reducing active muscle volume (Holt et al. 2016). However, the increased energy storage in, and release from, the tendon is associated with a higher muscle force, which in turn increases the metabolic cost, offsetting the effects of increased energy storage and release (Fletcher and MacIntosh 2017). Yet, in theory, if the whole muscle-tendon unit length changes could be attributed to the tendon only, the muscle fibres would operate under isometric conditions and therefore, the level of muscle activation required would be lower since muscle force is greater under isometric conditions compared to when the muscle is actively shortening (Alexander 1991). Indeed, Fletcher and MacIntosh (2017) recently hypothesised that tendon behaviour could reduce the energy expended during contraction by reducing the amount and rate of muscle shortening. These theoretical notions were supported by recent studies of Bohm et al. (2019) and Monte et al. (2020), which revealed a quasi-isometric behaviour of the plantar flexor muscles during running at different speeds. Furthermore, Bohm and co-workers found a negative significant correlation between the force-length-velocity potential of the soleus muscle and the energy cost of running at 10 $km \cdot h^{-1}$, suggesting that the higher the force potential the lower the energy expended. Therefore, the ankle plantar flexors seem to play an important role in the mechanical and physiological demand of human running.

The human ankle plantar flexors produce forces of up to 12 times body weight during running at increasing speed (Komi 1990) and are the main force producers amongst all the major lower-limb muscle groups (Dorn et al. 2012). Due to their unique design (short muscle fibres connected to the heel via a long and compliant Achilles tendon), the ankle plantar flexors, have the capacity to generate

high amounts of power with minimal energy expenditure. In fact, thanks to their long tendon, the plantar flexors can store elastic energy up to about 60% of the MTU work during running (Monte et al. 2020; Farris and Sawicki 2012; Lai et al. 2014) and their contribution increases as a function of speed. This behaviour seems to be particularly relevant for determining energy expenditure, mechanical work and therefore, "apparent" efficiency; however, there are no studies that have investigated the role of plantar flexor tendons on "apparent" running efficiency.

The aim of this study was to verify experimentally the theoretical link between human plantar flexor muscle-tendon behaviour and "apparent" running efficiency. In particular, we combined *in vivo* ultrasound, kinematic and kinetic measurements during running at different speeds and we calculated the relative contribution of GM muscle fascicles and Achilles tendon to the mechanical work done by the MTU to investigate the role of Achilles tendon behaviour on the mechanical power output at whole-body level (W_{TOT}) and on the energy demands ($\dot{V}O_{2net}$ and C_{net}) during running at increasing speeds. Our main hypothesis was that the contribution of tendon work to the total work done by the MTU would increase with running speed and that this increase could, at least partially, explain the concurrent increase in "apparent" efficiency.

MATERIALS AND METHODS

Subjects

The experiments were performed on fifteen male endurance athletes, as a part of a larger study partly submitted elsewhere. All participants (24±2.4 years of age; 74±2.8 kg of body mass; 1.77±0.04 m of stature; 8.5±2.2 years of training: 5±1 workouts per week) received written and oral instructions before the study and gave their written informed consent to the experimental procedure. The experimental protocol was approved by the Ethical Committee of Liverpool John Moores University (protocol number: 18/SPS/028) and performed in accordance with the Helsinki Declaration.

Experimental Design

During each running trial the participants ran at steady speed using a self-selected cadence, step length and running technique. All participants used a forefoot running pattern.

The trajectories of 50 reflective markers were recorded using 12 camera system (Vicon Vero 2.2, Oxford Metrics, United Kingdom), sampling at 250 Hz. The markers were placed at specific anatomical position on the subjects' head, trunk, arms, pelvis, lower limbs and foots. This marker set was proposed by Lai et al. (2018) to investigate the ankle moment generation. Moreover, we added another 14 markers (four on the right and left knee, six on the right shank/foot and one at the great trochanter and cheekbones, bilaterally) to measure the tendon lever arm during running as described

by Rasske et al. (2017) and the internal work (see below) with the marker set proposed by Minetti et al. (1993) which considers the body as composed by 11 body segments: head-trunk, thigh, shank, foot, upper arm, forearm.

Ground reaction forces (GRFs) were recorded using an instrumented treadmill (M-GAIT, MOTEK) with two 3-axial (horizontal, vertical and mediolateral) force plates sampling at 1500 Hz (Lai et al., 2018). Resultant GRFs, center of pressure and free moment vectors were measured and recorded by the treadmill's software.

A B-mode ultrasound apparatus (Telemed Echo Blaster 128) with a linear probe operated at a scanning depth and with of 6 cm (sample frequency 7 MHz) was used to record the GM fascicles at a sampling rate of 60 Hz. Ultrasound images were recorded from the right leg of each athlete during each running trial, with the probe placed in the sagittal plane at the mid-belly of the muscle. The transducer was manipulated until the superficial and deep aponeuroses and the connective tissue that surrounds the muscle fascicles were clearly visible (Lichtwark et al., 2007; Cronin & Finni, 2013).

All signals were synchronized by a digital output generated by the ultrasound scanner that triggered all instrumentations (the Vicon cameras, ground reaction forces and ultrasound).

Finally, a metabolic gas analysis was performed in order to measure oxygen consumption during each running trial ($\dot{V}O_2$) by means of a breath by breath metabolimeter (CORTEX Metalyzer 3B, CORTEX Biophysik, Germany); 6 min of baseline data collection in a standing position was performed before these tests, the running trials were separated by 5 min of rest and data collected in the last minute of rest/exercise were averaged and used in further analyses. Net energy cost C_{net} was calculated by dividing net oxygen uptake ($\dot{V}O_{2net}$, in $mlO_2 \cdot kg^{-1} \cdot min^{-1}$, above resting values) to the treadmill velocity (v, expressed in $m \cdot min^{-1}$) and by using an energy equivalent that takes into account the RER: $\dot{V}O_{2net} \cdot (4.94 \cdot RER + 16.04)$ $J \cdot mlO_2^{-1}$ (Gabry & Astrup, 1987); C_{net} is thus expressed in $J \cdot kg^{1} \cdot m^{-1}$ and represents the energy expended to cover a unit distance.

Data analysis

In the last minute of each running trial, kinematic, kinetic and ultrasound data were analyzed for ten stance phases for each participant. This timing was selected because at the same time as for the determination of oxygen uptake. Data of each instrumentation (except for the oxygen consumption data) were interpolated to 200 sample points.

Kinetics and mechanical work

Marker trajectories were filtered with a forward and reverse low-pass Butterworth filter (second order: cut-off 10 Hz), whereas GRF was filtered through a forward and reverse low pass, 4th order

Butterworth filter with a cut off frequency of 30 Hz (consistent with the Nyquist theorem). Spectral analysis showed peaks of noise frequencies at 41, 47 and 100 Hz, which were speed and gait independent and consequently induced by the treadmill engine.

An inverse kinematics and dynamics approach were used to calculate the angular rotation for each body segment (Lai et al., 2018) and to compute the net joint moment at the ankle (Lai et al., 2018, Schache et al., 2011), respectively. Finally, based on the intrinsic characteristics of the limbs (mass of each segment and the radius of gyration determined according to Dempster inertial parameters (Winter, 1979) and their 3D angular velocity and acceleration, the work necessary to rotate and accelerate the limbs with respect to BCoM (the internal work, $W_{INT,}$ $J \cdot kg^{-1} \cdot m^{-1}$) was calculated (Cavagna & Kaneko, 1977; Minetti, 1998; Pavei et al., 2017).

The work done to raise and accelerate the body center of mass with respect to the environment ($W_{EXT,}$ $J \cdot kg^{-1} \cdot m^{-1}$) was calculated based on the summation of all increases in total mechanical energy ($E_T = E_P + E_K$), where the time course of potential (E_P) and kinetic ($Ek = Ek_x + Ek_y + Ek_z$) energy were calculated based on the BCoM trajectory. The BCoM position was calculated from the GRF by a double integration of the force signal, according to Cavagna (8) and by using as integration constant the treadmill speed (as described by Saibene & Minetti, 2003).

The sum of internal and external work represents the total mechanical work generated to move the body over a unit distance ($W_{TOT,}$ $J \cdot kg^{-1} \cdot m^{-1}$). "Apparent" efficiency (AE) was then calculated from the ratio W_{TOT} / C_{net} (both expressed in $J \cdot kg^{-1} \cdot m^{-1}$, see above).

Fascicle and series elastic element behavior

In vivo muscle fascicle length and pennation angle were measured from the ultrasound videos. The length of the muscle fascicle was defined as the distance between the deep and superficial aponeuroses. The pennation angle was defined as the angle between the collagenous tissue and the deep aponeurosis (Lichtwark et al., 2007; Seynnes et al., 2015). A validated automatic tracking algorithm was used to quantify the muscle fascicle length and pennation angle (Cronin & Finni, 2013; Gillet et al., 2013). At the end of the auto-tracking, every frame of the tracked muscle fascicle lengths and pennation angles was visually examined to check the algorithm accuracy. Whenever the muscle fascicle length or pennation angle was deemed inaccurate, the two points defining the muscle fascicles were manually repositioned. The instantaneous MTU length of GM in the stance phase was computed at each instant using instantaneous joint angles as proposed by Hawkins and Hull (1990); the instantaneous tendon length was calculated as the difference between the MTU length and the muscle belly length, taking into account the effect of pennation angle (Fukunaga et al., 2001; Randhawa et al., 2012; Wakeling et al., 2011). The average muscle-tendon unit (MTU) length,

fascicle length and tendon length during ankle moment development and ankle moment decline are reported in Table 1 along with tendon strain (the maximum value during the stance phase) and tendon recoil (the maximum value during the propulsive phase). Fascicles and tendon velocities were computed by differentiating the lengths of each component with respect to time in the stance phase (Lai et al., 2018).

Muscle fiber and Tendon mechanical work

The mechanical work done by the MTU, by the muscle fibers and by the Achilles tendon was calculated by integrating the corresponding power curves over the entire stance phase. In turn, the power developed by each component was obtained by multiplying the corresponding force and velocity values. Force production was determined as proposed by Farris & Sawicki (2011) whereas the velocity was calculated as first derivative of the length changes. Briefly, tendon force was calculated as the net ankle torque divided by the tendon lever arm (estimated as suggested by Rasske et al. (2017). The contribution of the antagonist moment to the net joint moment, was taken into account and subtracted to that of the agonist muscles. The force attributable to GM was estimated by multiplying "overall" tendon force by the relative PCSA of this muscle which, according to the literature, amounts to 15.9% of the PCSA of plantar flexors (Kurokawa et al., 2003; Fukunaga et al., 1992; Akim et al., 1995). To estimate the force of the muscle fascicles, tendon force was divided by the cosine of the pennation angle, as proposed by Lichtwark & Wilson (2006).

The positive work done by the MTU (W_{MTU}) was calculated in the portion of stance where the MTU generates positive power (Anderson and Pandy, 1993). Positive muscle fiber work (W_{fas}) was calculated as the positive muscle fiber work done during the propulsion phase; from these data positive tendon work (W_{ten}) was finally calculated, it represents the mechanical energy that can be derived from tendon recoil during the propulsion phase.

Statistics

A one-way ANOVA for repeated measures was conducted to test for possible differences among running speeds for all the investigated variables. When significant main effects were found, a post-hoc pairwise comparison using Fisher's least significant difference was used to determine the effect of speed. To determine the relationships between W_{ten} and C_{net} and W_{TOT} the Pearson's correlation coefficient was used. Statistical analysis was performed with SPSS (v24.0). All data extracted for statistical analysis were normally distributed (Shapiro-Wilk normality test, $P > 0.05$).

RESULTS

Table 6.1 reports the average values of muscle-tendon unit length, fascicle length and tendon length during ankle moment development and ankle moment decline (during the stance phase) as well as the values of tendon strain and recoil; all these parameters increased significantly as a function of speed (main effect: $P < 0.001$) but for GM fascicle length that decreased as a function of speed both during ankle power development and decline. Significant differences were observed among speeds in all investigated muscle and tendon parameters and the majority of the MTU displacement was accommodated by the Achilles tendon.

		Running parameters		
		10 km·h^{-1}	13 km·h^{-1}	16 km·h^{-1}
MTU length (cm)	Development	47.41±3.4	53.33±3.9**#	58.87±4.2***#
	Decline	44.32±3.2	42.88±2.7*#	40.04±2.8**#
Fascicle length (cm)	Development	4.37±1.01	4.28±0.97*#	4.19±0.83**#
	Decline	3.99±0.98	3.81±0.98*#	3.62±0.98**#
Tendon length (cm)	Development	22.53±2.2	23.78±1.97*##	24.51±1.89**##
	Decline	21.12±1.9	20.02±2.01*#	19.48±1.88**#
Tendon strain (cm)		1.10±0.49	1.35±0.52**##	1.62±0.57***##
Tendon recoil (cm)		0.89±0.55	1.11±0.48**##	1.35±0.51***##

Table 6. 1 Average muscle-tendon unit (MTU) length, fascicle length and tendon length during ankle moment development and ankle moment decline at 10, 13 and 16 km·h^{-1}. Tendon strain (the maximum value during the stance phase) and tendon recoil (the maximum value during the propulsive phase) also reported. Data are means ± SD and are expressed in cm. Significant differences from 10 km·h^{-1} (P<0.05; ** P<0.01; ***P<0.001); significant differences between 13 and 16 km·h^{-1}(# P<0.05; ## P<0.01; ###P<0.001).*

Figure 6.1 shows the average joint power at the ankle level during the stance phase at each running velocity (upper panel). During the propulsion phase (positive values in the second half of the stance), the average joint power was: 5.40±0.88, 7.38±0.96, 9.72±0.91 W·kg^{-1} at 10, 13 and 16 km·h^{-1}, respectively. Significant differences were observed among all running velocities (main effect: P<0.001). The mechanical work generated by the MTU, by the muscle fascicles and by the Achilles tendon during the propulsion phase are reported in the lower panel of Figure 6.1. All variables increased as a function of speed (MTU: P<0.001; Fascicle: P<0.05; Tendon: P<0.01) and significant differences were observed among running speed in all the investigated parameters. The majority of the MTU work is attributable to the Achilles tendon.

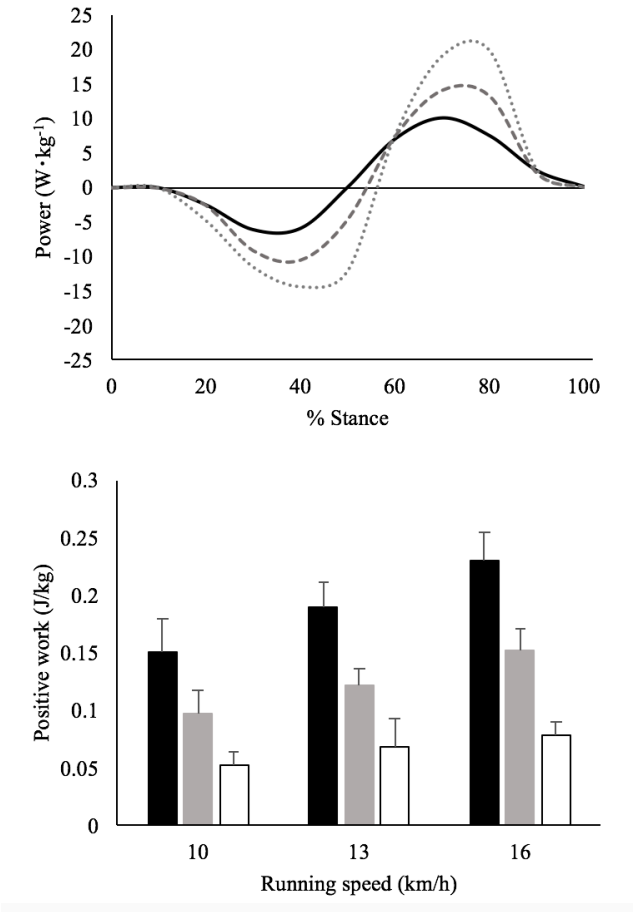

Figure 6. 1: Upper panel: average net joint power (normalised to body mass) calculated at the ankle level when running at three steady speeds (solid line: 10 km·h^{-1}; thick dashed line: 13 km·h^{-1}; thin dashed line: 16 km·h^{-1}). Lower panel shows the average net joint work done by the GM MTU (black columns), by the Achilles tendon (dark grey columns) and by the muscle fascicles (light grey columns).

Table 6.2 reports mechanical and metabolic data at the three investigated running speeds. With running speed, W_{EXT} decreased (main effect: $P < 0.001$), whereas $\dot{V}O_{2net}$, AE, W_{INT} and W_{TOT} increased (main effect: $P < 0.001$, for all variables). The comparisons among speeds showed significant differences among running trials for each of these variables. No differences in C_{net} were observed as a function of speed.

	W_{EXT} ($J \cdot kg^{-1} \cdot m^{-1}$)	W_{INT} ($J \cdot kg^{-1} \cdot m^{-1}$)	W_{TOT} ($J \cdot kg^{-1} \cdot m^{-1}$)	$\dot{V}O_2$ ($ml \cdot kg^{-1} \cdot min^{-1}$)	Cnet ($J \cdot kg^{-1} \cdot m^{-1}$)	AR
10 $km \cdot h^{-1}$	1.60 ± 0.09	0.31 ± 0.05	1.91 ± 0.04	32.2 ± 5.4	3.98 ± 0.42	0.49 ± 0.03
13 $km \cdot h^{-1}$	1.49 ± 0.08$^{**\#}$	0.67 ± 0.07$^{***\#\#\#}$	2.16 ± 0.03$^{**\#\#}$	42.9 ± 4.6$^{***\#\#\#}$	4.04 ± 0.38	0.53 ± 0.03$^{**\#\#}$
16 $km \cdot h^{-1}$	1.33 ± 0.08$^{***\#}$	0.95 ± 0.08$^{***\#\#\#}$	2.28 ± 0.06$^{***\#\#}$	52.6 ± 04.2$^{***\#\#\#}$	4.08 ± 0.34	0.57 ± 0.05$^{***\#\#}$

Table 6. 2: Mechanical and metabolic data (mean±SD) during running at 10, 13 and 16 $km \cdot h^{-1}$. W_{EXT}, mechanical external work; W_{INT}, mechanical internal work; W_{TOT}, mechanical total work; $\dot{V}O_2$, oxygen uptake; C_{net}, energy cost of running; AE, "apparent" efficiency. Significant difference from 10 $km \cdot h^{-1}$ (P<0.05; ** P<0.01; ***P<0.001); significant difference between 13 and 16 $km \cdot h^{-1}$(# P<0.05; ## P<0.01; ###P<0.001).*

Correlations between tendon work and running parameters

Figure 6.2 shows the correlations between Achilles tendon work and W_{TOT}, C_{net} and "apparent" efficiency (AE) at each running speed (10, 13 and 16 $km \cdot h^{-1}$, from top to bottom). Significant correlations were observed for all the investigated parameters at all the investigated speeds. The subjects with the highest tendon work were those with the highest total mechanical work (upper panel, $P < 0.01$ in all cases) and with the lower energy cost (middle panel, $P < 0.01$ in all cases). Positive significant correlations were observed between tendon work (W_{ten}) and AE at all the investigated speeds (lower panel, $P < 0.001$ in all cases): the subjects with the highest the tendon work were those with the highest "apparent" efficiency.

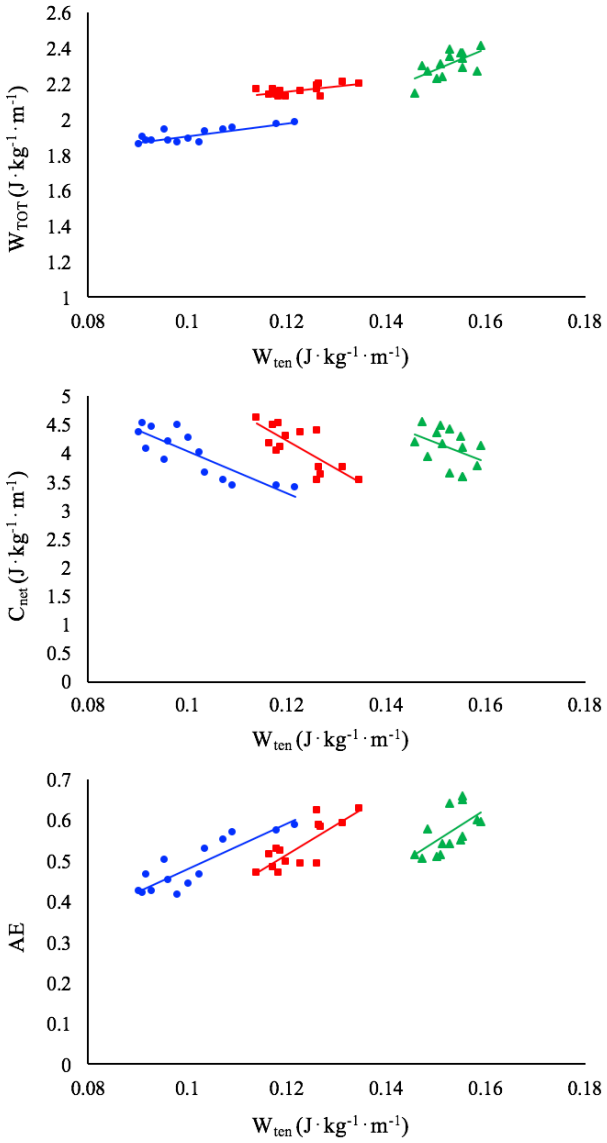

Figure 6. 2: Correlations between tendon work and total mechanical work (at the whole-body level), energy cost of running and "apparent" efficiency at the three investigated speeds (blued dots: 10 km·h^{-1}, red squares: 13 km·h^{-1}, green triangles: 16 km·h^{-1}). Upper panel: correlations between tendon work and total mechanical work at 10 km·h^{-1} (W_{TOT} = 3.34·W_{ten} + 1.57, R^2 = 0.65, P<0.01), 13 km·h^{-1} (W_{TOT} = 2.82·W_{ten}+ 1.81, R^2 = 0.52, P<0.05) and 16 km·h^{-1} (W_{TOT} = 11.40·W_{ten} + 0.56, R^2 = 0.55, P<0.05). Middle panel: correlations between tendon work and energy cost of running at 10 km·h^{-1} (C_{net} = -36.56·W_{ten} + 7.68, R^2 = 0.72, P<0.001), 13 km·h^{-1} (C_{net} = -49.43·W_{ten} + 10.15, R^2 = 0.60, P<0.01) and 16 km·h^{-1} (C_{net} = -35.36·W_{ten} + 9.49, R^2 = 52, P<0.05). Lower panel: correlations between tendon work and "apparent" efficiency at 10 km·h^{-1} (AE = 5.61·W_{ten} – 0.08, R^2 = 0.75, P<0.001), 13 km·h^{-1} (AE = 7.43·W_{ten} – 0.38, R^2 = 0.65, P<0.01) and 16 km·h^{-1} (AE = 7.96·W_{ten} – 0.65, R^2 = 54, P<0.05).

DISCUSSION

In this study we investigated the role of elastic strain energy (Achilles tendon work) on locomotion ("apparent") efficiency at increasing running speeds. Our results reveal that the work provided by the recoil of the Achilles tendon at each speed is linked to: 1) a reduction in the energy cost of running, 2) an increase in the mechanical work at whole-body level and 3) an increase in the "apparent" efficiency. These novel *in vivo* experimental results support the notion of elastic energy reutilization impacting positively on the economy/efficiency of running.

Apparent efficiency

Although the contribution of the Achilles tendon to the economy/efficiency of running through the reutilization of elastic energy is a mechanism since long postulated, data reported in this paper constitute a novel observation for in vivo human running, allowing for a better interpretation of the changes in AE in different experimental conditions. In this study, AE was calculated based on values of (total) mechanical work (i.e. the sum of internal and external work), an approach sometimes debated in the literature. However, an increase in efficiency attributable to elastic energy reutilization was also observed in studies where mechanical work was calculated based on a different (joint power) approach. As an example, Farris and Sawicki (2011) calculated values of efficiency of about 0.45 during running at 11 $km \cdot h^{-1}$ and Voigt et al. (1995) reported values of efficiency of about 0.65 during hopping (with a frequency of 2 Hz). This supports the idea that measuring "apparent" efficiency can help in understanding whether mechanical work has been "recycled" via storage and release of elastic energy, thus indicating the presence of an energy saving mechanism (as suggested by Alexander 1991).

Muscle and tendon contribution

Regarding the underpinning mechanisms, a possible explanation for the increase in "apparent" efficiency with speed is that the plantar flexor muscles favour the use of tendon elastic strain energy over muscle fibre work (Lichtwark et al. 2007), and that this energy is enhanced when running speed advances towards maximum running velocity (Cavagna and Kaneko 1977; Cavagna 2009). Our data are in line with these considerations and are comparable to those of previous studies that have estimated the relative contribution of tendon elastic strain energy to the positive work done by the MTU for the ankle plantar flexors during running (Hof et al. 2002; Farris and Sawicki 2012; Lai et al. 2014).

This mechanism may be a consequence of the plantar flexor muscle fibres remaining relatively isometric as running speed increases, a behaviour that allows to generate large muscle forces and facilitates the storage and recovery of tendon elastic strain energy. This was recently verified by *in vivo* studies that analysed the muscle and tendon behaviour of the plantar flexors during running at increasing speed (Lai et al. 2018; Werkhausen et al. 2019; Monte et al. 2020; Bohm et al. 2019). For instance, Monte et al. (2020) demonstrated that the Gastrocnemius Medialis muscle fascicles shorten during the entire stance phase, but that the series elastic components accommodate much of the displacement of the MTU, allowing the series-elastic components to provide the larger amount of mechanical power of the MTU. This result suggests that fibres in distal limb muscles, such as the

ankle plantar flexors, act like isometric struts to facilitate greater storage and recovery of tendon elastic strain energy at fast locomotion speeds (as indicated by Biewener and Roberts 2000).

The strong relationship between tendon work and total mechanical work at whole-body level we observed (middle panel of Figure 2) suggests that the elastic energy provided by the Achilles tendon recoil during the propulsive phase would affect the total mechanical work provided by the body. Indeed, as showed by Monte et al. (2020) with faster running speed, the GM muscle fascicle operating range shifts towards smaller lengths, on the ascending limb of the F-L relationship. This muscle fascicle shortening allows the elastic elements to provide more elastic energy during the propulsion phase and therefore to produce more positive power as speed increases.

What is the benefit of a larger tendon work? The most obvious answer is that the work done by tendons does not have to be done by the muscles, since muscle work is metabolically expensive (Roberts and Azizi 2011). In particular, if the whole MTU length changes were attributable to the tendon alone, the muscle fibres would operate under "pure" isometric conditions, requiring the lowest level of muscle activation (Fletcher and MacIntosh 2017). This phenomenon was recently verified by Bohm et al. (2019), who observed that the subjects with the higher soleus muscle force-potential were those with the lower energy cost of running, suggesting that, the lower the shortening velocity of the soleus muscle the lower the energy demand during running. Furthermore, these authors suggested that the main mechanism for the underlying reduction of the fascicle shortening velocity during the stance phase was a greater tendon gearing (i.e. larger tendon displacement with respect to the muscle fascicles).

However, the utilization of tendon elasticity does not come entirely "free-of-charge". Tendons operate in series with muscles and can only act as useful springs when muscles generate force. Force generation by muscles requires metabolic energy, and thus there is a cost to operate tendon springs. It has been proposed that the net metabolic benefit of tendon elasticity in running is best understood in the context of two properties of skeletal muscle (Roberts 2002; Roberts and Scale 2002). The first is the 'Fenn effect', which states that active muscles use more energy when performing work than when generating force isometrically (Fenn 1924). Thus, to the extent that tendons allow muscles to generate force without doing work (or while doing less work), they reduce the rate of energy consumption in the muscle. The second mechanism is the influence that tendon mechanics can have on the recruited muscle volume during running. Owing to the F-V properties of muscles, force can be produced with fewer active muscle fibres if the muscle operates at low or zero (i.e. isometric) shortening velocity (Fletcher and MacIntosh 2017). A larger mechanical work provided by the tendons is thus expected to reduce the metabolic demands of running and to increase locomotion efficiency. Our data support this notion.

Final remarks and conclusions

Besides Achilles tendon recoil, there are several other parameters that could affect energy expenditure as running speed increases and have not been considered in our analysis. For instance, higher activation of other agonist and antagonist muscles in the lower limbs, torso and upper limbs would contribute to the increase in metabolic energy expenditure with increasing speed (Arellano and Kram 2014). On the other hand, elastic mechanisms other than Achilles tendon recoil, such as the arch of the foot, could provide extra energy savings with increasing speed and make the running task less energy demanding. Furthermore, elastic energy could be stored also in the transversal plane of the MTU; indeed, biaxial loading of aponeuroses allows for variation in tendon stiffness and energy storage in a variety of locomotor behaviours (such as running, jumping and landing; e.g. Arellano et al. 2019).

Data reported for the first time in this study support the notion that GM tendon strain and recoil allow the muscle fascicles to operate with smaller length changes and indicate that this mechanism is enhanced when running speed increases. Although the reutilization of elastic energy is a well-known mechanism through which tendons are expected to contribute to the economy of movement, the novel observation of this study is that this increase is indeed associated with a concomitant decrease in metabolic energy expenditure and an increase in the "apparent" efficiency of locomotion.

CHAPTER 7
CONCLUSIONS

Summary

In this chapter, the novel findings of the five studies are briefly summarized and some general conclusions are drawn along with some considerations about future developments.

SUMMARY OF THE THESIS RESULTS

The aim of the present thesis was to enhance our knowledge about the energetics and mechanics of human locomotion and the underpinning role of muscle and tendon behaviour. To this aim: 1) the mechanical and energetic demands during non-steady locomotion were investigated by using sprints and shuttles; and 2) a detailed description of muscle and tendon behaviour during running at constant (and increasing) speed was provided; finally, 3) the effects of this behaviour on the mechanics and energetics of (constant speed linear) running were investigated.

The results of the five studies can be summarized as follows:

Study 1: This study provides information about how the architectural characteristics of knee extensors, plantar flexors and Achilles tendon contribute to (external, horizontal) power generation during a sprint running acceleration phase. Muscle-tendon parameters show a stronger correlation with peak values of horizontal power, force and speed than with average values of velocity over the first 20 meters and this indicates that the relationship between muscle-tendon parameters and sprinting performance is particularly evident in the sprint acceleration phase were the largest (horizontal) forces are exerted and peak power is attained.

Study 2: In a 20 m sprint, the power to accelerate the body forward (external, horizontal power) accounts for only 50% of total power, the internal power accounts for 41% and the power to rise BCoM accounts for 9% of total power. All the components of total mechanical power increase linearly with mean sprint velocity. In this study we adapted a published equation for internal power prediction in steady locomotion to unsteady conditions (e.g. the acceleration phase); this equation can be used to include internal power also in the methods that estimate external horizontal power only (as in Study 1).

Study 3: In shuttle runs, total mechanical work (internal + external) is larger the faster the velocity and the shorter the distance covered whereas mechanical (apparent) efficiency shows an opposite trend. At maximal speed, over all distances, braking/negative power is twice the positive power. The latter result highlights that running humans can exert a larger negative than positive power, in agreement with the fundamental proprieties of skeletal muscles in vivo (the Force-Velocity relationship in concentric and eccentric conditions). A greater relative importance of the constant speed phase, associated to a better exploitation of the elastic energy saving mechanism, is likely responsible of the higher apparent efficiency at the longer shuttle distances.

Study 4: With increasing running speed, the operating length of the muscle fascicles in the stance phase shifts towards smaller lengths in vastus lateralis (VL) and longer lengths in gastrocnemius medialis (GM). However, both muscles contract near-isometrically, close to their optimal length. The GM and VL series elastic element (SEE) show similar values of strain and recoil, but whereas the length of VL SEE does not change as a function of speed, GM lengthens and shortens more at higher speeds. With increasing running speed, the contribution of elastic strain energy to the positive power generated by the MTU increases similarly for GM and VL. These results indicate that VL and GM have similar muscle and tendon behaviors during running at increasing speed and that both muscle tendon units prioritize the storage and recovery of elastic strain energy over muscle power.

Study 5: In running GM muscle fascicles shorten during the entire stance phase but is the Achilles tendon that accommodates much of the displacement of the MTU. The values of tendon strain and recoil increase as a function of running speed and the contribution of tendon elastic energy to the positive work generated by the MTU increases linearly with speed. Tendon work and metabolic energy (energy cost) are negatively correlated at each running speed: the larger the tendon recoil the lower the metabolic demands. When data at all speeds are pooled, a significant correlation is observed between tendon work and apparent mechanical efficiency. These data indicate (as in Study 3) that apparent efficiency can be considered as an index of tendon function, since it is associated to a better exploitation of the elastic energy saving mechanism.

Conceptual diagrams summarizing the parameters investigated in each study and the most relevant and original results (in the framework of what is already known from the literature on these topics) are reported in Figures 7.1 and 7.2. These diagrams are based on the classification of tendon function (and relative locomotory tasks) proposed by Roberts and Azizi (2011), that are described in detail in the Introduction (see also Figure 1.30).

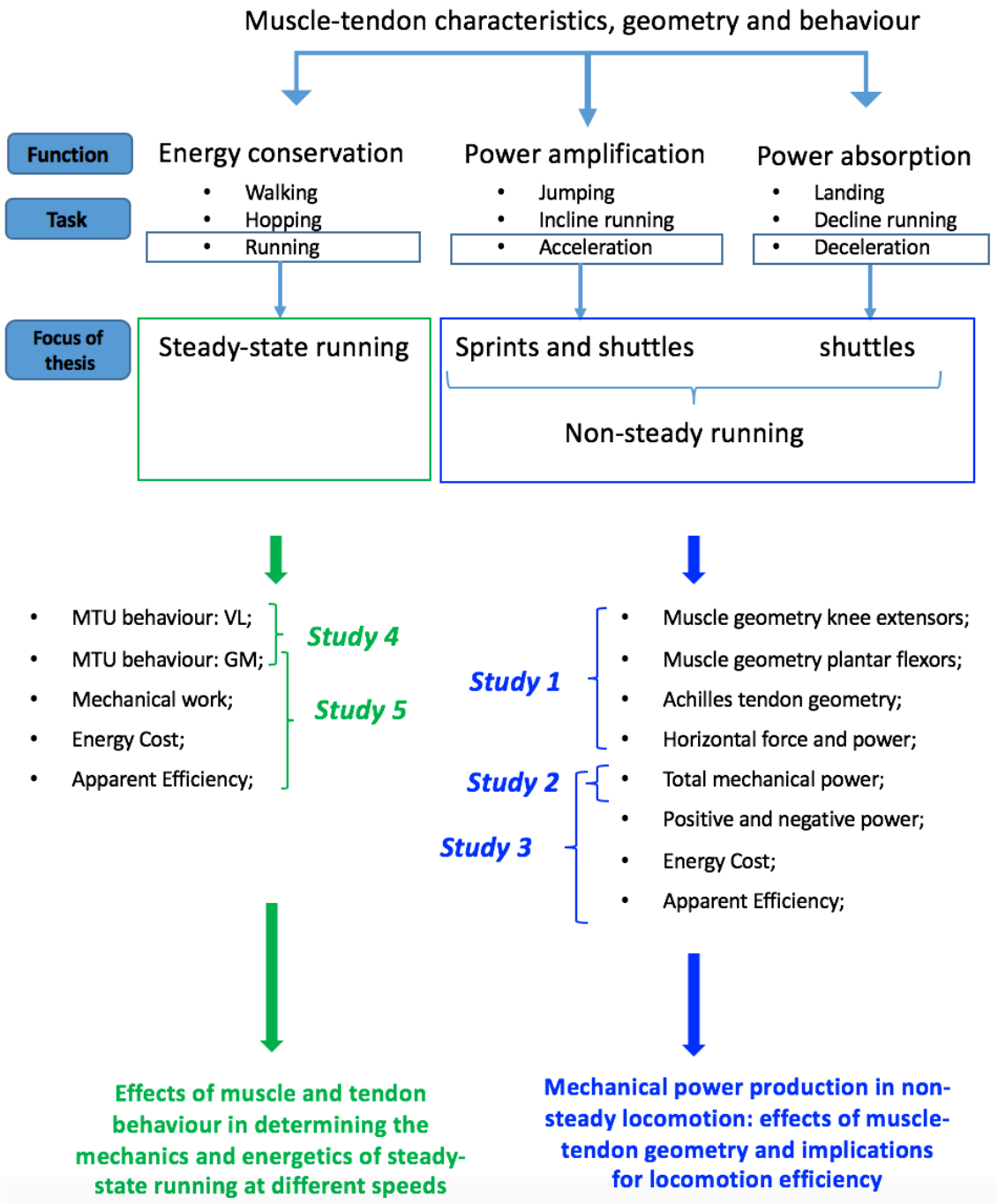

Figure 7. 1: muscle-tendon behaviour determines mechanical function in human locomotion: energy conservation, power amplification and power absorption. Five different studies were conducted to analyse the relationship between muscle-tendon behaviour and the mechanics and energetics of steady and non-steady locomotion. The most important parameters determined in each study are represented as well.

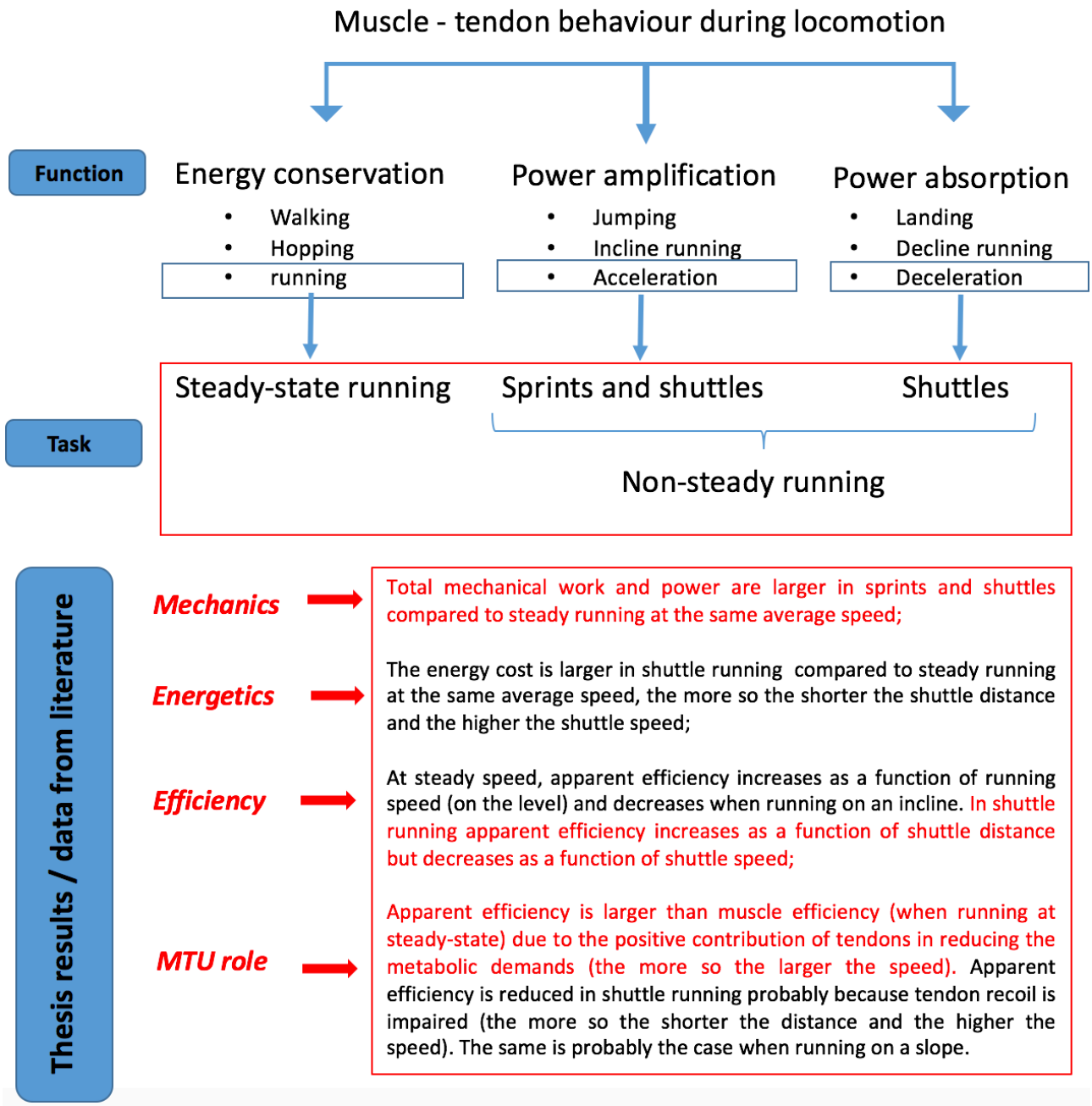

Figure 7. 2: the main results of this thesis (in red) are reported along with what we already know from the literature (in black) on these topics.

LIMITATIONS, ASSUMPTIONS, SPECULATIONS AND FUTURE PERSPECTIVES

Each study has its own limitations, which are discussed in the respective chapters.

One "general limitation" of this thesis is the approach to calculate total mechanical work as the sum of external and internal work. This approach was firstly proposed by Cavagna and Kaneko (1977) and is based on the calculations of whole body mechanical energy (and its changes) during motion in the 3D space, which is quite different from a muscle-tendon approach, where more complex interactions among non-linear properties of springs and actuators are involved. Total mechanical work estimation with this approach is still debated in the literature (Aleshinsky 1986 a, b, c, d, e) as also acknowledged for some aspects by the original authors (Willems et al., 1995). In this thesis we kept on adding W_{INT} and W_{EXT} to approximate W_{TOT} by considering as only energy transfer the one within body limbs segments. The only component left behind with this approach (besides the rotational work over the twist axis at change of direction in shuttles) is the internal friction in body tissues, which could affect the total mechanical work done.

The approach used in this thesis considers that all the measurable whole body mechanical energy decrease is "negative work" and all the measurable positive energy increase is "positive work". However, the positive work due to muscle contraction cannot exceed the equivalent work of metabolic consumption (converted according to reasonable muscle efficiency); if this should happen (as in the case of running at constant speed on the level), the only possibility is to refer the "extra positive work" to some energy previously stored as negative work, as in the case of the elastic energy stored into the elastic elements. This lead to say that "apparent efficiency", when exceeding 0.25-0.30, reveals the existence of a relevant amount of mechanical energy that is "kept" in the system (to allow bouncing) by an elastic storage-release system.

Data reported in this thesis allow to put forward a tentative answer to this hypothesis.

In Figure 7.3 the relationship between apparent efficiency (AE) and tendon work (W_{ten}) is reported (based on data reported in Chapter 6): when data from the three running speeds are considered together (black symbols) this relationship can be described by a linear function of the form: $AE = 1.99\ W_{ten} + 0.28$, $N = 45$, $R = 0.72$, $P < 0.001$. Even if correlation is not causation and even if the Achilles tendon is not the only "elastic storage-release system" of the human body, this relationship supports previous suggestions that a value of apparent efficiency of 0.25-0.30 should be expected when no elastic energy can be stored into the elastic elements (tendon work = 0 and AE = 0.28); on the other hand, when AE exceed these values some elastic recoil is probably at work.

In Figure 7.3 are also reported the values of AE as measured during shuttle running at maximal speed over the three investigated shuttle distances (data from Chapter 4). W_{ten} can thus be estimated based on this equation and on the values of AE: it is indeed lower in short shuttles than in shuttles

over long distances (as indeed suggested and discussed in Chapter 4). Interestingly, over the shortest shuttle distance, AE is lower than 0.28 and this suggests that, besides elastic recoil, also muscle efficiency is impaired in these conditions (e.g. when acceleration is high muscles may work far from the optimal operating range in their F-V relationship). The negative values of tendon work, over the shortest shuttle distance, could indicate a certain degree of dissipation (energy absorption).

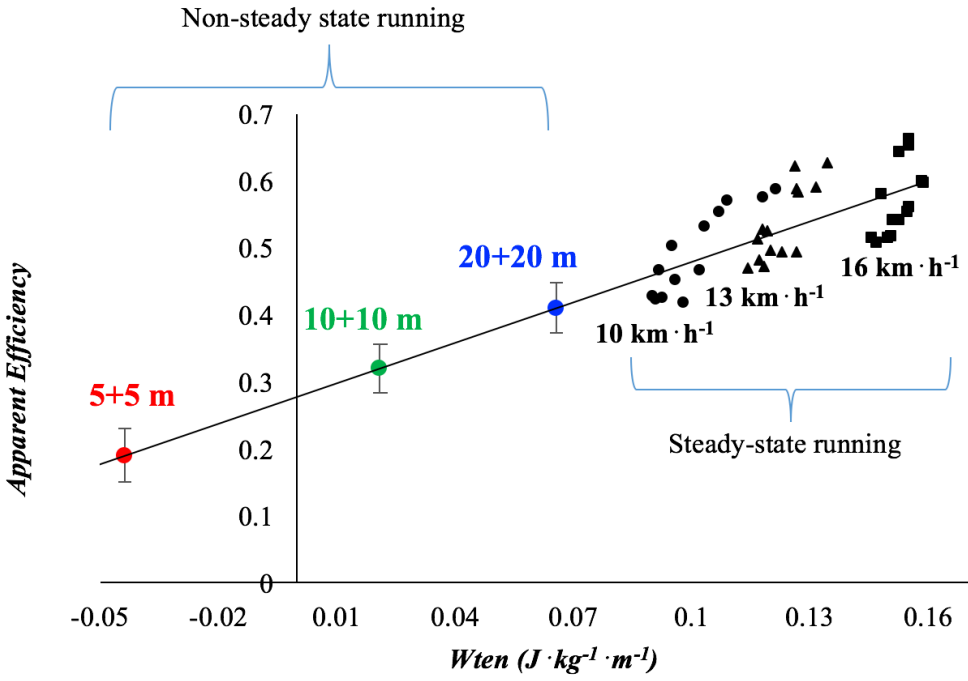

Figure 7.3. apparent efficiency (AE) as a function of tendon work (positive work during tendon recoil) during running at steady speed (black symbols). The values of AE as measured during shuttle running at maximal speed over three investigated shuttle distances are also reported (see text for details).

A future development of this thesis will be to check whether this is indeed the case by measuring, besides AE, also muscle-tendon behaviour during shuttle running and sprint running, as well as during running on a slope; these are, indeed, all conditions where AE decreases compared with constant speed linear running suggesting a concomitant decrease in tendon work. This is an unexplored field of study mainly because of methodological difficulties in measuring muscle-tendon behaviour *in vivo* in these conditions; the simplest way to check the validity of these estimations is to start with gradient locomotion.

What is the advantage of measuring AE over energy expenditure alone, given the limitations of the approach we used to calculate whole body mechanical work? The advantage is that it is possible to estimate the energy expended were the elastic recoil nil. Indeed, measuring only metabolic energy

cannot provide any indication on how much energy is spared by tendon work in a given locomotor task.

Data reported in Chapter 5 and 6 indicate that during steady-state running the muscles operate at higher force potential and close to their optimal length and that this allows the tendon to accommodate much of the MTU displacement increasing positive tendon work (Chapter 5). This is expected to reduce oxygen consumption and, indeed, the subjects with the higher tendon work are those with the lower $\dot{V}O_2$ (at a given speed) (Chapter 6). From data reported in Chapter 6 is, however, not possible to quantify the energy spared; in other words, it is not so simple to quantify the energy saving due to tendon work by measuring just $\dot{V}O_2$. Based on values of AE some rough estimations could be attempted (see Figure 7.4).

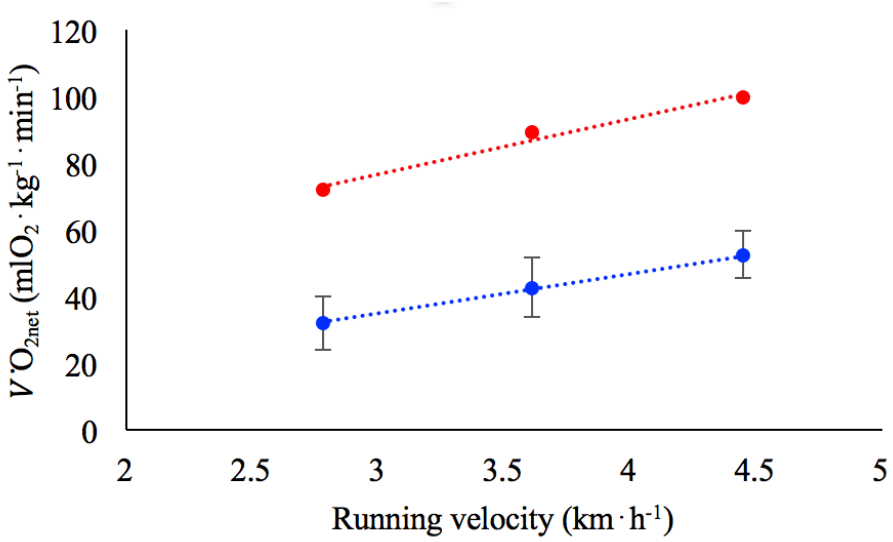

Figure 7.4: Net oxygen uptake ($\dot{V}O_{2net}$) as a function of running speed. Blue dots refer to the experimental data recorded during running at 10, 13 and 16 km·h^{-1} ($y = 11.8x$; $R^2 = 0.99$), whereas red dots represent the calculated values of $\dot{V}O_{2net}$ ($y = 16.59x + 27.14$; $R^2 = 0.98$) (see text for details). The difference between the two lines represents the metabolic energy saved by Achilles tendon work.

In figure 7.4 the average values of $\dot{V}O_2$ at three running speeds are reported (blue dots, data from Chapter 6). The red dots are calculated as follows: to the corresponding values of AE (see Table 5.1 in Chapter 6) a value of 0.28 is subtracted (e.g. the intercept of the linear relationship of Figure 7.3); the implicit assumption is thus made that the "excess in AE" above this value can provide an indication of the occurrence of some elastic recoil. The values of total mechanical work (W_{tot}, J · m^{-1} · kg^{-1}, see Table 5.1 in Chapter 6) can thus be divided by the "excess in AE" to obtain the "overall" energy expended in the unit of distance (C, J · m^{-1} · kg^{-1}; indeed: AE = W_{tot} / C and C = W_{tot} / AE). The values of C can be finally converted in mlO_2 · min^{-1} · kg^{-1} by knowing the energy equivalent of

oxygen and the running speed (see Introduction). These "overall-estimated" $\dot{V}O_2$ values represent the energy (in the unit of time) that would be requested were the tendon work nil; the difference between the red and blue lines thus represents the "metabolic energy spared" (+44, +48 and +53 of "overall-estimated" -red- values at 10 $km \cdot h^{-1}$, 13 $km \cdot h^{-1}$ and 16 $km \cdot h^{-1}$, respectively).

Unfortunately, this set of calculations could not be applied to estimate the energy spared in un-steady locomotion (e.g. shuttle running) because the difference between the calculated values of AE and the intercept on the ordinate in Figure 7.3 could be nil or even negative (e.g. for the shorter shuttle distance).

The theoretical considerations put forward in the conclusions of this thesis must, of course, be verified by experimental analysis even if, from a methodological point of view, measuring muscle and tendon behavior during non-steady locomotion represents a real challenge. Modelling studies could provide important evidences about the role of muscles and tendons during unsteady locomotion, but real data are still necessary to fully understand their effects on the economy/efficiency of locomotion.

CHAPTER 8
REFERENCES

Aagaard P, Simonsen EB, Andersen JL, Magnusson SP, Halkjaer- Kristensen J, Dyhre-Poulsen P (2000) Neural inhibition during maximal eccentric and concentric quadriceps contraction: effects of resistance training. J Appl Physiol 89: 2249–2257

Albracht K & Arampatzis A (2013) Exercise-induced Changes in Triceps Surae Tendon Stiffness and Muscle Strength Affect Running Economy in Humans. Eur J Appl Physiol 13:1605-15

Alexander RM (1988) Elastic Mechanisms in Animal Movement Cambridge: Cambridge University Press

Alexander RM (1991) Energy-saving mechanisms in walking and running. J Exp Biol 160: 55-69

Alexander RM (2002) Tendon elasticity and muscle function. Comp Biochem Physiol 133: 1001-1011

Alexander RM (1984) Elastic energy stores in running vertebraties. American Zoologist 24: 85- 94

Alexander RM (2000) Optimization of Muscles and Movement for Performance or Economy of Energy. Neth J Zool 50: 101–112

Anderson FC, Pandy MG (1993) Storage and utilization of elastic strain energy during jumping. J Biomech 26: 1413 – 1427

Arampatzis A, Stafilidis S, Demonte G, Karamanidis K, Morey-Klapsing G, Bruggermann GP (2005) Strain and elongation of the human gastrocnemius tendon and aponeurosis during maximal plantarflexion effort. J Biomech 38: 833–841

Arampatzis, A, Karamanidis, K, Mademli, L, Albracht, K (2009) Plasticity of the human tendon to short- and long-term mechanical loading. Exerc Sport Sci Rev 37: 66–72

Arellano CJ & Kram R (2014) Partitioning the metabolic cost of human running: a task-by-task approach Integrative and Comparative Biology 54: 1084-1098

Arellano CJ, Konow N, Gidmark NJ, Roberts TJ (2019) Evidence of a tunable biological spring: elastic energy storage in aponeuroses varies with transverse strain in vivo. Proc R Soc B 286: 20182764

Arnold EM, Hamner SR, Seth A, Millard M, Delp SL (2013) How muscle ber lengths and velocities affect muscle force generation as humans walk and run at different speeds. J Exp Biol 216: 2150–2160

Avery NC, Bailey AJ (2005) Enzymic and non-enzymic cross-linking mechanisms in relation to turnover of collagen: relevance to aging and exercise. Scand J Med Sci Sports 15: 231– 240

Azizi E, Brainerd EL, Roberts TJ (2008) Variable gearing in pennate muscles. PNAS 105: 1745–1750

Bailey AJ, Paul RG, Knott L (1998) Mechanisms of maturation and ageing of collagen. Mech Ageing Dev 106: 1–56

Baltzopoulos V (1995) A videofluoroscopy method for optical distortion correction and measurement of knee-joint kinematics. Clin Biomech 10: 85–92

Bekenecker P, Raiteri B, Hahn D (2019) Patella tendon moment arm function considerations for human vastus lateralis force estimates. J Biomech 27: 225-231

Benjamin M, Kumai T, Milz S, Boszczyk BM, Boszczyk AA, Ralphs JR (2002) The skeletal attachment of tendons—tendon "entheses". Comp Biochem Physiol A Mol Integr Physiol 133: 931–945

Benjamin M, Ralphs JR (1997) Tendons and ligaments - an overview. Histol Histopathol 12: 1135–1144

Biewener AA, Roberts TJ (2000) Muscle and tendon contributions to force, work, and elastic energy savings: a comparative perspective. Exerc Sport Sci Rev 28: 99 – 107

Billeter R & Hoppeler (2003) Muscular basis of strength. Strentgth and power in sports, Willey 10.1002/9780470757215

Blickhan R (1989) The spring mass model for running and hopping. Journal of Biomechanics 22: 1217-1227

Bohm S, Marzilger R, Mersmann F, Santuz A, Arampatzis (2018) A Operating length and velocity of human vastus lateralis muscle suring walking and running. Scientific Reports 8: 5066

Bohm S, Mersmann F, Santuz A, Arampatzis A (2019) The force–length–velocity potential of the human soleus muscle is related to the energetic cost of running. Proc Biol Sci 286 (1917):20192560

Bøje O (1944) Energy production, pulmonary ventilatioa, and length of steps in well-trained runners working on a treadmill. Acta Physiologica Scandinavica

Butler DL, Grood ES, Noyes FR, Zernicke RF (1978) Biomechanics of ligaments and tendons. Exerc Sport Sci Rev 6: 125–181

Cavagna GA, Komarek L, Mazzoleni S (1971) The mechanics of sprint running. J Physiol 217: 709 – 721

Cavagna GA (1975) Force platforms as ergometers. J Appl Physiol 39: 174–179

Cavagna GA, Kaneko M (1977) Mechanical work and efficiency in level walking and running Journal of Physiology-London 268: 467-481

Cavagna GA, Margaria R (1966) Mechanics of walking. Journal of Applied Physiology 21: 271-278

Cavagna GA, Thys H, Zamboni A (1976) Sources of external work in level walking and running Journal of Physiology-London 262: 639-657

Cronin NJ, Carty CP, Barrett RS, Lichtwark G (2011) Automatic tracking of medial gastrocnemius fascicle length during human loco- motion. J Appl Physiol 111: 1491-1496

Cronin NJ, Finni T (2013) Treadmill versus overground and barefoot versus shod comparisons of triceps surae fascicle behaviour in human walking and running. Gait Posture 38: 528-533

Csapo R, Maganaris CN, Seynnes OR, Narici MV (2010) On muscle, tendon and high heels. J Exp Biol 213: 2582-2588

di Prampero PE, Atchou G, Bruckner JC, Moia C (1986) The energetics of endurance running. Eur J Appl Physiol 55:259-66

Dorn TW, Schache AG, Pandy MG (2012) Muscular strategy shift in human running: dependence of running speed on hip and ankle muscle performance. J Exp Biol 215: 1944-1956

Elliott DH (1965) Structure and Function of Mammalian Tendon. Biol Rev 40: 392–421

Eng CM, Azizi E, Roberts TJ (2018) Structural determinants of muscle gearing during dynamic contractions. Inter Comp Biol 58: 207-218

Ettema GJC (2001) Muscle efficiency: the controversial role of elasticity and mechanical energy conversion in stretch-shortening cycles. Eur J Appl Physiol 85: 457-465

Farris DJ & Sawicki GS (2012) Human medial gastrocnemius force-velocity behavior shifts with locomotion speed and gait. Proceedings of the National Academy of Sciences 109: 977- 982

Fenn WO (1930a) Frictional and kinetic factors in the work of sprint running. American Journal of Physiology 92: 583-611

Fenn WO (1930b) Work against gravity and work due to velocity changes in running movements of the center of gravity within the body and foot pressure on the ground. American Journal of Physiology 93: 433-462

Ferri A, Scaglioni G, Pousson M, Capodaglio P, Van Hoecke J, Narici MV (2003) Strength and power changes of the human plantar flexors and knee extensors in response to resistance training in old age. Acta Physiol Scand 177: 69-78

Finni T, Peltonen J, Stenroth,L, Cronin NJ (2013) Viewpoint: On the hysteresis in the human Achilles tendon. J Appl Physiol 114: 515–517

Fletcher JR and MacIntosh BR (2017) Running Economy from a Muscle Energetics Perspective. Front Physiol 8: 433 doi: 103389/fphys201700433

Fridén J, Lieber R (1992) Structural and mechanical basis of exercise-induced muscle injury. Med Sci Sports Exerc 24:521–30

Fukashiro S, Ito M, IchinoseY, Kawakami Y, Fukunaga T (1995) Ultrasonography Gives Directly

but Noninvasively Elastic Characteristic. Eur J Appl Physiol 71: 555–557

Fukunaga T, Kubo K, Kawakami Y, Fukashiro S, Kanehisa H, Maganaris C (2001) In vivo behaviour of human muscle tendon during waling. Proc R Soc Lond B 268: 229-233

Fukunaga T, Kawakami Y, Kuno S, Funato K, Fukashiro S (1997) Muscle architecture and function in humans. J Biomech

Fukuta S, Oyama M, Kavalkovich K, Fu FH, Niyibizi C (1998) Identification of types II, IX and X collagens at the insertion site of the bovine Achilles tendon. Matrix Biol J Int Soc 17: 65–73

Garby L, Astrup A (1987) The relationship between the respiratory quotient and the energy equivalent of oxygen during simultaneous glucose and lipid oxidation and lipogenesis. Acta Physiol Scand 129: 443-447

Gillett JG, Barrett RS, Lichtwark GA (2013) Reliability and accuracy of an automated tracking algorithm to measure controlled passive and active muscle fascicle length changes from ultrasound. Comput Methods Biomech Biomed Engin 16: 678-687

Gordon AM, Huxley AF, Julian FJ (1966a) The variation in isometric tension with sarcomere length in vertebrate muscle fibres. J Physiol 184: 170–192

Gordon AM, Huxley AF, Julian FJ (1966b) Tension development in highly stretched vertebrate muscle fibres. J Physiol 184: 143–169

Gordon SE, Flück M, Booth FW (2001) Selected Contribution: Skeletal muscle focal adhesion kinase, paxillin, and serum response factor are loading dependent. J Appl Physiol 90: 1174–1183

Halper J, Kjaer M (2014) Basic components of connective tissues and extracellular matrix: elastin, fibrillin, fibulins, fibrinogen, fibronectin, laminin, tenascins and thrombospondins. Adv Exp Med Biol 802: 31–47

Harridge SDR (2007) Plasticity of human skeletal muscle: gene expression to in vivo function. Exp Physiol 92: 783–97

Harridge SD, Kryger A, Stensgaard A (1999) Knee extensor strength, activation, and size in very elderly people following strength training. Muscle & nerve 22: 831–839

Hawkins D, Hull ML (1990) A method for determining lower extremity muscle-tendon lengths during exion/extension movements. J Biomech 23: 487–494

Haxton HA (1944) Absolute muscle force in the ankle flexors of man. J Physiol 103: 267–273

Heinemeier KM, Kjaer M (2011) In vivo investigation of tendon responses to mechanical loading. J Musculoskelet Neuronal Interact 11: 115–123

Hermens HJ, Freriks B, Merletti R, Rau G, Disselhorst-Klug C, Stegeman DF, Hägg GM (1999) European Recommendations for Surface Electromyography: Results of the SENIAM Project Roessingh Research and Development, Enschede, Netherlands

Herzog W, Abrahamse SK, Lter Keurs HE (1990) Theoretical determination of force-length relations of intact human skeletal muscles using the cross-bridge model. Plugers Arch 416: 113–119

Hill AV (1938) The heat of shortening and the dynamic constants of muscle. Proc R Soc B 126: 136-195

Hill A V (1938) The Heat of Shortening and the Dynamic Constants of Muscle. Proc R Soc B, 126: 136–195

Hof AL, Van Zandwijk JP, Bobbert MF (2002) Mechanics of human triceps surae muscle in walking, running and jumping. Acta Physiol Scand 174: 17-30

Hogberg P (1952) How do stride length and stride frequency influence the energy-output during running? Euro J Appl Physio O Physiol 14: 437- 441

Holt NC, Danos N, Roberts TJ, Azizi E (2016) Stuck in gear: age-related loss of variable gearing in skeletal muscle. J Exp Biol 219: 998-1003

Huxley A F (1974) Muscular contraction. J Physiol 243: 1–43

Huxley AF, Simmons RM (1971) Proposed mechanism of force generation in striated muscle. Nature, 233: 533–538

Ishikawa M, Pakaslahti J, Komi PV (2007) Medial gastrocnemius muscle behavior during human running and walking. Gait Posture 25: 380–384

Józsa LG, Kannus P (1997) Human Tendons: Anatomy, Physiology and Pathology Human Kinetics, Champaign, IL

Kastelic J, Galeski A, Baer E (1978) The Multicomposite Structure of Tendon. Connect Tissue Res 6: 11–23

Katz, B (1939) The relation between force and speed in muscular contraction. J Physiol, 45–64

Kawakami Y, Abe T, Fukunaga T (1993) Muscle-fiber pennation angles are greater in hypertrophied than in normal muscles. J appl Physiol 74: 2740–2744

Kellis E, Baltzopoulos V (1998) Muscle activation differences between eccentric and concentric isokinetic exercise. Med Sci Sports Exer 30: 1616-1623

Ker RF, Alexander RMcN, Bennett MB (1998) Why are mammalian tendons so thick? Journal of Zoology216: 309–324

Ker RF, Bennett MB, Bibby SR, Kester R, Alexander RM (1987) The spring in the arch of the human foot. Nature 325: 147-149

Kjaer M (2004) Role of extracellular matrix in adaptation of tendon and skeletal muscle to mechanical loading. Physiol Rev 84: 649–698

Komi PV (1990) Relevance of in vivo force measurements to human biomechanics. J Biomech 23: 23-34

Kubo K, Kawakami Y, Fukunaga T (1999) Influence of elastic properties of tendon structures on jump performance in humans. J Appl Physiol 87: 2090–2096

Kurokawa S, Fukunaga T, Fukashiro S (2001) Behavior of fascicles and tendinous structures of human gastrocnemius during vertical jumping. J Appl Physiol 90:1349–1358

Lai A, Lichtwark GA, Schache AG, Pandy MG (2018) Differences in in vivo muscle fascicle and tendinous tissue behaviour between the ankle plantarflexors during running. Scand J Med Sci Sports; DOI: 101111/sms13089

Lai A, Schache AG, Lin YC, Pandy MG (2014) Tendon elastic strain energy in the human ankle plantar-flexors and its role with increased running speed. J Exp Biol 217: 3159-3168

Lejeune TM, Willems PA, Heglund NC (1988) Mechanics and energetics of human locomotion on sand. J Exp Biol 201: 2071-80,

Lichtwark GA, Bougoulias K, Wilson AM (2007) Muscle fascicle and series elastic element length changes along the length of the human gastrocnemius during walking and running. J Biomech 40: 157-164

Lichtwark GA, Wilson AM (2006) In vivo mechanical properties of the human Achilles tendon during one-legged hopping. J Exp Biol 208: 4715-4725

Lichtwark GA, Cresswell AG, Ker RF, Reeves ND, Maganaris CN, Magnusson SP, Svensson RB, Coupe C, Hershenhan A, Eliasson P, Nordez A, Fouré A, Cornu C, Arampatzis A, Morey-Klapsing G, Mademli L, Karamanidis K, Vagula MC, Nelatury SR (2013) Commentaries on viewpoint: On the hysteresis in the human Achilles tendon. J Appl Physiol Bethesda Md 114: 518–520

Lichtwark GA and Wilson AM (2005) In vivo mechanical properties of the human Achilles tendon during one-legged hopping. J Exp Biol 208: 4715-4725

Lieber RL, Leonard ME, Brown-Maupin CG (2000) Effects of muscle contraction on the load-strain properties of frog aponeurosis and tendon. Cells Tissues Organs 166: 48-54

Lieber RL, Fridén J (2000) Functional and clinical significance of skeletal muscle architecture. Muscle nerve 23: 1647–66

Lin R, Chang G, Chang L (1999) Biomechanical properties of muscle-tendon unit under high-speed passive stretch. Clin Biomech 14: 412-417

Lombardi V, Piazzesi G (1990) The contractile response during steady lengthening of stimulated frog muscle fibres. J Physiol, 431: 141–171

Maganaris CN and Paul JP (2000) Hysteresis measurements in intact human tendon. J Biomech 33: 1723-1727

Maganaris CN (2002) Tensile properties of in vivo human tendinous tissue. J Biomech 35: 1019-

1027

Magnusson SP, Narici MV, Maganaris CN, Kjaer M (2008) Human tendon behaviour and adaptation, in vivo. J Physiol 586: 71 –81

Margaria R (1976) Biomechanics and energetics of muscular exercise. Claredon Press, Oxford, United Kingdom

Margaria R, Cerretelli P, Aghemo P, Sassi G (1963) Energy cost of running. J Appl Physiol 18: 367-370

McGeer T (1990a) Passive bipedal running Proceedings of the. Proc R Soc B 240: 107-134

McMahon TA, Cheng GC (1990) The mechanics of running-How does stiffness couple with speed? J Biomech 23: 65-78

Mero A, Luhtanen P, Komi PV (1983) A biomechanical study of the sprint start. Scand J Sport Sci 5: 20 – 28

Michna H (1983) A peculiar myofibrillar pattern in the murine muscle-tendon junction. Cell Tissue Res 233: 227–231

Minetti AE (1998) A model equation for the prediction of mechanical internal work of terrestrial locomotion. J Biomech 31:463–468

Minetti AE, Ardigò LP, Saibene F (1993) Mechanical determinants of gradient walking energetics in man. J Physiol 472: 725-735 Erratum in: J Physiol 475: 548

Minetti AE, Moia C, Roi G S, Susta D, Ferretti G (2002) Energy cost of walking and running at extreme uphill and downhill slopes. J Appl Physiol 93: 1039-1046

Minetti AE, Pinkerton J, Zamparo P (2001) From bipedalism to bicylism: evolution in energetics and biomechanics of historic bicycles. Proc Biol Sci 268: 1351-1360

Minetti AE (1998) A model equation for the prediction of mechanical internal work of terrestrial locomotion. J Biomech 31: 463–468

Muraoka T, Muramatsu T, Fukunaga T, Kanehisa H (2004) Influence of tendon slack on electromechanical delay in the human medial gastrocnemius in vivo. J Appl Physiol 96: 540-544

Narici MV (1999) Human skeletal muscle architecture studied in vivo by non- invasive imaging techniques: functional significance and applications Journal of electromyography and kinesiology : official journal of the. International Society of Electrophysiological Kinesiology, 9(2), 97–103

Narici MV, Binzoni T, Hiltbrand E, Fase, J, Terrier F, Cerretelli, P (1996) In vivo human gastrocnemius architecture with changing joint angle at rest and during graded isometric contraction. J Physiol 496: 287–297

Narici MV, Maganaris C, Reeves N (2005) Myotendinous alterations and effects of resistive loading in old age. Scand J Med Sci Sports 15: 392–401

Narici MV, Roi GS, Landoni L, Minetti AE, Cerretelli P (1989) Changes in force, cross-sectional area and neural activation during strength training and detraining of the human quadriceps. Eur J Appl Physiol 59: 310– 319

Neptune RR, Sasaki K (2005) Ankle plantar flexor force production is an important determinant of the preferred walk-to-run transition speed. J Exp Biol 208: 799 –808

Nigg BM, Herzog W (1999) Biomechanics of the musculoskeletal system Wiley

Nikolaidou ME, Marzilger R, Bohm S, Mersmann F, Arampatzis A (2017) Operating length and velocity of human M vastus lateralis fascicles during vertical jumping. R Soc Open Sci 4: 170185

O'Brien TD, Reeves ND, Baltzopoulos V, Jones DA, Maganaris CN (2010) Mechanical properties of the patellar tendon in adults and children. J Biomech 216: 631-642

O'Brien M (1992) Functional anatomy and physiology of tendons. Clin Sports Med 11: 505– 520

Pavei G, Seminati E, Cazzola D, Minetti AE (2017) On the estimation accuracy of the 3D body centre of mass trajectory during human locomotion: Inverse vs Forward Dynamics. Front Physiol 8: 129

Pins GD, Christiansen DL, Patel R, Silver FH (1997) Self-assembly of collagen fibers Influence of fibrillar alignment and decorin on mechanical properties. Biophys J 73: 2164–2172

Prilutsky BI, Zatsiorsky V (1994) Tendon action of two-joint muscles: transfer of mechanical energy between joints during jumping, landing and running. J Biomech 27: 25-34

Rasske K, Thelen DG, Franz JR (2017) Variation in the human Achilles tendon moment arm during walking. Comput Methods Biomech Biomed Engin 20: 201-205

Reiser K, McCormick RJ, Rucker RB (1992) Enzymatic and nonenzymatic cross-linking of collagen and elastin. FASEB J 6: 2439–2449

Roberts TJ, Azizi E (2011) Flexible mechanisms: the diverse roles of biological springs in vertebrate movement. J Exp Biol 214: 353-361

Roberts TJ, Marsh EL, Weyand PG, Taylor CR (1997) Muscular force in running turkeys: the economy of minimizing work. Science, 275:1113–1115

Roberts TJ, Scales JA (2002) Mechanical power output during running accelerations in wild turkeys. J Exp Biol 205, 1485 – 1494

Roberts TJ (2002) The integrated function of muscles and tendons during locomotion. Comp Biochem Physiol 133: 1087-1099

Rosager S, Aagaard P, Dyhre-Poulsen P, Neergaard K, Kjaer M, Magnusson SP (2002) Load-

displacement properties of the human triceps surae aponeurosis and tendon in runners and non-runners. Scand J Med Sci Sports 12: 90-98

Rubenson J, Pires NJ, Loi HO, Pinniger GJ, Shannon DG (2012) On the ascent: the soleus operating length is conserved to the ascending limb of the force-length curve across gait mechanics in humans. J Exp Biol 215: 3539- 3551

Saibene F, Minetti AE (2003) Biomechanical and physiological aspects of legged locomotion in humans. Eur J Appl Physiol 88: 297–316

Santuz A, Ekizos A, Janshen L, Baltzopoulos V, Arampatzis A (2017) On the Methodological Implications of Extracting Muscle Synergies from Human Locomotion. Int J Neural Syst 27: 1750007

Sawicki GS, Lewis CL, Ferris DP (2009) It pays to have a spring in your step. Exerc Sport Sci Rev 37: 130

Schache AG, Blanch PD, Dorn TW, Brown NA, Rosemond D, Pandy MG (2011) Effect of running speed on lower limb joint kinetics. Med Sci Sports Exerc 43:1260-71

Seynnes OR, Bojsen-Moller J, Albracht K, Arndt A, Cronin NJ, Finni T, Magnusson SP (2015) Ultrasound based testing of tendon mechanical properties: a critical evaluation. J Appl Physiol 118:133-141

Silver FH, Freeman JW, Seehra GP (2003) Collagen self-assembly and the development of tendon mechanical properties. J Biomech, Bone Cell and Tissue Mechanics 36: 1529– 1553

Stafilidis S, Karamanidis K, Morey-Klapsing G, Demonte G, Bruggermann GP, Arampatzis (2005) A Strain and elongation of the vastus lateralis aponeurosis and tendon in vivo during maximal isometric contraction. Eur J Appl Physiol 94: 317–322

Stevens TG, de Ruiter CJ, van Maurik D, van Lierop CJ, Savelsbergh GJ, Beek PJ (2015) Measured and estimated energy cost of constant and shuttle running in soccer players. Med Sci Sport Exerc 47: 1219–1224

Thompson JI, Czernuszka JT (1995) The effect of two types of cross-linking on some mechanical properties of collagen. Biomed Mater Eng 5: 37–48

Tidball JG (1991) Myotendinous junction injury in relation to junction structure and molecular composition. Exerc Sport Sci Rev 19: 419–445

Tijs C, van Dieën JH, Maas H (2015) No functionally relevant mechanical effects of epimuscular myofascial connections between rat ankle plantar flexors. J Exp Biol 218: 2935-2941

Tsaopoulos DE, Baltzopoulos V, Maganaris CN (2006) Human patellar tendon moment arm length: measurement considerations and clinical implications for joint loading assessment. Clin Biomech 21: 657–667

Walker SM, Schrodt GR (1974) I segment lengths and thin filament periods in skeletal muscle fibers of the Rhesus monkey and the human. The Anatomical record 178: 63–81

Wang JH (2006) Mechanobiology of tendon. J Biomech 39:1563-1582

Wang JH-C, Guo Q, Li B (2012) Tendon Biomechanics and Mechanobiology—A Minireview of Basic Concepts and Recent Advancements. J Hand Ther 25: 133–141

Wang JHC, Thampatty BP (2006) An introductory review of cell mechanobiology. Biomech Model Mechanobiol 5: 1–16

Werkhausen A, Cronin NJ, Albracht K, Bojsen-Møller J, Seynnes OR (2019) Distinct muscle-tendon interaction during running at different speed and in different loading conditions. J Appl Physiol 127: 246-253

Westing SH, Seger JY, Karlson E, Ekblom B (1988) Eccentric and concentric torque-velocity characteristics of the quadriceps femoris in man. Eur J Appl Physiol 58: 100–104

Weyand PG, Sandell RF, Prime DNL, Bundle MW (2010) The biological limits to running speed are imposed from the ground up. J Appl Physiol 108: 950-961

Williams KR, Cavanagh PR (1987) Relationship between distance running mechanics, running economy, and performance. J Appl Physiol 63:1236–1245

Winter D (1987) A new definition of mechanical work done in human movement. J Appl Physiol 64:79–83

Woledge RC, Curtin NA, Homsher E (1985) Energetic aspects of muscle contraction London: Academic Press

Yin Z, Chen X, Chen JL, Shen WL, Nguyen TMH, Gao L, Ouyang HW (2010) The regulation of tendon stem cell differentiation by the alignment of nanofibers. Biomaterials 31: 2163–2175

Zajac FE (1989) Muscle and tendon: properties, models, scaling, and application to bio- mechanics and motor control. Crit Rev Biomed Eng 17:359-411

Zamparo P, Pavei G, Monte A, Nardello F, Otsu T, Numazu N, Fujii N, Minetti AE (2019) Mechanical work in shuttle running as a function of speed and distance: implications for power and efficiency. Hum Mov Sci 66:487-496

Zamparo P, Pavei G, Nardello F, Bartolini D, Monte A, Minetti AE (2016) Mechanical work and efficiency of 5+5 m shuttle running. Eur J Appl Physiol 116: 1911-1919

Zamparo P, Pendergast DR, Termin B, Minetti AE (2002) How fins affect the economy and efficiency of human swimming. J Expl Biol 205: 2665-2676